



NUCLEAR WASTE MANAGEMENT ORGANIZATION SOCIÉTÉ DE GESTION DES DÉCHETS NUCLÉAIRES

Phase 2 Geoscientific Preliminary Assessment, Acquisition, Processing and Interpretation of High- Resolution Airborne Geophysical Data

TOWNSHIP OF SCHREIBER, ONTARIO



APM-REP-06145-0006

FEBRUARY 2015

This report has been prepared under contract to the NWMO. The report has been reviewed by the NWMO, but the views and conclusions are those of the authors and do not necessarily represent those of the NWMO.

All copyright and intellectual property rights belong to the NWMO.

For more information, please contact:

Nuclear Waste Management Organization

22 St. Clair Avenue East, Sixth Floor

Toronto, Ontario M4T 2S3 Canada

Tel 416.934.9814

Toll Free 1.866.249.6966

Email contactus@nwmo.ca

www.nwmo.ca

 Sander Geophysics	Airborne Geophysics Acquisition and Interpretation	Issue Date:	February 2015
--	--	-------------	---------------

PHASE 2 GEOSCIENTIFIC PRELIMINARY ASSESSMENT

**ACQUISITION, PROCESSING AND INTERPRETATION OF
HIGH-RESOLUTION AIRBORNE GEOPHYSICAL DATA**

TOWNSHIP OF SCHREIBER, ONTARIO

Prepared for:

Nuclear Waste Management Organization (NWMO)

by:

Sander Geophysics Limited (SGL)

NWMO REPORT NUMBER:

APM-REP-06145-0006

Signatures

Martin Bates, Ph.D.



Martin Mushayandevu, Ph.D.

M. M. Feb 20, 2015.

Executive Summary

This technical report documents the results of the acquisition, processing and interpretation of high-resolution airborne geophysical data conducted as part of the Phase 2 Geoscientific Preliminary Assessment, to further assess the suitability of the Schreiber area to safely host a deep geological repository (Geofirma, 2015). This study followed the successful completion of a Phase 1 Geoscientific Desktop Preliminary Assessment (NWMO, 2013; AECOM, 2013). The desktop study identified two potentially suitable areas warranting further studies such as high-resolution surveys and geological mapping.

The purpose of the Phase 2 acquisition, processing and interpretation of geophysical data was to provide an updated interpretation of the geological characteristics of the potentially suitable bedrock units identified in Phase 1 and to provide additional information to further assess the geology of the Schreiber area. Both magnetic and gravimetric data were acquired during the surveys in order to provide data to interpret the geometry and thickness of the potentially suitable bedrock units; the nature of geological contacts; bedrock lithologies; the degree of geological heterogeneities and the nature of intrusive phases within the batholith in the area; as well as the nature of structural features such as faults, shears zones, and alteration zones.

The grids of the acquired magnetic and gravimetric data and associated processed grids (first, second and horizontal derivatives, total gradient amplitude, trend analysis solutions and tilt angle) were analyzed and interpreted together with the mapped bedrock geology and other available geological information (e.g. magnetic susceptibility and rock density). The geophysical data and derivative products were used to estimate the locations of geological boundaries related to magnetic susceptibility and density changes, reveal regions of different geophysical character giving insight into variations in composition of the batholiths, and provide additional insight into the presence of potential faults, dykes, and other heterogeneities within and surrounding the batholiths. The Crossman Lake batholith in the survey area shows a pattern of low magnetic signal interspersed with linear features (both high and low) associated with dykes and faults, a number of which have not been previously mapped.

Preliminary forward modelling was completed on four profile lines that transect the batholith to estimate the shape, depth, thickness and the distribution of geological units within the geophysical survey area. The preliminary modelling indicates that the batholith is particularly deep in the centre and east of the western part of the Crossman Lake batholith, with maximum depths reaching approximately 7 km. However, the area of the batholith close to the metasedimentary rock appears to be significantly shallower and modelled as having depths of around 1.6 km. The preliminary modelling suggests that the eastern part of the Crossman Lake batholith may have depths of at least 2 km throughout.

1	INTRODUCTION.....	1
1.1	Study Objective.....	1
1.2	Geophysical Survey Area.....	1
2	SUMMARY OF GEOLOGY	3
2.1	Geologic Setting	3
2.2	Bedrock Geology	3
2.2.1	Crossman Lake Batholith	3
2.2.2	Schreiber-Hemlo Greenstone Belt	4
2.2.3	Mafic Dykes	4
2.3	Structural History and Mapped Structures	4
2.4	Metamorphism.....	5
2.5	Quaternary Geology	5
3	DATA SOURCE ACQUISITION AND QUALITY.....	6
3.1	Magnetic Data	7
3.2	Gravity Data	7
3.3	Digital Elevation Data.....	8
3.4	Additional Data Sources.....	9
3.4.1	OGS Mapped Bedrock Geology.....	9
3.4.2	OGS PETROCH Lithogeochemical Database	9
3.4.3	Magnetic Susceptibility Measurements.....	9
4	GEOPHYSICAL DATA PROCESSING METHODS.....	10
4.1	Gravity Data Processing.....	10
4.1.1	Bouguer Correction	11
4.1.2	Static and Level Corrections.....	11
4.1.3	Gridding and Filtering.....	11
4.2	Magnetic Data Processing	12
4.2.1	Levelling.....	12
4.2.2	Micro-Levelling.....	13
4.2.3	Gridding.....	13
4.3	Gravity and Magnetic Derivative Products.....	13
4.3.1	Total Magnetic Intensity Reduced to Pole.....	13

4.3.2	Vertical Derivatives of Total Magnetic Intensity and Bouguer Gravity	14
4.3.3	Total Horizontal Gradient of Total Magnetic Intensity and Bouguer Gravity	14
4.3.4	Total Gradient Amplitude of Total Magnetic Intensity	15
4.3.5	Tilt Angle	15
4.3.6	Trend Analysis Method	15
5	GEOPHYSICAL INTERPRETATION.....	16
5.1	Results of Qualitative Analysis	16
5.1.1	Crossman Lake Batholith	17
5.2	Preliminary 2.5D Modelling	18
5.2.1	Model Descriptions	19
5.2.2	Model Results	21
6	SUMMARY OF RESULTS	26
7	REFERENCES	28
8	FIGURES.....	31

1 Introduction

This technical report documents the results of the acquisition and interpretation of high-resolution airborne geophysical data (gravity and magnetic) conducted as part of the Phase 2 Geoscientific Preliminary Assessment, to further assess the suitability of the Schreiber area to safely host a deep geological repository (Geofirma, 2015). This study followed the successful completion of a Phase 1 Geoscientific Desktop Preliminary Assessment (NWMO, 2013; AECOM, 2013). The desktop study identified two potentially suitable areas warranting further studies such as high-resolution surveys and geological mapping.

1.1 Study Objective

The purpose of the interpretation of the acquired magnetic and gravity data is as follows:

- Acquire high-resolution airborne magnetic and gravimetric data within a geophysical survey area that encompasses the general potentially suitable areas identified in the Phase 1 Geoscientific Desktop Preliminary Assessment (AECOM, 2013a; NWMO, 2013).
- Characterize the geophysical response of the bedrock units (e.g. bedrock contacts, intrusive phases, potential for natural resources, etc).
- Characterize the extent of bedrock heterogeneity (e.g. ductile fabric, complexity, etc).
- Interpret the geophysical character of potential structures (faults, dykes, joints, etc).
- Develop initial models of bedrock units at depth (2.5D forward modeling).

1.2 Geophysical Survey Area

The Schreiber area encompasses the eastern portion of the Crossman Lake batholith which is bounded to the north by the Quetico metasedimentary rocks and to the southeast by the Schreiber-Hemlo greenstone belt. The Township of Schreiber is located along the north shore of Lake Superior approximately 150 km east of Thunder Bay (~200 km by road). The geophysical survey area is located approximately 15 km north of the Township of Schreiber, Ontario. It consists of two separate survey areas totaling an area of 174 km². Topography in the area comprises moderate to high relief over short distances, with rugged terrain consisting of knobby bedrock hills and steep escarpments. The location of the geophysical survey area is shown in Figure 1.1, and the full set of survey lines are shown in Figure 1.2. The survey lines that were flown in an east-west direction link the two survey areas together. The survey areas are bounded by the following coordinates presented in Table 1.1 (NAD83 datum, UTM zone 16N)

Table 1.1: Coordinates of the survey areas

Easting (m)	Northing (m)
Western Block	
464,222	5,430,741
471,657	5,430,741
471,657	5,418,469
464,222	5,418,469
Eastern Block	
491,043	5,425,584
491,043	5,416,950
481,490	5,416,950
481,490	5,425,584

2 Summary of Geology

Details of the physical geography and geology of the area of Schreiber were described in the Phase 1 Geoscientific Desktop Preliminary Assessment (AECOM, 2013a). The following sub-sections provide a summary of the geologic setting, bedrock geology, structural history and mapped structures, metamorphism and Quaternary geology, with a focus on the general potentially suitable areas in the Crossman Lake batholith identified during Phase 1 (AECOM, 2013), as well as the surrounding bedrock units and important structural features.

2.1 Geologic Setting

The Schreiber area is located in the Archean Wawa Subprovince of the Superior Province. The Wawa Subprovince comprises a volcano-sedimentary-plutonic terrane bounded to the east by the Kapuskasing structural zone (beyond the Schreiber geophysical survey area) and to the north by the metasedimentary-dominated Quetico Subprovince. The western end of the Wawa Subprovince is bordered by the Proterozoic Trans-Hudson orogen. In the Schreiber area the Wawa Subprovince is flanked to the south by the Early Proterozoic Southern Province.

The Wawa Subprovince is composed of two semi-linear zones of greenstone belts, the northern of which includes the Shebandowan, Schreiber-Hemlo, Manitouwadge-Hornepayne, White River, Dayohessarah, and Kabinakagami greenstone belts. The Proterozoic Coldwell alkalic complex divides the Schreiber-Hemlo greenstone belt (sometimes referred to as the Terrace Bay-Schreiber greenstone belt) into an eastern and western portion, the latter of which falls within the Schreiber area. The Schreiber-Hemlo greenstone belt is intruded by large granitoid bodies, including the Crossman and Whitesand Lake batholiths within the Schreiber area.

2.2 Bedrock Geology

The main geological units in the Schreiber area that occur within the airborne geophysical survey area include two large granitoid intrusions (Crossman Lake and Whitesand Lake batholiths), portions of the supracrustal rocks of the Schreiber-Hemlo greenstone belt, and several swarms of mafic diabase dykes (Figure 1.1). These bedrock units in the Schreiber area are overprinted by several orientations of brittle faults and the individual rock units have been subjected to varying amounts of metamorphism. The following subsections include a brief description of the Crossman Lake batholith, the Schreiber-Hemlo greenstone belt and diabase dykes that occur within the geophysical survey area.

2.2.1 Crossman Lake Batholith

The Crossman Lake batholith occupies the majority of the northern part of the Schreiber area (Figure 1.1). The batholith is predominantly massive and consists of a mixture of medium-grained quartz-monzonite and monzodiorite, (alkali-feldspar) granite, tonalite, and granodiorite. Minor dykes and irregular masses of microgranite, quartz (-feldspar) porphyry and aplite occur along the margins of the batholith.

The boundary between the mostly massive (alkali-feldspar) granite of the Whitesand Lake batholith and Crossman Lake batholith is poorly defined. Carter (1988) placed the boundary between the two batholiths along narrow septa of east-trending greenstone belt rocks along the western margin of the Schreiber area (Figure 1.1).

2.2.2 Schreiber-Hemlo Greenstone Belt

The Schreiber-Hemlo greenstone belt is highly complex structurally and lithologically. Supracrustal rocks of this greenstone belt occurring in the Schreiber area are considered to be part of the Schreiber assemblage (Williams et al., 1991; Figure 1.1).

Carter (1988) identified three major types of supracrustal rocks in the Schreiber assemblage: 1) tholeiitic, mafic, massive or schistose, and variably metamorphosed up to amphibolite facies metavolcanic rocks comprising mainly massive to pillow basalt, tuff and related breccias; 2) calc-alkalic, mafic to felsic metavolcanic rocks dominated by massive, aphanitic to fine-grained flows with minor tuff and felsic amygdaloidal interbeds; and 3) clastic metasedimentary rocks, mainly wacke and silicified shale (including graphitic intervals) of turbiditic origin interbedded with minor banded iron formation.

2.2.3 Mafic Dykes

Several suites of diabase dykes crosscut the Schreiber area (Figure 1.1), including:

- Northwest-trending Matachewan Suite dykes (ca. 2.473 Ga; Buchan and Ernst, 2004). This dyke swarm is one of the largest in the Canadian Shield. Individual dykes are generally up to 10 metres wide, and have vertical to subvertical dips. The Matachewan dykes comprise mainly quartz diabase dominated by plagioclase, augite and quartz (Osmani, 1991).
- North-trending Marathon Suite dykes (ca. 2.121 Ga; Buchan et al., 1996). These dykes form a fan-shaped distribution pattern around the northern, eastern, and western flanks of Lake Superior. The dykes vary in orientation from northwest to northeast, and occur as steep to subvertical sheets, typically a few metres to tens of metres thick, but occasionally up to 75 metres thick (Hamilton et al., 2002). The Marathon dykes comprise quartz tholeiite dominated by equigranular to subophitic clinopyroxene and plagioclase.
- East-west-trending, reversely polarized Keweenaw Suite dykes related to the ca. 1.100 Ga Midcontinent Rift that was centred on proto-Lake Superior (Thurston, 1991).

Potentially, a western extension of the ca. 2.167 Ga Biscotasing dyke swarm also occurs in the Schreiber area (Hamilton et al., 2002). These dykes generally trend northeast; however, how these dykes may be distinguished from the northeast-trending Marathon dykes in the Schreiber area is undefined.

2.3 Structural History and Mapped Structures

In the Schreiber area, several faults are indicated on public-domain geological maps (Figure 1.1). These include the major (from west to east) Sox Creek, and Ross Lake southeast-trending faults, as well as several northeast-trending faults including the Worthington Bay fault (with the Syenite Lake fault along its extension), and the Ellis Lake fault. The timing and kinematics of these faults are not described in the available literature.

Carter (1988) conducted a field mapping program and developed a geological map for the Schreiber area, primarily on the basis of 1:15,840 scale aerial photographs and north-south trending traverse mapping at roughly quarter mile intervals. As a result of this mapping program, Carter (1988) attempted an interpretation of the fault movement along some of the faults shown on public domain geological maps. No supporting structural information was included in Carter (1988), so it is assumed that the fault movement interpretation was derived from aerial photographs. Carter's (1988)

interpretation is only included here for historical reference. Carter (1988) interpreted the Sox Lake fault as a dextral strike-slip fault, the Cook Lake fault and Syenite Lake fault as dip-slip faults, and the Worthington Bay fault as a sinistral strike-slip fault.

2.4 Metamorphism

Overall, most of the Canadian Shield preserves a complex episodic history of Neoproterozoic tectonometamorphism overprinted by Paleoproterozoic tectonothermal events culminating at the end of the Grenville orogeny ca. 0.950 Ga. The distribution of contrasting metamorphic domains in the Canadian Shield is a consequence of relative uplift, block rotation and erosion resulting from Neoproterozoic orogenesis, subsequent local Proterozoic orogenic events and broader epeirogeny during later Proterozoic and Phanerozoic eons.

In the Schreiber area, the metamorphic grade of exposed Archean rocks is upper greenschist facies (Williams et al., 1991). Locally, higher metamorphic grades up to upper amphibolite facies are recorded in rocks along the margins of plutons. No records exist that suggest that rocks in the Schreiber area may have been affected by thermotectonic overprints related to post-Archean events.

2.5 Quaternary Geology

Quaternary geology in the Schreiber area is described in detail in AECOM (2013b). A brief summary is provided here for reference.

The Quaternary sediments, commonly referred to as drift, soil or overburden, are glacial and post-glacial materials which overlie the bedrock in the Schreiber area. For the majority of the area of Schreiber drift thickness over bedrock is limited and the ground surface reflects the bedrock topography. Over the majority of the area bedrock outcrops are common and the terrain is classified, for surficial purposes, as a bedrock-drift complex, i.e., thin drift cover that only locally achieves thicknesses that mask or subdue the bedrock topography.

The most common glacial deposits in the area of Schreiber are outwash deposits and ground moraine (till), generally less than 2 to 3 m thick. Greater accumulations of till are found within bedrock depressions, large scale lineaments, and on the down-ice (lee) side of bedrock highs.

Glaciofluvial outwash deposits occur as relatively level areas within some narrow, bedrock controlled valleys. The thicknesses of these deposits are likely to be variable, and may be locally substantial. Outwash deposits are generally well-sorted and comprised of stratified sand, gravel, and local boulders. The ground moraine (till) deposits have a silty-sand matrix and contain abundant clasts in the pebble to cobble size range. The thickness of the till in the Schreiber area, based on exploration borehole records and surficial mapping, is generally on the order of 1 to 3 m (AECOM, 2013b).

Bogs and organic-rich alluvial deposits are present along water courses in the area and in rock floored basins. These deposits tend to have a limited thickness, as determined by regional studies, and areal extent.

3 Data Source Acquisition and Quality

Sander Geophysics Limited (SGL) completed a fixed-wing high-resolution airborne magnetic and gravity survey in the Schreiber area between April 12 and April 24, 2014. The survey area comprised two small survey blocks located northeast and northwest of the Township of Schreiber (Figure 1.1). These survey blocks were designed to cover the two general potentially suitable areas identified in the Phase 1 preliminary assessment and capture relevant geological features.

The survey included a total of 3,397 km of flight lines covering a surface area of approximately 174 km² (Figure 1.2). Flight operations were conducted out of the Greenstone Regional Airport, in Geraldton, Ontario using a Britten-Norman BN-2 Islander. Data were acquired along traverse lines flown in an east-west direction spaced at 100 m, and control lines flown north-south spaced at 500 m. The survey was flown at an altitude of 80 m above ground level, with an average ground speed of 100 knots (approximately 185 km/h or 50 m/s). Airborne magnetic and gravity data were acquired using equipment with very high sensitivity and accuracy. The airborne magnetic data was recorded using a magnetometer sensor mounted in a single fibreglass stinger extending from the tail of the aircraft. The airborne gravity data was recorded using a gravimeter, which includes three orthogonal accelerometers that are mounted on a stabilized platform inside the cabin of the aircraft. Table 3.1 gives a quick reference of the details of the survey.

Table 3.1: Survey Details

Survey Particulars	
Survey Start Date:	April 12, 2014
Survey End Date:	April 24, 2014
Field Office Location:	Geraldton, Ontario
Airport Used:	Greenstone Regional Airport (Geraldton)
Aircraft Type:	Britten-Norman Islander
Total line kilometers:	3,397 km
Traverse Line numbers:	3000 - 3141
Traverse Line direction:	East-West
Traverse Line spacing:	100 m
Control Line numbers:	300-354
Control Line direction:	North-South
Control Line spacing:	500 m
Survey Altitude:	Smoothed drape with target height of 80 m above ground.
Digital Terrain Source:	SRTM
Number of Flights (numbers):	8 (1001 to 1008)
Aircraft Target Ground Speed:	100 knots
Magnetic Field Reference location:	478775mE 5424161mN (NAD83):UTM 16N
Magnetic Field Inclination (+ve down):	74.45° at reference station
Magnetic Field Declination (+ve east):	-5.79 ° at reference station
Approximate total field value:	56,900 nT
Magnetic Reference Field Model:	International Magnetic Reference Field (IGRF 2010-2015), interpolated to date and location of acquisition

Fundamental Gravity Network Ties:	Tied to the gravity station established by SGL in Hearst. The Hearst gravity station was in turn tied our Ottawa office gravity station.
Survey Base Gravity Value:	980935.82 mGal at centre of gravimeter when aircraft parked on the ramp at Greenstone Regional Airport.
Survey Base Parking Location (NAD83):	504978.48mE 5514348.63mN UTM 16N Height: 312.0 m (location of gravimeter centre, 1.62 m above the ground.)
Base Station Locations (NAD83):	GND1: 503401.88mE 5506207.79mN UTM 16N Height: 298.859 m GND2: 503403.18mE 5506207.61mN UTM 16N Height: 298.672 m
Field Acquisition Datum:	WGS84
UTM Projection:	UTM 16N

3.1 Magnetic Data

Total magnetic field measurements were recorded with a single cesium magnetometer mounted in a fibreglass stinger extending from the tail of the survey aircraft. SGL's hardware and software system, AIRComp, was used to remove the effects of the aircraft and its manoeuvres from the recorded magnetic data. The data were recorded for post-processing. Coefficients to be used for compensation were derived by processing the calibration flight data, based on principles presented by Leliak (1961). The compensation coefficients were applied to data recorded during normal survey operations to produce compensated magnetic data.

Low-pass filtered reference station diurnal was subtracted from the airborne data on a reading by reading basis. If more than one reference station is used, the reference station value could be interpolated, based on the relative distance of the reading from each reference station.

Both the ground and airborne systems used the Geometrics G-822A cesium magnetic sensor. Total magnetic field measurements were recorded at 160 Hz in the aircraft, and then later down sampled to 10 Hz in the processing. The ground systems recorded magnetic data at 11 Hz.

A pre-planned drape surface was prepared for the survey to guide the aircraft over the topography in a consistent manner, as close to the minimum clearance as possible. The drape surface was prepared with digital elevation model (DEM) data obtained from the Shuttle Radar Topography Mission (SRTM) (<http://srtm.usgs.gov/>) for the area. The DEM included an extension beyond the survey boundary to allow the aircraft to achieve the drape clearance before coming on line.

Details of the processing of the magnetic data are provided in Section 4.2 of this report.

3.2 Gravity Data

Gravity data were acquired with SGL's propriety AIRGrav (*Airborne Inertially Referenced Gravimeter*) system, which uses a Schuler tuned inertial platform supporting three orthogonal accelerometers, which remain fixed in inertial space, independent of the manoeuvres of the aircraft, allowing precise isolation from the effects of the movement of the aircraft. The gravity sensor used in AIRGrav is a very accurate accelerometer with a wide dynamic range. The system is not affected by the strong vertical motions of the aircraft, allowing the final gravity data to be almost completely unaffected by in-flight conditions classified as "moderate turbulence" or better. The instrument is also considered to be an inertial navigator, and as such the platform levelling was essentially unaffected by horizontal accelerations.

In typical survey flying, accelerations in an aircraft can reach 0.1 G, equivalent to 100,000 milligal. Data processing must extract gravity data from this very noisy environment. This was achieved by modelling the gravity due to movements of the aircraft in flight as measured by extremely accurate Global Positioning System (GPS) measurement. These measurements are affected by noisy conditions in the ionosphere, and by the variable conditions (e.g. temperature, pressure and humidity) within the troposphere. SGL has developed a full suite of programs to carry out all the necessary corrections.

The GPS data are extracted from the airborne and reference station acquisition system and reformatted. Differential corrections to correct the airborne ranges for variations calculated from the base station GPS data were performed. Each recorded position was recalculated based on these ranges. The original reference system for all GPS data was the WGS-84 datum. Positions were then converted to the local datum, reference system and desired projection. Each line was then checked for data continuity and quality.

An extremely accurate location of the base station GPS receiver was determined using an IGS permanent GPS Reference Station to apply differential corrections (<http://igs.org/network>). This technique provides a final base station receiver location with an accuracy of better than a few decimetres. The entire airborne data set was then reprocessed differentially using the recalculated base station location.

Gravity data were recorded at 128 Hz. Accelerations were filtered and resampled to 10 Hz to match the GPS, using specially designed filters to avoid biasing the data. Gravity was calculated by subtracting the GPS derived accelerations from the inertial accelerations. The calculated gravity was corrected for the Eötvös effect and normal gravity, and the sample interval was then reduced to 2 Hz. These operations were all performed by SGL's proprietary GravGPS software. A detailed description of gravity processing is provided in Section 4.1 of this report.

3.3 Digital Elevation Data

Digital elevation data were collected during the survey using a laser altimeter (Riegl LD90-31K-HiP) mounted to the base of the aircraft. The elevation data were sampled at a rate of 3.3 Hz, which is consistent with a sample roughly every 16 m along the profile line. Even though the laser altimeter can record returns from more than 700 m above the ground with a high degree of certainty, some laser data dropouts occurred while flying over the areas of poor reflectivity. The laser data shows the effects of the dense tree cover; variable penetration of the canopy results in a high frequency variation of recorded altitude. The raw laser data were processed with an iterative de-spiking routine designed to remove many of the early laser returns from trees.

Digital elevation data were also collected using a King radar altimeter mounted to the base of the aircraft. Data were sampled at a rate of 10 Hz, which is consistent with a sample roughly every 6m. The radar data penetrates the canopy less as it records the first return within the footprint of its signal. The radar altimeter data were filtered to remove high-frequency noise using a 67-point low pass filter.

A digital elevation model (DEM) was derived by subtracting the laser altimeter data from the differentially corrected DGPS altitude with respect to the Canadian Geodetic Vertical Datum 2013 (CGVD2013). Short sections of poor laser data due to locally weak reflectivity were replaced using King radar data. The DEM reflects the presence of vegetation (for example trees) and buildings and

thus is not considered to be a digital terrain model (DTM).

The digital elevation data were gridded to form a DEM grid using a cell size of 25 m over the Schreiber survey area. The 25 m gridding cell was applied to present the highest resolution of the digital elevation model within the boundaries of the two survey blocks comprising the principal survey area (Figure 3.1).

3.4 Additional Data Sources

In addition to the acquired data, a number of other publically available data sources were used. These are summarized below.

3.4.1 OGS Mapped Bedrock Geology

The Precambrian Geoscience Section of the Ontario Geological Survey has compiled a 1:250,000 scale map of the bedrock geology of Ontario (OGS, 2011). These maps were recently revised and issued as 'Miscellaneous Release – Data 126 – Revision 1'. The data is publicly available as a seamless GIS data set and includes such details as bedrock units, major faults, dyke swarms, iron formations and kimberlites. This resource was of fundamental importance in assisting with the geophysical interpretation of the acquired potential field data. The mapped bedrock geology was used for both qualitative and quantitative aspects of the interpretation. In the case of the qualitative interpretation, the mapped bedrock geology gave the overall context for the magnetic and gravity data. For the 2.5D modelling, the mapped bedrock geology provided initial surface constraints.

3.4.2 OGS PETROCH Lithogeochemical Database

The Ontario Geological Survey has a publicly available PETROCH Lithogeochemical Database (Haus and Pauk 2010). The database contains detailed rock chemical data collected by OGS geoscientists, which includes information about rock type, chemical composition, age, stratigraphy, major oxide values, sample location and specific gravity. A few dozen of these data points occur in the south and east of the survey area. This information was used in the interpretation to: 1) obtain further information on the composition of major mapped rock units where samples have been taken; and 2) constrain the density of rock units used in the 2.5D modelling.

3.4.3 Magnetic Susceptibility Measurements

The Ontario Geological Survey has a publicly available Ontario Precambrian Bedrock Magnetic Susceptibility Geodatabase for 2001 to 2012 (Muir, 2013), which is known as Miscellaneous Release – Data 273 (MRD 273-Rev). This GIS database contains measurements of magnetic susceptibilities and rock classifications for points across Ontario. In the Schreiber survey area, the data points are limited to sections of the greenstone belt to the northeast of the Crossman Lake batholith.

4 Geophysical Data Processing Methods

4.1 Gravity Data Processing

Advanced gravity processing allows for the generation of high-resolution gravity data. These advances involve the use of GPS phase angle corrections, the integration of GPS processing with inertial data from the gravimeter and the advanced analysis of system states and uncertainties. This processing helps reduce system noise and allows for the generation of high quality, low noise raw gravity data through a wider range of survey conditions than was previously possible. The following standard corrections were applied to the gravity data (Telford et al., 1990; Blakely, 1996):

- a. Eötvös correction,

$$\delta g_{Eötvös} = - \frac{v_x^2}{\frac{r}{(1 - e_2 \sin^2 \Phi)^{1/2}} + h} - 2 W_s v_x \cos \Phi - \frac{v_y^2}{\frac{r(1 - e_2)}{(1 - e_2 \sin^2 \Phi)^{3/2}} + h}$$

where Φ is the latitude of the aircraft, v_x and v_y are the velocities of the aircraft in the x (east) and y (north) direction, r is the Earth's radius at the equator (6,378,137 m), e_2 is a correction for Earth's flattening towards the poles ($6.69437999013 \times 10^{-3}$), W_s is the angular velocity of Earth's rotation ($7.2921158553 \times 10^{-5}$ rad/s), and h is the altitude of the plane above the WGS84 datum;

- b. Normal gravity,

$$g_{Normal} = \frac{9.7803267714 (1 + 0.00193185138639 \sin^2 \Phi)}{\sqrt{1 - 0.00669437999013 \sin^2 \Phi}}$$

where Φ is the latitude of the aircraft;

- c. Free air correction,

$$g_{fa} = - (0.3087691 - 0.0004398 \sin^2 \Phi) h + 7.2125 \times 10^{-8} h^2$$

where h is the height of the aircraft in metres above the WGS84 datum;

- d. Bouguer Slab,

$$g_{sb} = 2 \pi \gamma \rho h = 0.041925 \rho h$$

where γ is the Universal Gravity constant, ρ is the average density for the project in g/cm^3 , and h is height of the surface of land or sea in metres above the WGS84 datum;

- e. Curvature of the Earth,

$$g_{ec} = \frac{\rho}{2.67} [1.464 h - 0.3533 h^2 + 0.000045 h^3]$$

where h is height of the surface of land or sea in kilometres above the WGS84 datum and ρ is the density for the project.

- f. Full Bouguer correction, g_b . See below in subsection 4.1.1 for a description of the Bouguer correction technique;
- g. Static correction, g_{sc} , based on static ground recordings and repeat lines;
- h. Level Correction, g_{lc} , based on line intersections. See below in subsection 4.1.2 for a more

detailed description of the Static correction (g_{sc}) and Level correction (g_{lc}) techniques.

The final Bouguer anomaly equals $G - g_{fa} - g_b - g_{sc} - g_{lc}$, where G is the calculated gravity adjusted for Eötvös effect and normal gravity.

4.1.1 Bouguer Correction

Shuttle Radar Terrain Mission (SRTM) digital elevation model data were used to calculate the Bouguer corrections for gravity processing. The SRTM data contains information in a grid with a 3 arcsecond spacing, approximately equal to 100 m cell spacing, which has a higher density than the line spacing for this survey, and therefore provides terrain data at a better resolution between the survey lines. Coverage up to 160 km from the survey block was kept for accurate regional corrections.

Terrain corrections were computed using software developed by SGL. The algorithm calculates the topographic attraction of the terrain using a mass prism model with a constant density. The difference between the topographic attraction and the simple Bouguer correction is the terrain correction. The terrain and Bouguer corrections were calculated for the bedrock at the height of the aircraft using densities of 2.67 and 2.40 g/cm³.

Terrain corrections were filtered to match the degree of filtering applied to the gravity data, as described below.

4.1.2 Static and Level Corrections

The gravimetric data were levelled to compensate for instrument variations in two steps. A single constant shift determined from ground static recordings was applied on a flight-by-flight basis. The pre- and post-flight readings were averaged for each flight and the difference between the average value and the local gravity value was removed. This acts as a simple, but effective, coarse levelling of the data.

Intersection statistics were then used to adjust individual survey lines. Unlike magnetic levelling, individual intersections were not used to make corrections. Instead, intersection differences from whole lines were averaged and a single adjustment was applied to each survey line and each control line. Minor adjustments were calculated for sections of each line based on statistics from groups of intersections. The adjustments were smoothed and applied to line data that was filtered, as described below. Grids of adjusted data were inspected to determine that the adjustments were appropriate.

4.1.3 Gridding and Filtering

Statistical noise in the data was reduced by applying a cosine tapered low pass filter to the time series line data. For this survey, a 20 second (1000 m) half-wavelength filter was employed. The data were gridded using a minimum curvature algorithm that averages all values within any given grid cell and interpolates the data between survey lines to produce a smooth grid. The algorithm produces a smooth grid by iteratively solving a set of difference equations by minimizing the total second horizontal derivative while attempting to honour the input data (Briggs, 1974). Grids were generated using a 25 m grid cell size.

Low-pass spatial filtering was applied to the grid to achieve better noise reduction than by simply increasing the degree of line filtering. A range of grid filters were used and evaluated for their effectiveness in removing noise from the data, and highlighting signal content. The final data was filtered with a 1.0 km half-wavelength grid filter.

The gravity data were gridded using a cell size of 25 m and 250 m over the Schreiber area. The 25 m gridding cell was applied to present the highest resolution of the data within the boundaries of the two survey blocks comprising the principal survey area. The 250 m gridding cell was applied to include the extensions of the flight lines beyond the survey blocks comprising the extended survey area. The Bouguer gravity with a terrain correction of 2.67 g/cm³ is displayed in Figures 4.1 (principal survey area, grid cell size of 25 m) and Figure 4.2 (extended survey area, grid cell size of 250 m). The Free Air gravity is displayed in Figures 4.3 (principal survey area, grid cell size of 25 m) and Figure 4.4 (extended survey area, grid cell size of 250 m).

4.2 Magnetic Data Processing

The airborne magnetometer data were recorded at 160 Hz, and down sampled to 10 Hz for processing. A second order Butterworth 0.9 Hz low pass filter was utilized in the process for compensation and anti-aliasing. All magnetic data were plotted and checked for any spikes or noise. A 0.244 second static lag correction due to signal processing, in addition to a dynamic lag correction, was applied to each data point. The aircraft speed dependent dynamic lag was calculated using SGL's Dynlag software.

Ground magnetometer data were inspected for cultural interference and edited where necessary. All reference station magnetometer data were filtered using a 121 point low-pass filter to remove any high frequency noise, but retain the low frequency diurnal variations.

A correction for the International Geomagnetic Reference Field (IGRF) year 2010 model was applied to all ground magnetometer data using the fixed ground station location and the recorded date for each flight. The mean residual value of the reference station was calculated (-947.109nT) and subtracted to remove any bias when correcting the local anomalous field on the survey grid. Diurnal variations in the airborne magnetometer data were removed by subtracting the corrected reference station data.

The airborne magnetometer data were corrected for the IGRF using the location, altitude, and date of each point. IGRF values were calculated using the year 2010 IGRF model. The altitude data used for the IGRF corrections are DGPS heights above the WGS84 datum.

4.2.1 Levelling

Intersections between control and traverse lines were determined by a program which extracts the magnetic, altitude, and x and y values of the traverse and control lines at each intersection point. Each control line was adjusted by a constant value to minimize the intersection differences, calculated as follows:

$$\sum |i - a| \text{ summed over all traverse lines, where:}$$

i = (individual intersection difference)

a = (average intersection difference for that traverse line)

Adjusted control lines were further corrected locally to minimize any residual differences. Traverse line levelling was carried out by a program called CLEVEL that interpolates and extrapolates levelling values for each point based on the two closest differences at intersections. After traverse lines were levelled, the control lines were matched to them. This ensured that all intersections tie perfectly and permitted the use of all data in the final products.

CLEVEL provided a curved correction using a function similar to spline interpolation. A third degree polynomial was used to interpolate between two intersections. CLEVEL is an improved method, as it allows intersection points to be preserved with no mismatch and interpolation is smooth with the first

derivative continuously approaching the same value from both sides of the intersection points.

The levelling procedure was verified through inspection of the magnetic anomaly and vertical derivative grids by plotting profiles of corrections along lines, and by examination of levelling statistics to check for steep correction gradients.

4.2.2 Micro-Levelling

Micro-levelling was applied to remove any residual diurnal effects from the data, and was achieved by using directional filters to identify and remove artifacts that are long wavelength parallel to survey lines and short wavelengths perpendicular to survey lines. A limit of +/-0.20 nT was set for all micro-levelling corrections.

4.2.3 Gridding

The grid of the total magnetic intensity was made using a minimum curvature algorithm to create a two-dimensional grid equally sampled in the x and y directions following Briggs (1974). The final grids of the magnetic data were created with 25 m grid cell size appropriate for survey lines spaced at 100 m. Grids were also made that included the 1000 m spaced lines that extend out from the main block area. These were gridded with a cell size of 250 m.

The magnetic data were gridded using a cell size of 25 m and 250 m over the Schreiber area. The 25 m gridding cell was applied to present the highest resolution of the data within the boundaries of the two survey blocks comprising the principal survey area. The 250 m gridding cell was applied to include the extensions of the flight lines beyond the survey blocks comprising the extended survey area. The total magnetic intensity (or more precisely, the magnetic anomaly) is displayed in Figures 4.5 (principal survey area, grid cell size of 25 m) and Figure 4.6 (extended survey area, grid cell size of 250 m).

4.3 Gravity and Magnetic Derivative Products

Filters may be applied to the data to enhance different wavelength information that arises from different sources. In many cases, filtering is best achieved by transforming the data from the space domain to the frequency domain by Fourier transform since frequency characteristics of the filter to be applied are more precisely defined in the frequency domain. The filtered derivatives created to assist with interpretation are described below.

4.3.1 Total Magnetic Intensity Reduced to Pole

Reduction to the pole (RTP) transforms anomalies as if they were at the north magnetic pole. The basic assumption is that magnetic anomalies arise from induced magnetization. This assumption may not always be true where significant magnetic remanence occurs. The method allows direct comparison of anomaly shapes from different magnetic latitudes, and if the assumptions hold true the anomaly will be symmetrically disposed about the causative body. Reduction to pole is essentially a phase shift filter applied in the frequency domain, and is described by (Baranov and Naudy, 1964):

$$F(k_x, k_y) = \frac{1}{[\sin I + i \cos I \cos(D - \theta)]^2}$$

where

- θ is the angle in the k_x k_y plane
- I is the local magnetic inclination
- D is the local magnetic declination

For ease of calculation, this transformation was performed through filtering in the frequency domain using a constant (average/central) inclination and declination, which was considered valid throughout the entire grid. The inclination used was 74.46°, and the corresponding declination used was -5.75° representing a station approximately at the centre of the survey. The total magnetic intensity reduced to the pole is shown in Figure 4.7 (principal survey area, grid cell size of 25 m) and Figure 4.8 (extended survey area, grid cell size of 250 m).

4.3.2 Vertical Derivatives of Total Magnetic Intensity and Bouguer Gravity

If k_x and k_y are the wave numbers of the potential field in the two dimensional frequency domain, the n^{th} vertical derivative of the potential field is easily derived in the Fourier domain by applying the following filter (Blakely, 1996):

$$F(k_x, k_y) = (-k)^n \quad \text{where } k = \sqrt{(k_x^2 + k_y^2)}$$

Vertical derivatives act as high-pass filters that enhance high frequency data and suppress low frequency data. The first vertical derivative ($n=1$) enhances the rapid changes in gravity or magnetic field at the edges of anomalies and is therefore useful for delimiting the extents of causative bodies. The second vertical derivative ($n=2$) enhances high frequency signal variations even more, such that textural variations in the character or the potential field (especially for magnetic data) can be used to delimit domains of a specific geophysical response.

First vertical derivative of the reduced to pole total magnetic intensity is shown in Figure 4.9 (principal survey area, grid cell size of 25 m) and Figure 4.10 (extended survey area, grid cell size of 250 m). The first vertical derivative of the Bouguer gravity with a terrain correction using a density of 2.67 g/cm³ is shown in Figure 4.11 (principal survey area, grid cell size of 25 m) and Figure 4.12 (extended survey area, grid cell size of 250 m). The first vertical derivative of the Free Air gravity is shown in Figure 4.13 (principal survey area, grid cell size of 25 m) and Figure 4.14 (extended survey area, grid cell size of 250 m). The second vertical derivative of the reduced to the pole total magnetic intensity is shown in Figure 4.15 (principal survey area, grid cell size of 25 m) and Figure 4.16 (extended survey area, grid cell size of 250 m). The gravity data does not contain high-frequency information to render its second vertical derivative useful for interpretation.

4.3.3 Total Horizontal Gradient of Total Magnetic Intensity and Bouguer Gravity

Horizontal gradients are most conveniently calculated in the space domain. Total horizontal gradient of a potential field “T” is from the gradients in the horizontal x and y plane as follows (Blakely, 1996):

$$\text{Total horizontal derivative} = \sqrt{(\partial T/\partial x)^2 + (\partial T/\partial y)^2}$$

Horizontal gradient grids are used primarily for edge detection of causative bodies (contacts, faults with large vertical displacement), and the data may also be employed for trend analysis and depth to source calculations.

Total horizontal derivatives of the reduced to pole total magnetic intensity, Bouguer gravity (2.67g/cm³ terrain correction) and Free Air gravity are shown for the principal survey area, grid cell size of 25m and for extended survey area, grid cell size of 250 m in Figures 4.17, 4.18, 4.19, 4.20, 4.21 and 4.22, respectively.

4.3.4 Total Gradient Amplitude of Total Magnetic Intensity

The total gradient amplitude, otherwise known as the 3D analytic signal amplitude, of a potential field (T) is defined as (Nabighian, 1972):

$$|A(x, y)| = \sqrt{(\partial T / \partial x)^2 + (\partial T / \partial y)^2 + (\partial T / \partial z)^2}$$

$|A(x, y)|$ is the amplitude of the analytic signal and T is the magnetic intensity at a point (x, y) . The horizontal derivatives are easily calculated in the space domain, whilst the vertical derivative ($\partial T / \partial z$) is calculated using space and frequency domains. Analytic signal is independent of field direction and direction of magnetization, and is independent of the type of magnetization (induced or remanent). This means that all similar bodies have similar analytic signal response, and that peaks in the analytic signal are symmetric and centred over the middle of narrow bodies and the edges of wide bodies. The amplitude however is affected by the strike of a body such that north-south oriented bodies at low latitudes are relatively weak for magnetic data. It highlights areas where the field varies quickly in any direction, such as for contacts, and high or low anomalies.

The total gradient amplitude of the total magnetic intensity is shown in Figure 4.23 (principal survey area, grid cell size of 25 m) and Figure 4.24 (extended survey area, grid cell size of 250 m).

4.3.5 Tilt Angle

The tilt angle can be applied to the pole reduced total magnetic intensity to preferentially enhance the weaker magnetic signals. This is particularly useful for mapping texture, structure, and edge contacts of weakly magnetic sources. The arctan operator restricts the tilt angle to within the range of -90° to $+90^\circ$, irrespective of the amplitude and wavelength of the field and enhances weak anomalies compared to the stronger anomalies. The tilt angle (θ) is defined as (Miller & Singh, 1994; Verduzco, 2004; and Salem et al. 2007):

$$\theta = \tan^{-1} \frac{\text{vertical component of gradient}}{\text{horizontal component of gradient}} = \tan^{-1} \left[\frac{\partial T / \partial z}{\sqrt{(\partial T / \partial x)^2 + (\partial T / \partial y)^2}} \right]$$

The vertical and horizontal gradients of the reduced to pole total magnetic intensity calculations are described above in subsections 4.3.2 and 4.3.3. The tilt angle grid for the reduced to pole total magnetic intensity is displayed in Figure 4.25 (principal survey area, grid cell size of 25 m) and Figure 4.26 (extended survey area, grid cell size of 250 m).

4.3.6 Trend Analysis Method

Depth trend, as implemented by Phillips (1997), can be utilized for the depth estimation using the horizontal gradient grid (HG). It uses the horizontal gradient of the reduced to pole total magnetic intensity and gravity grids to estimate strikes of and depths to thick and thin edges, respectively (Phillips, 2000). The method relies on the general principle that shallow sources produce anomalies with steep gradients, whereas deep sources produce anomalies with broad gradients. Depth estimates from the RTP magnetic and gravity data estimate the minimum and maximum depths to the top edge of the layer, respectively (Phillips, 2000).

The program uses a 5 by 5 window to both locate the crests of maxima and determine their strike direction. Once a crest is located and the strike direction is known, data within the window and within a belt perpendicular to the strike can be used to determine the depth of the contact by performing a

least squares fit to the theoretical shape of the HG over a contact. If " h " is the horizontal distance to the contact, " d " is the depth to the top of the contact and " K " is a constant, then the theoretical curve is given by (Roest and Pilkington, 1993):

$$HG(h) = K/(h^2 + d^2)$$

The least-squares fit gives an estimate of both the depth and its standard error, which can be expressed as a percentage of the depth. Typically only depth estimates with standard errors of 15% or better are retained in the final interpretation.

Due to the assumption of thick sources, the depth estimates obtained using the above procedure represent minimum depths. It is also possible to assume very thin sources and use a standard "pseudogravity" transformation instead of reduction to the pole (Roest and Pilkington, 1993). In this case, the same analysis could be done on the HG of the pseudogravity field, and the depth estimates represent maximum depths. Figures 4.27 and 4.28 show the depth results from the trend analysis solutions for the Bouguer gravity and the reduced to pole total magnetic intensity.

5 Geophysical Interpretation

The geophysical interpretation of the acquired gravity and magnetic data in the Schreiber area involved qualitative analysis of the various products derived from the magnetic and gravity grids (described in Section 4) and 2.5D forward modelling of gravitational and magnetic data along four profile lines that cover the principle features of the Crossman Lake batholith within the survey area.

5.1 Results of Qualitative Analysis

Qualitative analysis of the gravity derivative products was used to provide general indications about the location and dip of the batholith edges; the variation in depth across the batholith; the internal variation in density within the batholith; and the presence of major or deep seated structures. Qualitative analysis of the magnetic derivative products was used to: identify the presence of potential features within the batholith, such as faults and dykes (documented in SRK, 2015); and evaluate variation in the magnetic character of the batholith that may indicate changing composition of the rock or other potential heterogeneities.

For the qualitative geophysical interpretation, the Bouguer gravity (Figure 5.1) and its horizontal derivative (Figure 5.2), as well as the RTP of the magnetic intensity (Figure 5.3) and its first vertical derivative (Figure 5.4), were useful. In addition, the total gradient amplitude was particularly useful for interpretation of magnetic data (Figure 4.23 and 4.24) because: (a) it has a maxima over vertical magnetic contacts; (b) this is true regardless of the direction of magnetization; and (c) the reduced to pole magnetic intensity requires the assumption of only induced magnetization with the result that anomalies from remanently and anisotropically magnetized bodies can be severely distorted. Unlike the RTP, the total gradient amplitude will produce maxima over the edges of vertical magnetic contacts regardless of the presence of remanent magnetism (MacLeod, 1993). The horizontal derivative of the Bouguer gravity (Figure 5.2) produces highs directly over major density contrasts, and is a good way of identifying near vertical fault structures.

The following observations were made about the Crossman Lake batholith within the Schreiber survey area:

5.1.1 *Crossman Lake Batholith*

- There are two distinct gravity lows associated with the western and eastern ends of the batholith (Figure 5.1, areas A1 and A2) which imply that these are areas where the batholith extends to its greatest depth. Both areas are associated with smooth low amplitude magnetic anomalies. From the first vertical derivative of the Bouguer gravity, area A2, though smaller has less internal density variations. Area A1 has more prominent internal density variations, more so to the south western section.
- A linear high in the horizontal derivative of the Bouguer gravity (Figure 5.2, feature F6) clearly matches the mapped edge of the northern greenstone unit adjacent to the Crossman Lake batholith, with some minor discrepancies, for example along the western edge of this greenstone unit, where the high lies somewhat to the east of the mapped boundary – this suggests that the Crossman Lake batholith may extend under the greenstone belt units here. The linear high is well traced by the Bouguer gravity trend analysis solutions. This supports the proposition of the greenstones overlie the granites at this location.
- There is a very gradual increase in the gravity anomaly to the north of the Crossman Lake batholith at its boundary with the metasedimentary rocks, and no strong features in the horizontal derivative of the Bouguer gravity. This implies that the density contrast between the Crossman Lake batholith and the metasedimentary rocks is relatively small. The magnetic boundary is north of mapped contact suggesting the granites may also underlie the non-magnetic metasediments.
- The southern edges of the mapped Crossman Lake batholith are generally closely aligned with linear highs in the horizontal derivative of the Bouguer gravity. The somewhat broader peak in the horizontal derivative of the Bouguer gravity in the centre-south (Figure 5.2, feature F9) suggests that the greenstone may slope under the batholith here rather than there being a purely vertical contact. The smooth transition could also indicate a transition to more gneissic country rocks.
- Within the western section of the Crossman Lake batholith there are three north-south-running peaks in the horizontal derivative of the Bouguer gravity, as well as an east-west running peak (Figure 5.2, features F1, F4, F5). These could represent faults or contacts. The north-south direction of these potential faults is consistent with a mapped fault in the Crossman Lake batholith to the west of the survey area. It is worth noting that the trend of these structures would parallel lineaments from magnetic data (running north – south), particularly for feature F1 and F4 supporting the presence of a fault. Many gravity trend analysis solutions line up with the most prominent of these features.
- In the eastern part of the survey area there exist mapped faults with a NNW to NW orientation which are consistent with the orientation of linear features in the horizontal derivative of the Bouguer gravity. On the other hand, all the other major mapped faults have an obvious magnetic response either as magnetic low lineaments or anomaly disruption.
- The unit of mafic to ultramafic rock on the eastern edge of the Crossman Lake batholith is clearly identified with peaks in the horizontal derivative of the Bouguer gravity (Figure 5.2, feature F14), although the location of these peaks imply that the western edge of this unit occurs to the west of where it has been mapped. This may alternatively suggest that the mafic-to-ultramafic rock dips underneath the batholith here.

- To the south of the western section of the Crossman Lake batholith, the gravity anomaly steadily rises implying that the Crossman Lake batholith is becoming progressively shallower as it comes into contact with the Whitesand Lake batholith. This area of the Crossman Lake batholith also shows a highly complex magnetic response. A northeasterly running linear peak in the horizontal derivative of the Bouguer gravity (Figure 5.2, feature F2) suggests that there may be an abrupt change in depth of the batholith along this line.
- A band of high magnetic variability in the vertical derivative data curves around the mapped northwestern section of the Crossman Lake batholith (Figures 5.3 and 5.4, area A4). Although regional bedrock geology maps identify this area as a continuation of the batholith, the magnetic results indicate this area comprises significant lithological heterogeneity that may indicate an extension of the metasedimentary and metavolcanic rocks from the adjacent greenstone belt from the east. Despite this unmapped unit being identified in the magnetic data, the rock density contrast of the unit compared to the Crossman Lake batholith does not appear to be sufficient to produce a response in the gravity data. It is also possible that the northern and southern section of this anomaly represent an alteration zone on the edges of the batholith or different phases of intrusion.
- In the area A3, Figures 5.3 and 5.4, the magnetic data exhibits a circular area with a uniform and weak response. This pattern in the magnetic data may correspond to a separate and distinct phase within the Crossman Lake batholith.
- Since the batholith is likely to be quite deep in this section (as indicated by the 2.5D gravity models, discussed in Section 5.2), these magnetic features are likely to be associated with the batholith itself rather than any underlying greenstone. Assuming the surface bedrock mapping is accurate here, it could be assumed that a slightly different phase of granodiorite is present with different magnetite content.
- The remainder of the Crossman Lake batholith shows a complex pattern of low magnetic signal interspersed with linear features (both high and low) associated with dykes and faults, a number of which have not been previously mapped. A detailed lineament interpretation of potential dykes and faults in the Schreiber area are presented in SRK (2015).
- In addition, there are a few local north-south running magnetic highs in the centre of the eastern section of the Crossman Lake batholith (Figures 5.3 and 5.4, areas A5 and A6). These highs run directly adjacent to a north-south running fault, and could indicate: (a) slivers of greenstone beneath the surface; or (b) isolated units of granodiorite with higher magnetite content. These features are similar to those discussed above in the west of the Crossman Lake batholith, and it is likely that the same process could be responsible for them.

5.2 Preliminary 2.5D Modelling

The purpose of the 2.5D modelling is to develop an idea of the relatively deep and relatively shallow parts of the batholith and rough approximation of the depth to the bottom of different parts of the batholiths. The preliminary 2.5D modelling used the gravity, magnetic and terrain data sets, accompanied with constraints from the qualitative interpretation of the geophysical data and the mapped bedrock geology to provide a preliminary image of the subsurface along the four profile lines shown on Figures 5.5 and 5.6.

For the purpose of this initial modelling attempt, density and magnetic susceptibility values were

assumed for the bedrock units mapped on the surface and to the bedrock units at depth based on readily available information (Figure 1.1). In the Schreiber area, several surface bedrock density and magnetic susceptibility values have been compiled from available literature (data sources discussed in Section 3) and incorporated as constraints into the models. These assumed density and magnetic susceptibility values should be considered as approximate values as site-specific information on the bedrock at depth is not available (i.e. data from borehole drilling).

In order to assess the influence of assumed bedrock characteristics on the modelled geometry and depth of the batholiths, a series of alternative models were also considered by varying the assumed physical bedrock properties, in particular the bedrock density, for the bedrock units at depth. As we have an idea of the range of likely density values, the resulting 2.5D models can give an idea of the upper and lower bounds on the depth of the batholith.

It is important to emphasize that the accuracy of these preliminary models is limited at this early stage of the assessment due to limited availability of measured bedrock densities and magnetic susceptibilities that are key for constraining the model. It is anticipated that the preliminary 2.5D models would be revised and refined if more field data is collected in the future.

5.2.1 Model Descriptions

The preliminary 2.5D forward modelling of gravity and magnetic data was carried out using GMSYS Software (copyright Northwest Geophysical Associates Inc) running under Geosoft Oasis Montaj (Geosoft, 2012). The modelling considered four profile lines. The locations of the profile lines are shown in Figure 5.5 superimposed on the reduced to pole magnetic field, and in Figure 5.6 superimposed on the free air gravity. The start and end points of the co-ordinates listed in Table 5.1.

Table 5.1: Coordinates of 2.5D Model Profiles (UTM 16N, NAD83)

Profile Line	Start		End	
	UTM X	UTM Y	UTM X	UTM Y
1	458830	5426800	477140	5426800
2	496640	5421800	496640	5421800
3	466250	5436200	466250	5413000
4	485220	5411510	485220	5431100

The process for constructing the models was as follows:

- Lines were chosen to reflect the features of most interest in the block. The profile lines were also chosen to run directly along survey lines and to include the extensions that continue outside the main area of the block.
- The profiles were modelled from the free air gravity and the reduced to pole total magnetic intensity data. The choice of free air gravity, rather than Bouguer gravity allowed terrain effects of variable density to be included in the model, which are taken into account by including the topography in the profile.
- Generally speaking, the gravity was modelled first to determine the broad large scale features, and the magnetic data were used to refine the model and include features such as faults, dykes, and to help model the overall shape of smaller rock units.

- Densities of greenstone belt units, batholiths and other units were assumed to be uniform throughout. This assumption was only otherwise violated if it was impossible to model the gravity using uniform densities. This can be restated by saying that gravity anomalies were generally accounted for by varying the shapes of the rock units after initial density assumptions were made, rather than by varying the densities within the rock units. Depth trend solutions of the Bouguer gravity were used for determining locations and dips of faults/contacts.
- The available mapped surface geology was used to determine the location of the points at which geological boundaries occurred at the surface of the models. This information was obtained from the publicly available bedrock geology maps (MRD126-Rev1; OGS, 2011) that include shape files of the mapped bedrock units.
- Density information was determined by compiling available PETROCH density measurements in each of the mapped units. The PETROCH database is an Ontario Geological Survey (OGS) lithochemical database of rocks in Ontario which includes specific gravity. These values were then averaged, and a uniform rock density of the averaged value was used for the rock unit in question. Where Petroch rock data were not available for a given unit, a typical density for the rock type was used.
- In determining the magnetic susceptibilities for modelling the magnetic data, initial values of susceptibility were chosen that were: (a) best able to match the amplitude of the magnetic variations that were obviously associated with terrain; and (b) best able to reproduce the overall long wavelength trend associated with the larger rock units. This approach was employed due to the uncertainties of the susceptibilities, since only a limited number of readings were available and none near the location of the profiles and generic susceptibility values for given rock types can vary over several orders of magnitude over short distances.
- In seeking to model magnetic variations within individual rock units, vertical boundaries were generally used in the absence of other indications. Indicators that were used included the presence of foliation orientations identified on bedrock geology maps, and faults and dykes as determined by the presence of linear features in the magnetic derivative grids. Trend analysis solutions for the reduced to pole magnetic field were also used as a guide in setting the dip of magnetic contacts. Trend analysis solutions are shown in the 2.5D model figures as x and + symbols on the profile lines for gravity and magnetic data, respectively. The solutions shown are those which occur within a 0.5 km wide band centered along the model line. The shallow trend analysis solutions were only used for to estimate the location of the top of modelled faults.
- The overburden has not been included in the modelling. It is deemed to be sufficiently shallow that its effect on the gravity and magnetic anomalies will be negligibly small for modelling purposes.
- Where the 2.5D model lines intersect, the geological boundaries, densities, and magnetic susceptibilities have been made to coincide at the model intersection points.

Table 5.2: Densities and magnetic susceptibilities used in the 2.5D models

Layer	Density (g/cm³)	Magnetic Susceptibility (S. I.)
<i>Crossman Lake batholith</i>	2.61	0.0120-0.0394
<i>Greenstone</i>	2.95	0.0123-0.0580
<i>Metasedimentary rock</i>	2.77	0.0139-0.0226
<i>Mafic to ultramafic rock</i>	2.95	0.0200-0.0280
<i>Dykes</i>	2.75	0.0200-0.390
<i>Mafic intrusive rock</i>	2.77	0.0350
<i>Gneissic rock</i>	2.68	0

5.2.2 Model Results

The 2.5D modeling results for the Schreiber area are shown on Figures 5.7 to 5.16. The figures show a plan view along the profile line (e.g. top panel Figure 5.7) in order to show the distribution of bedrock rock units that are included in the model calculations that are perpendicular to the strike of the profile line. The gravity view (e.g. second panel Figure 5.7) shows the observed gravity data along the profile line, as well as the calculated gravity data, and the RMS error (i.e. root mean square error). The RMS error is used as a measure of the difference between the observed gravity data and the modelled gravity results. The next gravity view (e.g. third panel Figure 5.7) shows the assignment of the rock density values to each of the bedrock units in the model. The magnetic view (e.g. fourth panel Figure 5.7) shows the observed and calculated magnetic data, as well as the RMS error between the two data sets. The next magnetic view (e.g. fifth panel Figure 5.7) shows the assignment of the magnetic susceptibility values to each of the bedrock units in the model. The structural view provides the overall interpretation of the modelled results, which are coloured based on geological unit (e.g. sixth panel on Figure 5.7). Each of these model views shows the depth on the y-axis in kilometers depth below mean sea level (MSL).

Several alternative models are presented to assess the influence of changing the bedrock density, and its impact on the geometry and thickness of the batholith units. These alternative models show only a subset of the panel views discussed above (e.g. Figure 5.9).

5.2.1.1 Results for Profile Line 1

Initial Model 1.5 (Figure 5.7)

As shown in Figure 5.5, Line 1 runs east-west across the northern part of the Crossman Lake batholith, and the greenstone unit to its east. The orientation of the line is almost perpendicular to the batholith-greenstone boundary, and runs through the centre of the broad oval area of quiet magnetic responses at the centre of the batholith.

- The Crossman Lake batholith can be divided into three distinct sections along the model line. To the west is a very shallow section of the batholith with a flat bottom with a depth of approximately 1.0 km. This section extends from the metasedimentary block west of the batholith for just over 4 km and concludes with a potential fault where there is a sudden increase in depth to approximately 3.8 km. Based on the large low gravity response in this

section of the profile line (distance of 4 km), intuitively, the depth of the batholith is expected to be deeper. However, the use of the free air gravity data in the 2.5D modelling show the influence of terrain effects along the profile line. These terrain effects are taken into account by including the topography in the model.

- The high magnetic anomaly extending around the northwestern part of the batholith, as seen in the reduced to pole magnetic anomaly grids, are accounted for in the magnetic model by incorporating a shallow section of the batholith having higher magnetic susceptibility.
- The deeper section of the mapped batholith has a depth of roughly 3.8 km which gradually shallows to 3.4 km to the east, at which point the batholith continues under the overlying greenstone belt units. Initially, the overlying greenstone belt is rather shallow (approximately 400 m), until the point at which a fault occurs and the batholith dips deeper under the greenstone. The batholith continues to deepen towards the eastern end of the model line where there is another significant fault.
- A very broad and low magnetic anomaly occurs in the centre of the Crossman Lake batholith. This has been modelled as an approximately 2 km wide band of uniform and low magnetic susceptibility, and appears to represent a fairly homogenous section of the batholith with little magnetic variability.
- The greenstone overlying the Crossman Lake batholith has been modelled as having a constant density, and as such the gravity anomaly here has been deemed to be indicative of the geometry of the Crossman Lake batholith that underlies it. The presence of alternating large positive and negative magnetic anomalies which flatten at the top and bottom suggest the presence of alternating units within the greenstone belt with different magnetic properties.

Alternative Model 1.6

This model interpretation (Figure 5.8) takes an alternative approach for modelling the western section of the Crossman Lake batholith along the model line, by incorporating two units of higher rock density and higher magnetic susceptibility within the batholith based on the qualitative interpretation of the magnetic data (Figures 5.3 and 5.4; area A4). The alternative approach indicates that the portions of the western part of the batholith may be deeper than predicted in the previous modelling results. However, overall the depth in the central portion of the batholith is roughly consistent with the previous model values, ranging from approximately 2.5 to 4.0 km.

The two units of higher rock density and higher magnetic susceptibility are interpreted as the potential extension of the greenstone belt units further to the east, which may underlie a thinner portion of the batholith. The top of these units are modelled with a depth of approximately 1.0 km.

Alternative Model 1.5

In this model (Figure 5.9), results from Figure 5.7 are modified in order to incorporate a gneissic basement with a density of 2.680 g/cm³. This new basement density is 0.27 g/cm³ lower compared to the density values used in the model shown in Figure 5.7, which was underlain by a greenstone belt unit (2.95 g/cm³). This basement density is now only marginally greater than that of the batholith (2.61 g/cm³), whereby the resulting model becomes less sensitive to the depth of the boundary. These model results indicate an overall increase in the thickness of the batholith, with depth estimates now

ranging from approximately 2.5 km in the west and up to 5.5 km in the central portion of the profile line (Figure 5.9).

Alternative models have been created for the other three 2.5D profile lines in the Schreiber area with the introduction of the same gneissic basement. Where each of the model lines intersects each other, the depths of the geological units, their densities, and magnetic susceptibilities have been made consistent.

5.2.1.2 Results of Profile Line 2

Initial Model 2.2

As shown in Figure 5.5, Line 2 runs east-west across the length of the Crossman Lake batholith. Near the central portion of the line the model run adjacent to the greenstone belt units approximately 1 km to the north. Although these units are not including along the line, their influence on the results is incorporated by 2.5D modeling (Figure 5.10).

- The western part of the Crossman Lake batholith shows a depth range between approximately 2.5 km to 4.0 km. The deepest portion of the batholith is midway along the model line, which is interpreted to be bounded by two large faults. The fault located at approximately 17 km along the profile line has a near vertical dip, and the dip angle of the fault at approximately 25 km is slopes rough 85° towards to the east. These fault dips are also characterized by several trend analysis solutions of the Bouguer gravity. Both of these faults are modelled with interpreted vertical offset of approximately 600 m and 2.0 km. The modelled depth of the batholith shows an increase towards the east from 3.2 km to 5.0 km.
- A significant and very sharp positive magnetic anomaly occurs in the eastern portion of the modeled line. This has been modelled as a section of higher magnetic susceptibility with a near vertical dip, possibly representing a dyke.
- Within the eastern part of the batholith there is a roughly 9 km long section that is characterized by a relatively uniform depth of approximately 2.0 km. Based on the magnetic data, a number of potential dykes have been modelled within this section of the batholith.
- Along the easternmost part of the model line, the batholith is interpreted to extend underneath an area of mapped greenstone belt. Interpreted faults in this area dip steeply in an easterly direction indicated by the occurrence of trend analysis solutions at depth using the magnetic data.

Alternative Model 2.1.2

This model (Figure 5.11) shows an alternative interpretation of the possible geometry of the Crossman Lake batholith that is consistent with the gravity data. The model differs from model 2.2.2 in two main ways:

- The bottom of the western half of the Crossman Lake batholith comprises a broad downward bulge that dips gently, rather than the more irregularly shaped bottom of model 2.2.2. The peak depth of the batholith in this section is approximately 3.0 km.
- The deep central section of the Crossman Lake batholith with the depth offset attributed to faulting has the same form as model 2.2.2, except that the batholith here is interpreted to be shallower, having a maximum depth of approximately 3.0 km.

Alternative Model 2.1.2

An alternative model for Line 2, Model 2.1.2 (Figure 5.12), assumes the batholith and greenstone belt units are underlain by gneissic basement rocks with a density of 2.68 g/cm³ in a manner similar to an alternate model for Line 1. This model results indicate an overall increase in the thickness of the batholith, with the thickest portion of the batholith (approximately 5.0 km) located at the western end of the profile line (Figure 5.12).

5.2.1.3 Results of Profile Line 3

Initial Model 3.4 (Figure 5.13)

As shown in Figure 5.5, Line 3 runs north-south across the centre of the western part of the Crossman Lake batholith, and extends into the metasedimentary rocks of the Quetico Subprovince.

- At the boundary of the Crossman Lake batholith and the metasedimentary rock, the batholith has a depth of approximately 7.0 km. For the next 5.5 km along the model line, the depth of the batholith diminishes to approximately 1.5 km – the shallowest point in the batholith along the model line. Intuitively, the depth of the batholith is expected to be the deepest where the gravity profile shows the lowest response (e.g. distance of 8 km). However, terrain effects, such as topography, are taken into account in the 2.5D models. As a result, the deepest portion of the batholith does not necessarily overlap with the lowest gravity response.
- To the south of this shallow point, the batholith bulges downwards to a depth of approximately 8.0 km. This section of the batholith may represent an individual phase of the batholith with a width of approximately 5.5 km.
- To the south of this feature, the base of the batholith gently ascends from a depth of 4.0 km to a depth of 3.0 km. At this point a significant fault is modeled to include a vertical offset of approximately 2.0 km. The batholith located at approximately 18 km along the profile line is roughly 5.0 km deep. Another fault is interpreted to mark the southern extent of this feature.
- This feature could plausibly have been modelled as a rounded granitic phase similar to that in the north, but the presence of the mapped faults suggested the likelihood of a faulting-induced offset.
- There is no clear division between the Crossman Lake and Whitesand Lake batholiths and they appear to be part of the same overall unit. Convention seems to indicate that the depth offset section of the batholith just discussed would be considered as being the northernmost extent of the Whitesand Lake batholith.
- The southernmost part of the modeled line shows the batholith has a flat bottom with a consistent depth of approximately 2.0 km.
- The magnetic susceptibility is fairly consistent throughout the batholith, the exception being in the far south where there are blocks of high magnetic susceptibility either side of the large fault.

Alternative Model 3.4 (Figure 5.14)

An alternative model for line 3, Model 3.4, assumes the batholith is underlain by a gneissic basement with a density of 2.68 g/cm³. Overall, the model results do not show significant change to the thickness

of the batholith units. The deepest portion of the batholith in Figure 5.13 shows a similar depth in the alternative model of approximately 7.0 km by incorporating the density of the gneissic basement.

5.2.1.4 Results of Profile Line 4

Initial Model 4.4.3.2 (Figure 5.15)

As shown in Figure 5.5, Line 4 runs north-south across the eastern arm of the Crossman Lake batholith, and the greenstone to its north.

- The northern most portion of the Crossman Lake batholith in profile Line 4 was modelled to extend under the greenstone belt unit, extending an additional 3 km northwards beyond its mapped surface extent and to a maximum depth of approximately 4.5 km. The shallowest point of the batholith has a depth of approximately 2.0 km
- The profile line crosses through a small fragment of greenstone belt, which has been modelled as having the Crossman Lake batholith extending underneath. The bottom of the batholith becomes gradually shallower to the south, ascending to a depth of approximately 2.0 km. Near the beginning of the profile line, the depth of the bottom of the batholith may shallow more quickly to a depth of approximately 400 m, where the batholith terminates.
- Based on the magnetic data the central portion of the batholith To the north of the greenstone fragment, there are a series of four dykes that have been incorporated into the model within the batholith. Two interpreted faults are also incorporated into the model based on the magnetic data.
- The magnetic susceptibility of the batholith is generally uniform, with the exception of an increased magnetic susceptibility in the southern section of the batholith, and two bands of higher susceptibility in the north. The dip of these bands follow the trend analysis solutions of the reduced to pole magnetic data. It is assumed that these bands represent regions of the batholith with higher magnetite content.
- The greenstone to the north of the batholith displays several large magnetic anomalies indicative of alternating units of metavolcanic rocks.

Alternative Model 3.4 Gneiss Basement (Figure 5.16)

An alternative model for Line 4, Model 3.4, assumes the batholith is underlain by a gneissic basement with a density of 2.68 g/cm³. Overall, the model results shown in Figure 5.16 display a similar depth to the base of the batholith and geometry as shown in Figure 5.15, despite the batholith and greenstone units now being underlain by the gneissic basement. The deepest portion of the batholith in Figure 5.15 remains at approximately 3.5 km at its northern end, which is interpreted to extend below the greenstone unit. The central portion of the batholith has a depth of approximately 3.0 km.

6 Summary of Results

The Schreiber survey area includes the western and eastern extent of the Crossman Lake batholith, and a small portion of the northernmost part of the Whitesand Lake batholith. The area of the Crossman Lake batholith encompassed by the survey contains mapped and interpreted numerous dykes and faults. Displacement along the faults has resulted in offsets within the batholith. The main results of the modelling and interpretation of these batholiths are as follows:

Eastern Part of the Crossman Lake Batholith

- The Crossman Lake batholith in the survey area shows a pattern of low magnetic signal interspersed with linear features (both high and low) associated with dykes and faults, a number of which have not been previously mapped. In addition, there are a few local north-south running magnetic highs in the eastern section of the Crossman Lake batholith. These highs run directly adjacent to a north-south running fault, and could indicate: (a) slivers of greenstone beneath the surface, or (b) isolated units of granodiorite with higher magnetite content.
- The horizontal gradient of the Bouguer gravity gives a good indication of the dip and location of the boundaries of the Crossman Lake batholith. The boundary with the greenstone to the north concurs with the location of linear highs in the horizontal gradient, and the slightly asymmetric nature of the peaks suggests that the batholith likely dips beneath the greenstone to the north.
- Towards the south, the gravity data imply that the greenstone dips slightly to the north underneath the batholith. It is possible that the southern fragment of the batholith may connect up with the main body of the batholith underneath the greenstone, although it is also possible to build models in which this does not occur.
- The unit of mafic to ultramafic rock on the eastern edge of the Crossman Lake batholith within the survey block is clearly identified with peaks in the horizontal derivative of the Bouguer gravity, although the location of the peaks imply that the western edge of this mafic to ultramafic unit occurs to the west of where it has been mapped. Alternatively this suggests that the mafic-to-ultramafic rock may dip significantly underneath the batholith in this area.
- Four major mapped faults run across the eastern area of the Crossman Lake batholith with orientations from south to east-southeast. These faults are associated with lows in the horizontal gradient of the Bouguer gravity. The gravity data suggests that these faults could be associated with depth offsets in the batholith. The most significant of these has been modelled as occurring between the southerly and southeasterly oriented faults in the centre of the eastern section of the batholith.
- The 2.5D modelling suggests that the eastern part of the Crossman Lake batholith has depths of at least 2 km throughout.

Western Part of the Crossman Lake Batholith

- The coverage of the western survey area of the Crossman Lake batholith includes a large part of the Crossman Lake batholith, as well as a small area of metasedimentary rock in the north, and the intersection with the greenstone belt in the east, were also covered by the survey.
- A band of high magnetic variability in the vertical derivative data curves around the mapped northwestern section of the Crossman Lake batholith. Although regional bedrock geology

maps identify this area as a continuation of the batholith, the magnetic results indicate this area comprises significant lithological heterogeneity that may indicate an extension of the metasedimentary and metavolcanic rocks from the adjacent greenstone belt from the east. Despite this unmapped unit being identified in the magnetic data, the rock density contrast of the unit compared to the Crossman Lake batholith does not appear to be sufficient to produce a response in the gravity data. As such, it is also possible that this anomaly represents an alteration zone on the edges of the batholiths, or different phases of intrusion.

- In the central portion of the survey area, the magnetic data exhibits a circular area with a uniform quiet and weak response. This pattern in the magnetic data may correspond to a separate and distinct phase within the Crossman Lake batholith. In this area, one linear magnetic low is evident that is potentially associated with a dyke.
- A linear high in the horizontal derivative of the Bouguer gravity occurs on the eastern edge of the batholith at the boundary with the greenstone, although this high lies somewhat to the east of the mapped boundary, suggesting that the batholith undercuts the greenstone here.
- To the south of the western section of the Crossman Lake batholith, the gravity anomaly steadily rises implying that the Crossman Lake batholith is becoming progressively shallower as it comes into contact with the Whitesand Lake batholith. A north-easterly running linear peak in the horizontal derivative of the Bouguer gravity suggests that there may be an abrupt change in depth of the batholith along this line.
- The area of the mapped batholith coincides clearly with a broad and deep low in the Bouguer gravity. The gravity anomaly is shallower in the northwest and south of the area of the batholith area surveyed. The modelling indicates that the batholith is particularly deep in the centre and east of the western part of the Crossman Lake batholith, with maximum depths reaching approximately 7 km, or more. However, the area of the batholith close to the metasedimentary rock appears to be significantly shallower and modelled as having depths of around 1.6 km. The batholith is modelled as deepening towards its northern boundary with the metasedimentary rock. Alternative modelling approach based on the assumption of the gneissic basement bedrock resulted in an overall increase in the depth to the base of the Crossman Lake batholith.

7 References

- AECOM Canada Ltd., 2013a. Phase 1 Geoscientific Desktop Preliminary Assessment of Potential Suitability for Siting a Deep Geological Repository for Canada's Used Nuclear Fuel, Township of Schreiber, Ontario. Prepared for Nuclear Waste Management Organization (NWMO). NWMO Report Number: APM-REP-06144-0035.
- AECOM Canada Ltd., 2013b. Phase 1 Geoscientific Desktop Preliminary Assessment, Terrain and Remote Sensing Study, Township of Schreiber, Ontario. Prepared for Nuclear Waste Management Organization (NWMO). NWMO Report Number: APM-REP-06144-0036.
- Baranov, V. and Naudy, H. 1964. Numerical Calculation of the Formula of Reduction to the Magnetic Pole. *Geophysics*, 29, pg. 67-79
- Blakely, R.J. 1996. *Potential Theory in Gravity and Magnetic Applications*. Cambridge University Press. pg 441
- Bostock, H.S. 1970. Physiographic Subdivisions of Canada. In *Geology and Economic Minerals of Canada*, Geological Survey of Canada, Economic Geology Report no. 1, p. 11-30.
- Briggs, I.C., 1974, Machine Contouring using Minimum Curvature, *Geophysics*, v. 39., no. 1, pp. 39-48.
- Buchan, K.L. and Ernst, R.E. 2004. Diabase Dyke Swarms and Related Units in Canada and Adjacent Regions. Geological Survey of Canada, Map 2022A, scale 1:5,000,000.
- Buchan, K.L., Halls, H.C. and Mortensen, J.K. 1996. Paleomagnetism, U-Pb Geochronology, and Geochemistry of Marathon Dykes, Superior Province, and Comparison with the Fort Frances Swarm. *Canadian Journal of Earth Sciences*, v. 33, p. 1583-1595.
- Carter, M.W. 1988. *Geology of Schreiber-Terrace Bay Area, District of Thunder Bay*. Ontario Geological Survey, Open File Report 5692, p. 287.
- Geofirma (Geofirma Engineering Ltd.), 2015. Phase 2 Geoscientific Preliminary Assessment, Findings from Initial Field Studies, Township of Schreiber, Ontario. Prepared for the Nuclear Waste Management Organization (NWMO), NWMO Report Number: APM-REP-06145-0005.
- Geosoft, 2012. Oasis Montaj Geophysical Processing System, v 7.5, Geosoft Inc.
- Golder Associates. 2011. Initial Screening for Siting a Deep Geological Repository for Canada's Used Nuclear Fuel, Township of Schreiber, Ontario; Nuclear Waste Management Organization, Report 10-1152-0110 (5000).
- Hamilton, M.A., David, D.W., Buchan, K.L. and Halls H.C. 2002. Precise U-Pb Dating of Reversely Magnetized Marathon Diabase Dykes and Implications for Emplacement of Giant Dyke Swarms along the Southern Margin of the Superior Province, Ontario. Geological Survey of Canada, Current Research 2002-F6, p. 10.
- Haus, M. and Pauk, T., 2010, Data from the PETROCH Litho-geochemical database, Ontario Geological Survey, Miscellaneous Release – Data 250, ISBN 978-1-4435-3732-2 [CD] ISBN 978-1-4435-3731-5 [zip file].
- Leliak, P. (1961). Identification and evaluation of magnetic field sources of magnetic airborne detector equipped aircraft. *IRE Transactions on Aerospace and Navigational Electronics*, 8(3), 95-105.

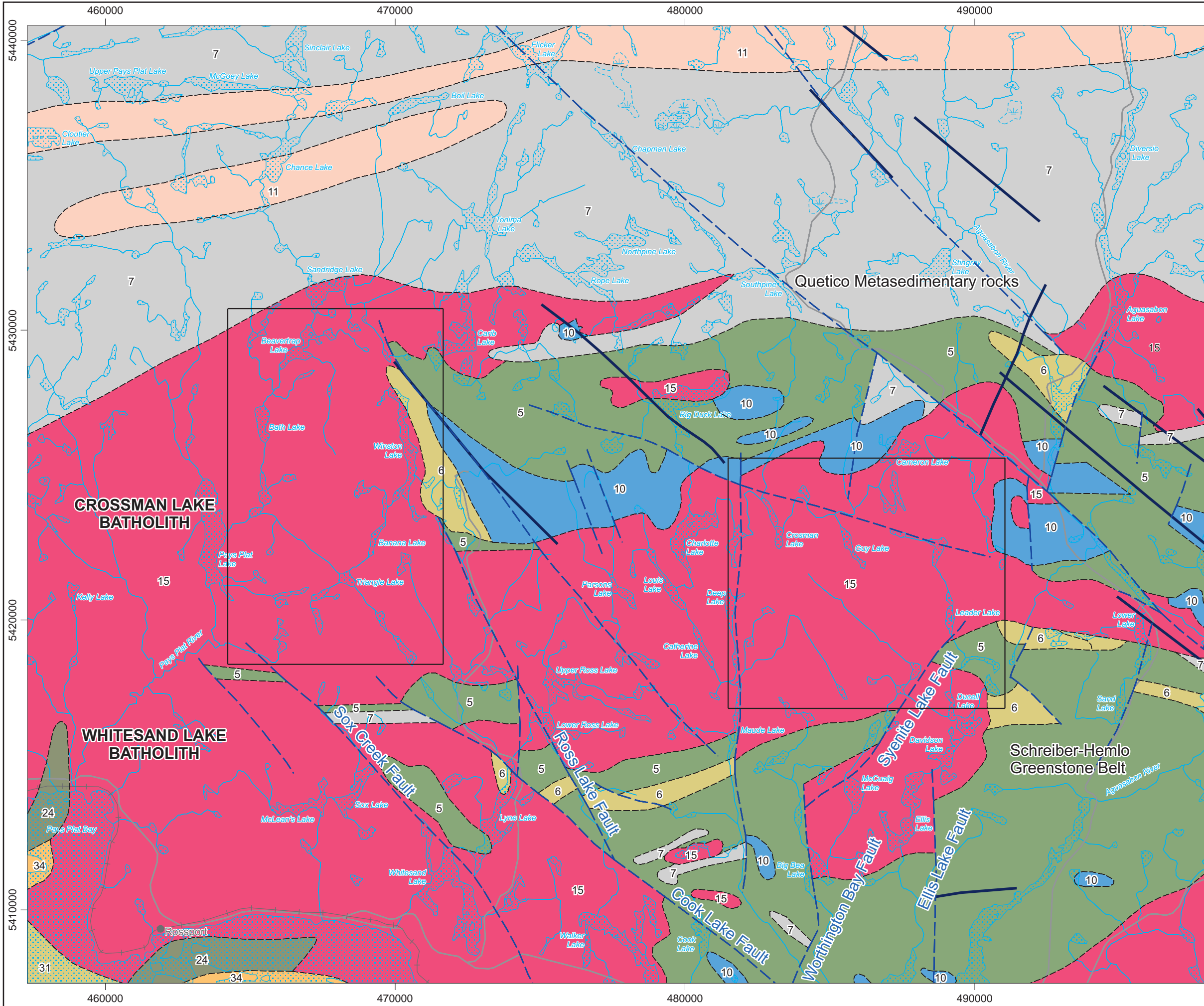
- equipped aircraft. IRE Transactions on Aerospace and Navigational Electronics, 8(3), 95-105.
- MacLeod, I.N., 1993, 3-D Analytic Signal in the Interpretation of Total Magnetic Field Data at Low Magnetic Latitudes, Exploration Geophysics, v. 24, pp. 679-688.
- Miller, H.G., and Singh, V., 1994, Potential Field Tilt – A New Concept for Location of Potential Field Sources, Journal of Applied Geophysics, v. 32, pp. 213-217.
- Muir, T. L., 2013, Ontario Precambrian Bedrock Magnetic Susceptibility Geodatabase for 2001 to 2012, Ontario Geological Survey, Miscellaneous Release – Data 273 – Revised.
- Nabighian, M.N. 1972. The analytic signal of two-dimensional magnetic bodies with polygonal cross-section: its properties and use for automated anomaly interpretation. Geophysics, 37, 507-517.
- NWMO, 2010. Moving Forward Together: Process for Selecting a Site for Canada's Deep Geological Repository for Used Nuclear Fuel, Nuclear Waste Management Organization. (Available at www.nwmo.ca)
- NWMO, 2013. Preliminary Assessment for Siting a Deep Geological Repository for Canada's Used Nuclear Fuel - Township of Schreiber, Ontario - Findings from Phase One Studies. NWMO Report Number APM-REP-06144-0033. (Available at www.nwmo.ca)
- OGS (Ontario Geological Survey), 2011. 1:250 000 Scale Bedrock Geology of Ontario, Ontario Geological Survey, Miscellaneous Release – Data 126 – Revision 1.
- Osmani, I.A. 1991. Proterozoic Mafic Dyke Swarms in the Superior Province of Ontario. In Geology of Ontario, Ontario Geological Survey, Special Volume 4, Part 1, p. 661-681.
- Phillips, J.D., 1997, Potential-Field Geophysical Software for the PC, Version 2.2, U.S. Geological Survey Open-File Report 97-725.
- Phillips, J.D., 2000, Locating Magnetic Contacts: A Comparison of the Horizontal Gradient, Analytic Signal, and Local Wavenumber Methods, Society of Exploration Geophysics, Expanded Abstracts with Biographies, 2000 Technical Program, v. 1, pp. 402-405.
- Roest, W., and Pilkington, M., 1993, Identifying Remanent Magnetization Effects in Magnetic Data, Geophysics, v. 58, no. 5, pp. 653-659.
- Salem, A., Williams, S., Fairhead, J. D., Ravat, D., and Smith, R., 2007, Tilt-Depth Method: A Simple Depth Estimation Method using First-order Magnetic Derivatives, The Leading Edge, 26, pp. 1502-1505.
- SRK (SRK Consulting Inc.), 2015. Phase 2 Geoscientific Preliminary Assessment, Lineament Interpretation, Township of Schreiber, Ontario. Prepared for Nuclear Waste Management Organization (NWMO). NWMO Report Number: APM-REP-06145-0007.
- Telford, W.M.; Geldart, L.P.; Sheriff, R.E. 1990. Applied Geophysics. 2nd edition. Cambridge university press. pg 770
- Thurston, P.C. 1991. Archean Geology of Ontario: Introduction. In Geology of Ontario, Ontario Geological Survey, Special Volume 4, Part 1, p. 3-25.
- Verduzco B., Fairhead J.D., Green C.M. and MacKenzie C., (2004), New Insights into Magnetic Derivatives for Structural Mapping, The Leading Edge, p. 116-119.
- Williams, H. R., G.M. Stott, K.B. Heather, T.L. Muir and R.P. Sage. 1991. Wawa Subprovince. In

Geology of Ontario, Ontario Geological Survey, Special Volume 4, Part 1, p. 485-525.

8 FIGURES

- 1.1 Survey Area
- 1.2 Flight Lines
- 3.1 Digital Elevation Model (25 m cell)
- 4.1 Bouguer Gravity (Density: 2.67g/cm^3) (25 m cell)
- 4.2 Bouguer Gravity (Density: 2.67g/cm^3) (250 m cell)
- 4.3 Free Air Gravity (25 m cell)
- 4.4 Free Air Gravity (250 m cell)
- 4.5 Total Magnetic Intensity (25 m cell)
- 4.6 Total Magnetic Intensity (250 m cell)
- 4.7 Reduction to the Pole of the Magnetic Field (25 m cell)
- 4.8 Reduction to the Pole of the Magnetic Field (250 m cell)
- 4.9 First Vertical Derivative of the Reduction to the Pole of the Total Magnetic Intensity (25 m cell)
- 4.10 First Vertical Derivative of the Reduction to the Pole of the Total Magnetic Intensity (250 m cell)
- 4.11 First Vertical Derivative of the Bouguer Gravity (Density: 2.67g/cm^3) (25 m cell)
- 4.12 First Vertical Derivative of the Bouguer Gravity (Density: 2.67g/cm^3) (250 m cell)
- 4.13 First Vertical Derivative of the Free Air Gravity (25 m cell)
- 4.14 First Vertical Derivative of the Free Air Gravity (250 m cell)
- 4.15 Second Vertical Derivative of the Reduction to the Pole of the Total Magnetic Intensity (25 m cell)
- 4.16 Second Vertical Derivative of the Reduction to the Pole of the Total Magnetic Intensity (250 m cell)
- 4.17 Total Horizontal Derivative of the Reduction to the Pole of the Total Magnetic Intensity (25 m cell)
- 4.18 Total Horizontal Derivative of the Reduction to the Pole of the Total Magnetic Intensity (250 m cell)
- 4.19 Total Horizontal Derivative of the Bouguer Gravity (Density: 2.67g/cm^3) (25 m cell)
- 4.20 Total Horizontal Derivative of the Bouguer Gravity (Density: 2.67g/cm^3) (250 m cell)
- 4.21 Total Horizontal Derivative of the Free Air Gravity (25 m cell)
- 4.22 Total Horizontal Derivative of the Free Air Gravity (250 m cell)
- 4.23 Analytic Signal of the Total Magnetic Intensity (25 m cell)
- 4.24 Analytic Signal of the Total Magnetic Intensity (250 m cell)
- 4.25 Tilt Angle of the Reduction to the Pole of the Total Magnetic Intensity (25 m cell)
- 4.26 Tilt Angle of the Reduction to the Pole of the Total Magnetic Intensity (250 m cell)

- 4.27 Trend Analysis Solutions of Bouguer Gravity (terrain correction density = 2.67 g/cc)
- 4.28 Trend Analysis Solutions of Reduction to the Pole of the Total Magnetic Intensity
- 5.1 Bouguer Gravity (terrain correction density = 2.67 g/cc) with Selected Interpreted Features and Trend Analysis Solutions
- 5.2 Horizontal Derivative of Bouguer Gravity (terrain correction density = 2.67 g/cc) with Selected Interpreted Features
- 5.3 Reduction to the Pole of the Total Magnetic Intensity with Interpreted Features
- 5.4 First Vertical Derivative of the Reduction to the Pole of the Total Magnetic Intensity with Selected Interpreted Features
- 5.5 Location of 2.5D Model Lines shown with Reduction to the Pole of the Total Magnetic Intensity
- 5.6 Location of 2.5D Model Lines shown with Free Air Gravity
- 5.7 Forward Modeling Results: Line 1, Model 1.5, Schreiber, Ontario
- 5.8 Forward Modeling Results: Line 1, Model 1.6, Schreiber, Ontario
- 5.9 Forward Modeling Results: Line 1, Alternative Model 1.5, Gneiss basement, Schreiber, Ontario
- 5.10 Forward Modeling Results: Line 2, Model 2.2, Schreiber, Ontario
- 5.11 Forward Modeling Results: Line 2, Model 2.1.2, Schreiber, Ontario
- 5.12 Forward Modeling Results: Line 2, Alternative Model 2.1.2, Gneiss Basement, Schreiber, Ontario
- 5.13 Forward Modeling Results: Line 3, Model 3.4, Schreiber, Ontario
- 5.14 Forward Modeling Results: Line 3, Alternative Model 3.4, Gneiss Basement, Schreiber, Ontario
- 5.15 Forward Modeling Results: Line 4, Model 4.4.3.2, Schreiber, Ontario
- 5.16 Forward Modeling Results: Line 4, Alternative Model 4.4.3.2, Gneiss Basement, Schreiber, Ontario



Legend

Hydrography

Road

Railway

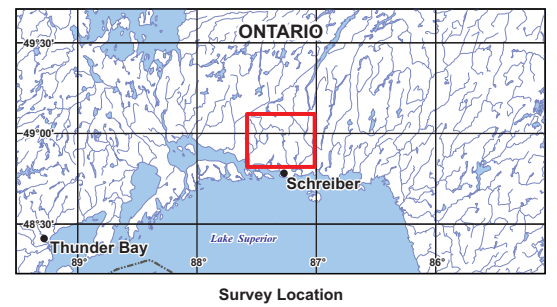
Geology

Fault

Dyke

- 5: Mafic to intermediate metavolcanic rocks
- 6: Felsic to intermediate metavolcanic rocks
- 7: Metasedimentary rocks
- 10: Mafic and ultramafic rocks
- 11: Gneissic tonalite suite
- 15: Massive granodiorite suite
- 24: Animikie Gp.
- 31: Sibley Gp.
- 32: Osler Gp., Mamaine Point Fm., Michipicoten Island Fm.
- 34: Mafic intrusive rocks (Keweenawan age)

Survey Area Boundary



BASE DATA: National Topographic Database - NRCAN
 GEOLOGY DATA: OGS Dataset MRD 126-Rev 1
 DATUM: NAD83
 PROJECTION: Universal Transverse Mercator (UTM Zone 16N)

N
E
S
W

Scale 1 : 130 000

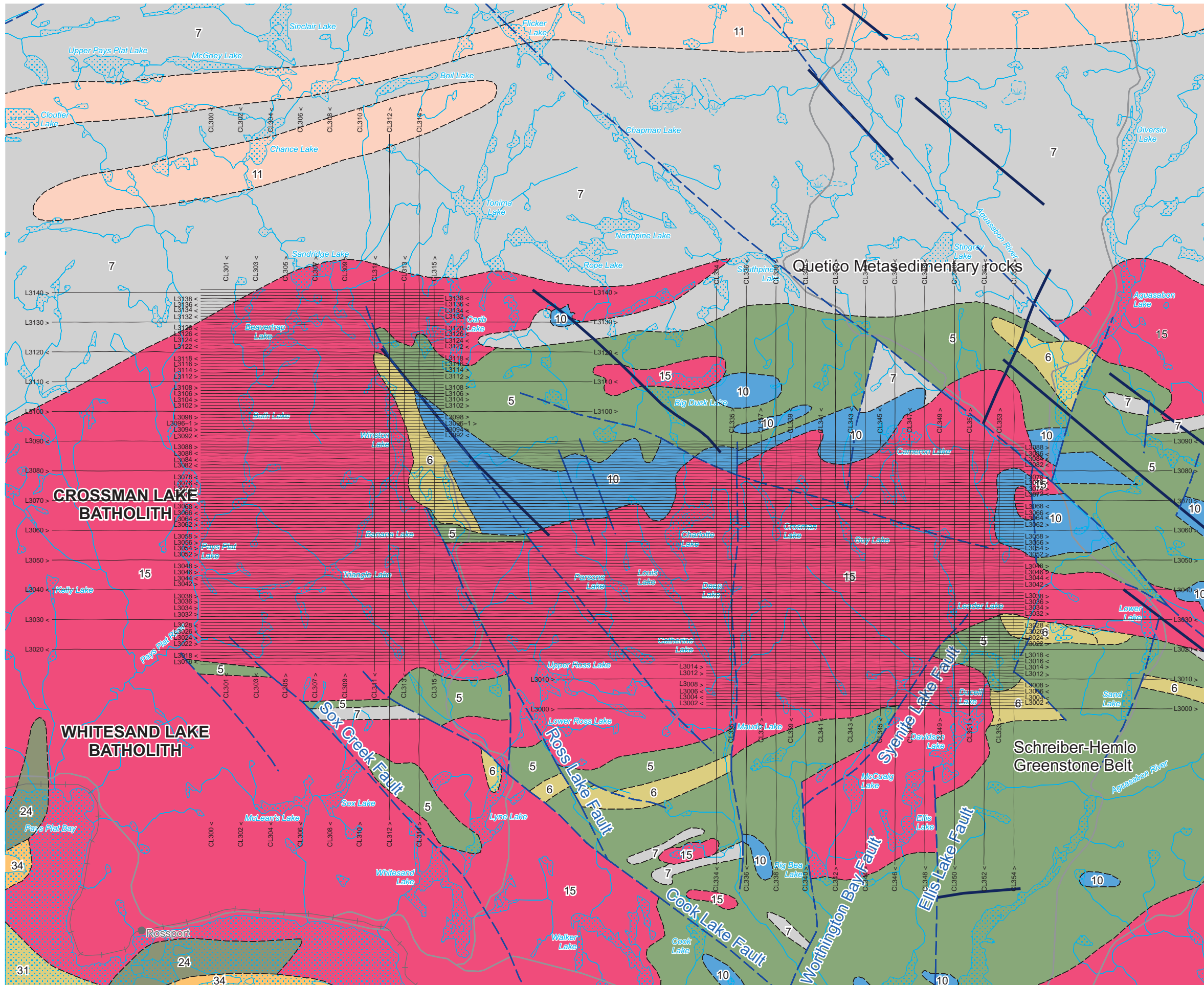
km 0 1 2 3 4 5 km

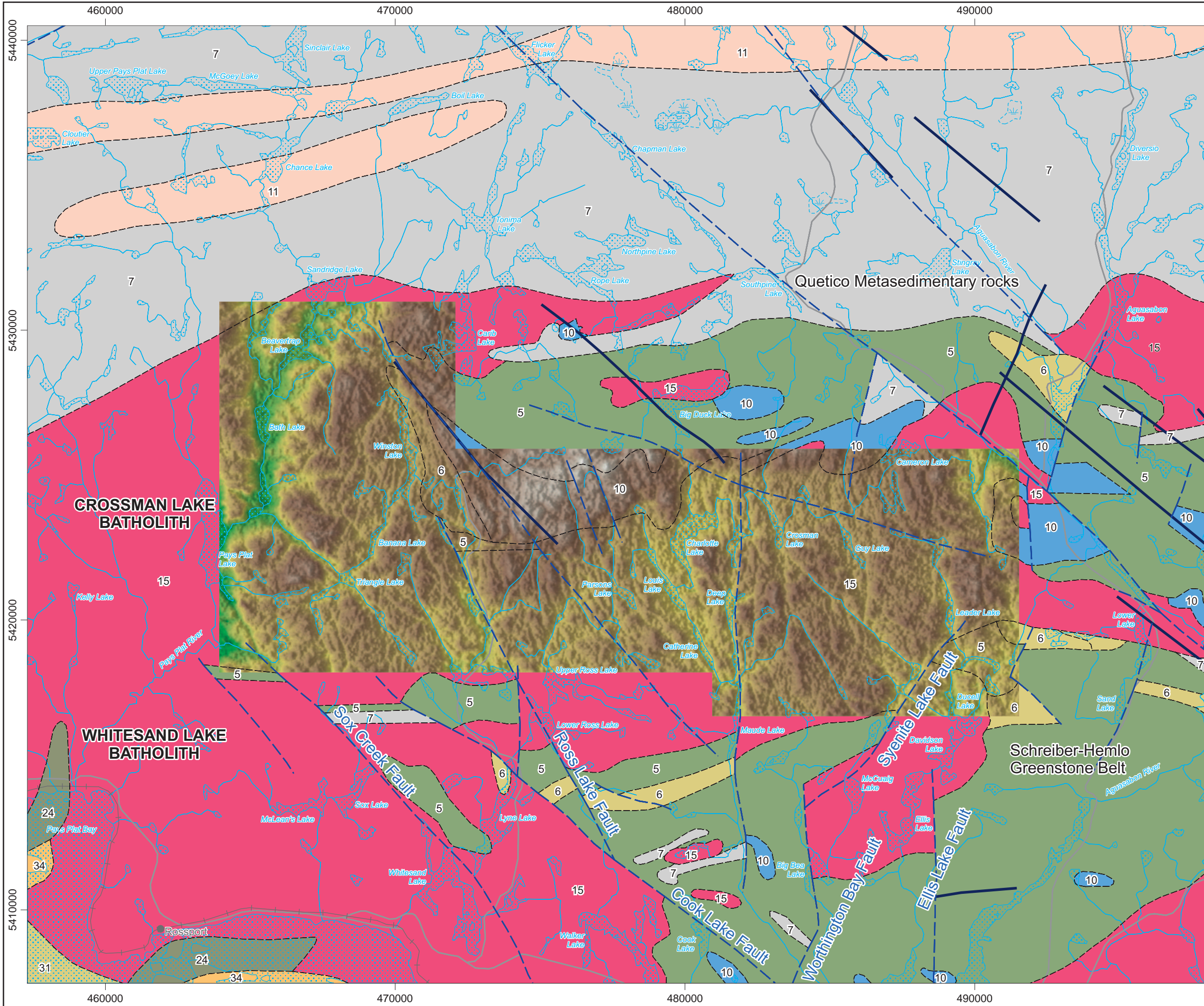
**Airborne Geophysics
 Acquisition and Interpretation**

Schreiber Area, Ontario 2014

Survey Area

	DESIGN	JK	29/01/2015	REV. 1.1
	GIS	YC, AP	04/02/2015	FIGURE: 1.1
	DATA	MM, DK	04/02/2015	
	QC	MB	04/02/2015	





Legend

Hydrography

Road

Railway

Geology

Fault

Dyke

5: Mafic to intermediate metavolcanic rocks

6: Felsic to intermediate metavolcanic rocks

7: Metasedimentary rocks

10: Mafic and ultramafic rocks

11: Gneiss tonalite suite

15: Massive granodiorite suite

24: Animikie Gp.

31: Sibley Gp.

32: Osler Gp., Mamainse Point Fm., Michipicoten Island Fm.

34: Mafic intrusive rocks (Keweenawan age)

Map Parameters

Illumination: inclination 50°, declination 270°

m



BASE DATA: National Topographic Database - NRCAN
 GEOLOGY DATA: OGS Dataset MRD 126-Rev 1
 DATUM: NAD83
 PROJECTION: Universal Transverse Mercator (UTM Zone 16N)

Scale 1 : 130 000

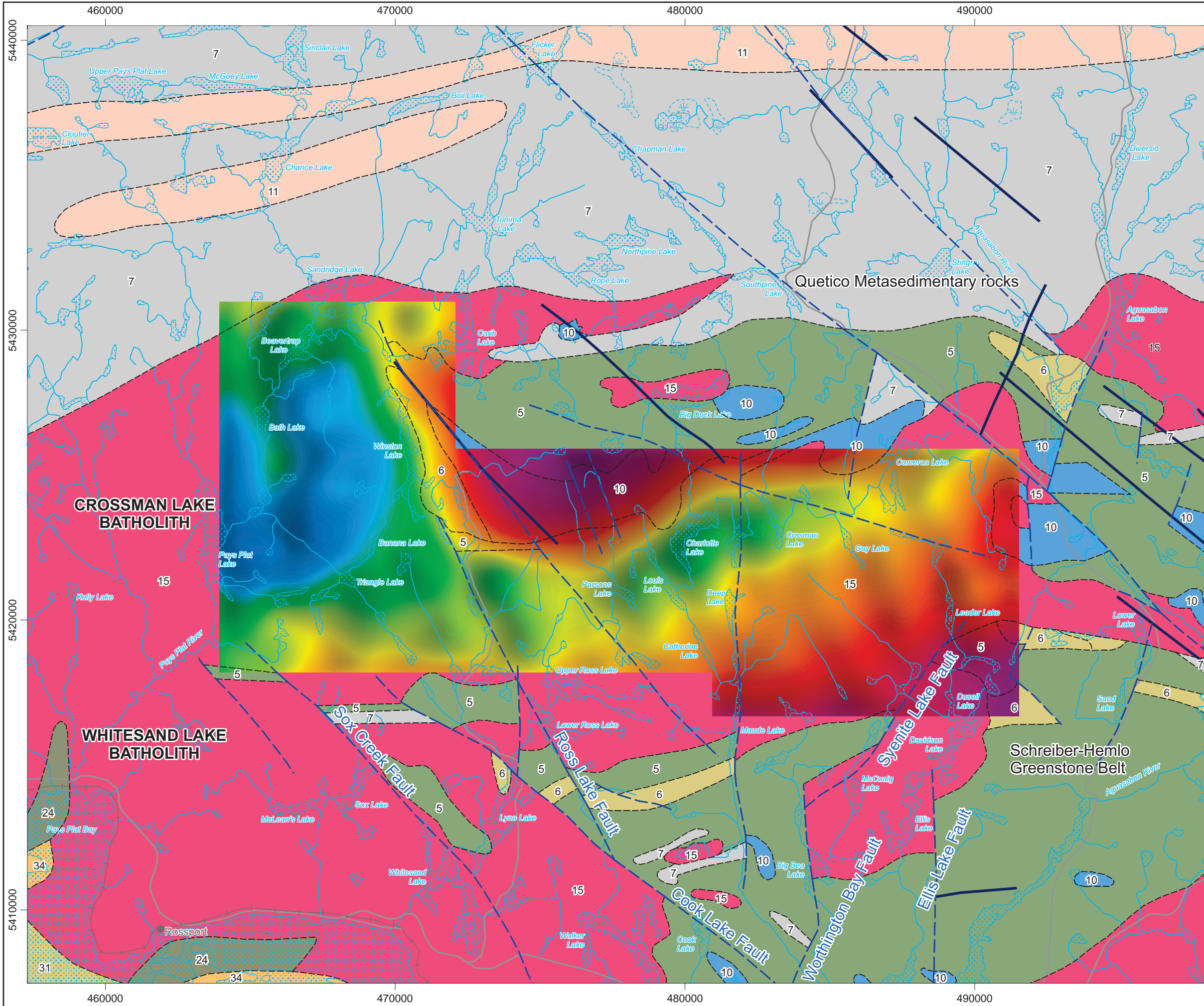
km 0 1 2 3 4 5 km

**Airborne Geophysics
 Acquisition and Interpretation**

Schreiber Area, Ontario 2014

Digital Elevation Model (25 m cell)

	DESIGN	JK	29/01/2015	REV. 1.1
	GIS	YC, AP	04/02/2015	FIGURE: 3.1
	DATA	MM, DK	04/02/2015	
	QC	MB	04/02/2015	



Legend

Hydrography

Road

Railway

Geology

Fault

Dyke

5: Mafic to intermediate metavolcanic rocks

6: Felsic to intermediate metavolcanic rocks

7: Metasedimentary rocks

10: Mafic and ultramafic rocks

11: Gneiss tonalite suite

15: Massive granodiorite suite

24: Animikie Gp.

31: Sibley Gp.

32: Osler Gp., Mamaise Point Fm., Michipicoten Island Fm.

34: Mafic intrusive rocks (Keweenawan age)

Map Parameters

Illumination: inclination 50°, declination 270°

Spatial Filter (half-wavelength): 1000 m

Bouguer Density: 2.67 g/cm³

mGal



BASE DATA: National Topographic Database - NRCAN
 GEOLOGY DATA: OGS Dataset MRD 126-Rev 1
 DATUM: NAD83
 PROJECTION: Universal Transverse Mercator (UTM Zone 16N)

Scale 1 : 130 000

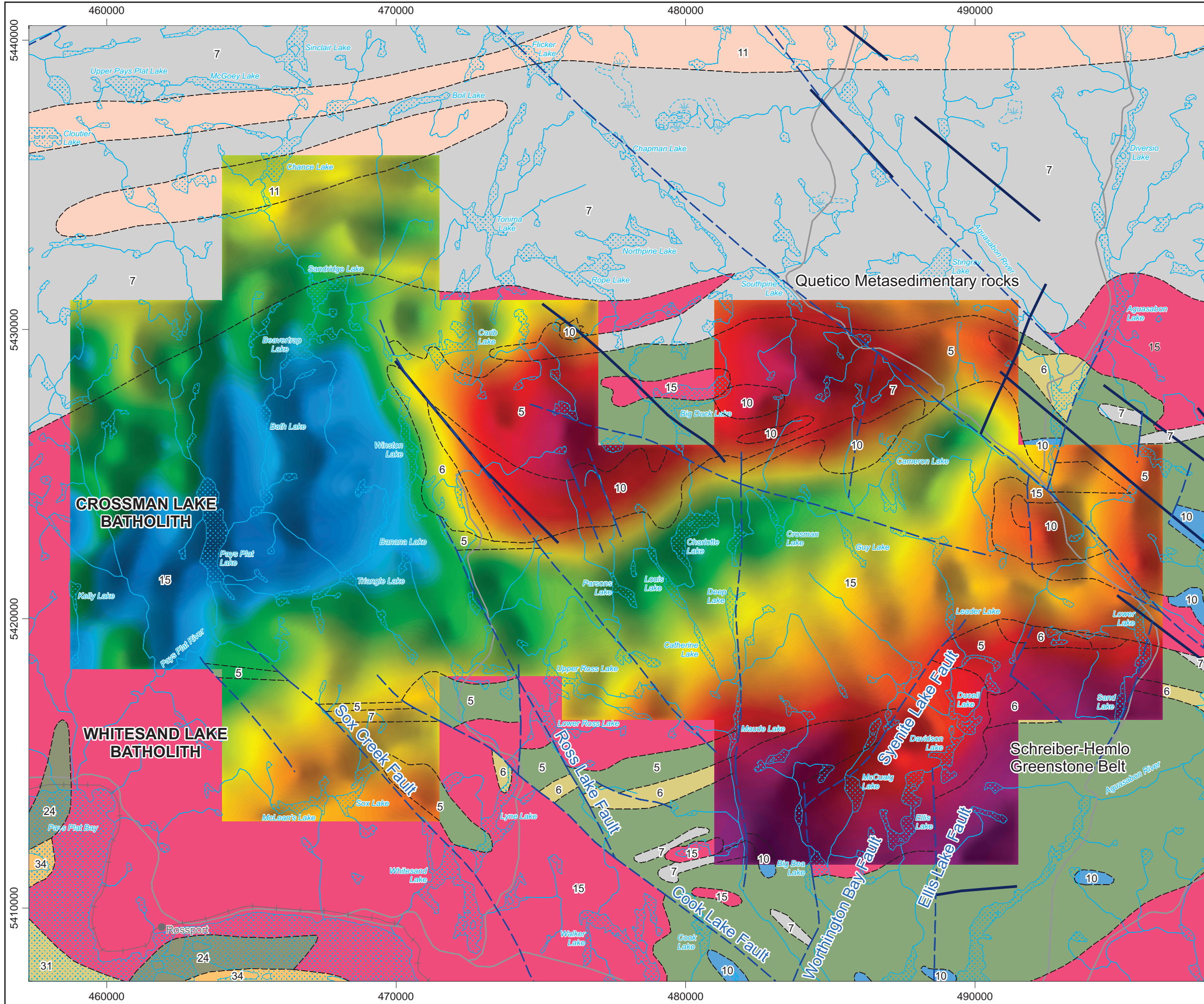
km 0 1 2 3 4 5 km

**Airborne Geophysics
 Acquisition and Interpretation**

Schreiber Area, Ontario 2014

Bouguer Gravity (Density: 2.67 g/cm³) (25 m cell)

	DESIGN	JK	29/01/2015	REV. 1.1
	GIS	YC, AP	04/02/2015	FIGURE: 4.1
	DATA	MM, DK	04/02/2015	
	QC	MB	04/02/2015	



Legend

Hydrography

Road

Railway

Geology

Fault

Dyke

5: Mafic to intermediate metavolcanic rocks

6: Felsic to intermediate metavolcanic rocks

7: Metasedimentary rocks

10: Mafic and ultramafic rocks

11: Gneissic tonalite suite

15: Massive granodiorite suite

24: Animikie Gp.

31: Sibley Gp.

32: Osler Gp., Mamaise Point Fm., Michipicoten Island Fm.

34: Mafic intrusive rocks (Keweenawan age)

Map Parameters

Illumination: inclination 50°, declination 270°

Spatial Filter (half-wavelength): 1000 m

Bouguer Density: 2.67 g/cm³

mGal



BASE DATA: National Topographic Database - NRCAN
 GEOLOGY DATA: OGS Dataset MRD 126-Rev 1
 DATUM: NAD83
 PROJECTION: Universal Transverse Mercator (UTM Zone 16N)

Scale 1 : 130 000

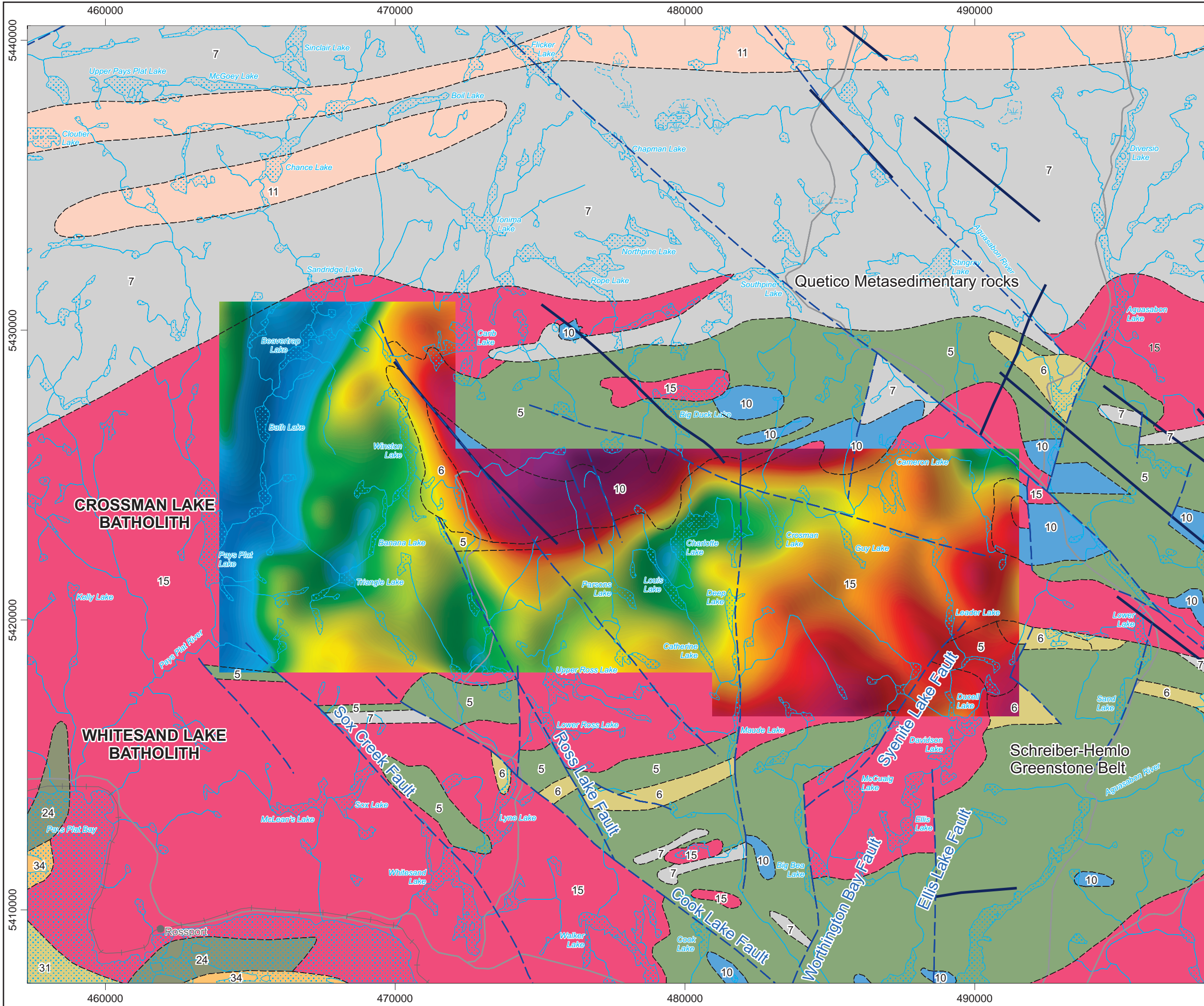
km 0 1 2 3 4 5 km

**Airborne Geophysics
 Acquisition and Interpretation**

Schreiber Area, Ontario 2014

Bouguer Gravity (Density: 2.67 g/cm³) (250 m cell)

	DESIGN	JK	29/01/2015	REV. 1.1
	GIS	YC, AP	04/02/2015	FIGURE: 4.2
	DATA	MM, DK	04/02/2015	
	QC	MB	04/02/2015	



Legend

Hydrography

Road

Railway

Geology

Fault

Dyke

- 5: Mafic to intermediate metavolcanic rocks
- 6: Felsic to intermediate metavolcanic rocks
- 7: Metasedimentary rocks
- 10: Mafic and ultramafic rocks
- 11: Gneissic tonalite suite
- 15: Massive granodiorite suite
- 24: Animikie Gp.
- 31: Sibley Gp.
- 32: Osler Gp., Mamainse Point Fm., Michipicoten Island Fm.
- 34: Mafic intrusive rocks (Keweenawan age)

Map Parameters

Illumination: inclination 50°, declination 270°

Spatial Filter (half-wavelength): 1000 m

mGal



BASE DATA: National Topographic Database - NRCAN
 GEOLOGY DATA: OGS Dataset MRD 126-Rev 1
 DATUM: NAD83
 PROJECTION: Universal Transverse Mercator (UTM Zone 16N)

Scale 1 : 130 000

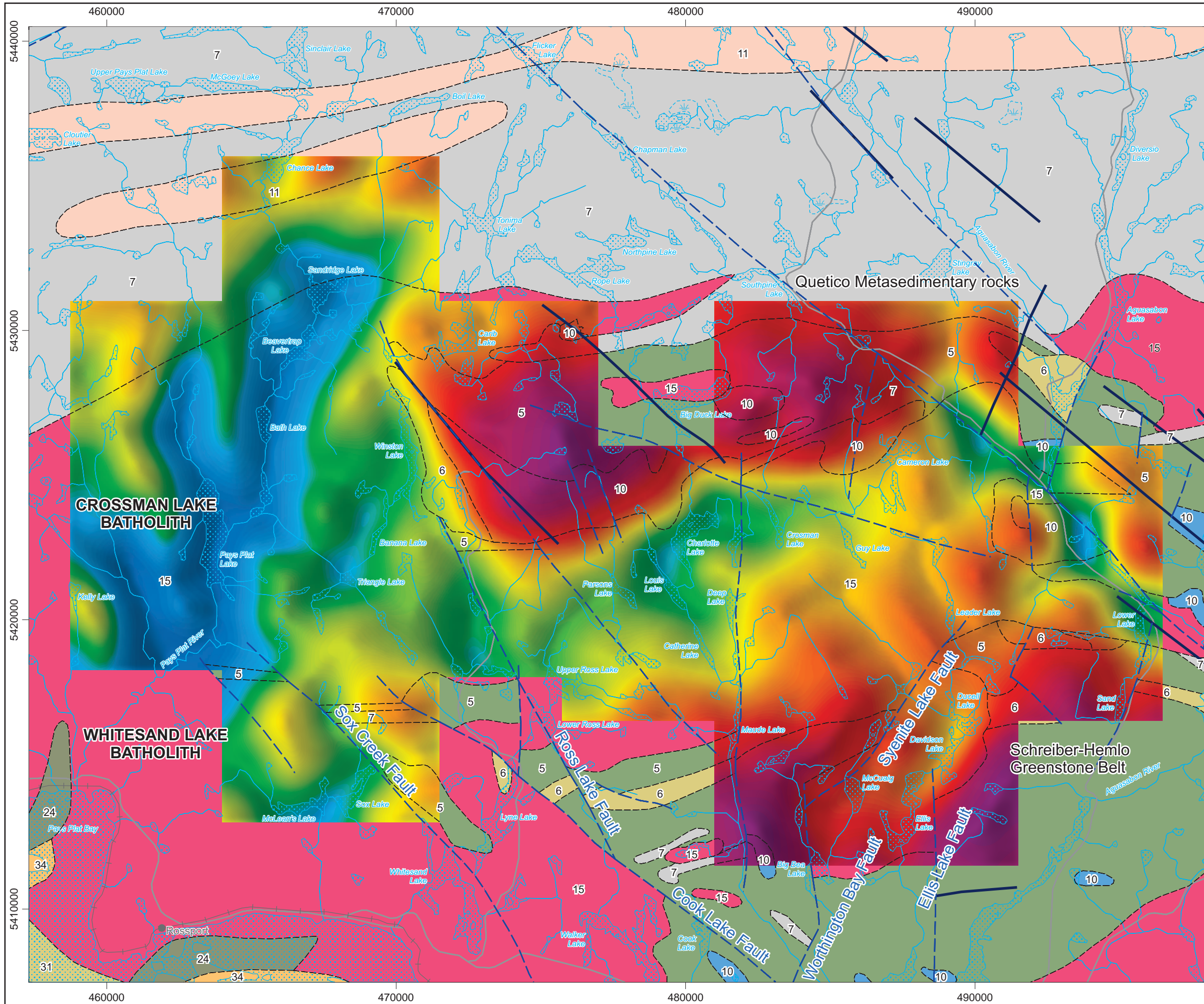
km 0 1 2 3 4 5 km

**Airborne Geophysics
 Acquisition and Interpretation**

Schreiber Area, Ontario 2014

Free Air Gravity (25 m cell)

	DESIGN	JK	29/01/2015	REV. 1.1
	GIS	YC, AP	04/02/2015	FIGURE: 4.3
	DATA	MM, DK	04/02/2015	
	QC	MB	04/02/2015	



Legend

Hydrography

Road

Railway

Geology

Fault

Dyke

5: Mafic to intermediate metavolcanic rocks

6: Felsic to intermediate metavolcanic rocks

7: Metasedimentary rocks

10: Mafic and ultramafic rocks

11: Gneissic tonalite suite

15: Massive granodiorite suite

24: Animikie Gp.

31: Sibley Gp.

32: Osler Gp., Mamainse Point Fm., Michipicoten Island Fm.

34: Mafic intrusive rocks (Keweenawan age)

Map Parameters

Illumination: inclination 50°, declination 270°

Spatial Filter (half-wavelength): 1000 m

mGal

-5.6

-7.8

-10.7

-13.3

-14.8

-16.0

-17.4

-18.7

-20.2

-21.5

-22.7

-23.9

-24.9

-25.6

-26.2

-26.8

-27.4

-28.0

-28.5

-28.9

-29.4

-29.8

-30.2

-30.8

-31.4

-32.0

-32.6

-33.2

-33.7

-34.1

-34.5

-34.9

-35.3

-35.7

-36.0

-36.4

-36.7

-37.1

-37.5

-38.0

-38.4

-38.8

-39.3

-39.9

-40.6

-41.7

-43.5

-45.3

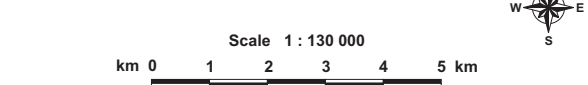
-47.2

-49.7

-57.6



BASE DATA: National Topographic Database - NRCAN
 GEOLOGY DATA: OGS Dataset MRD 126-Rev 1
 DATUM: NAD83
 PROJECTION: Universal Transverse Mercator (UTM Zone 16N)

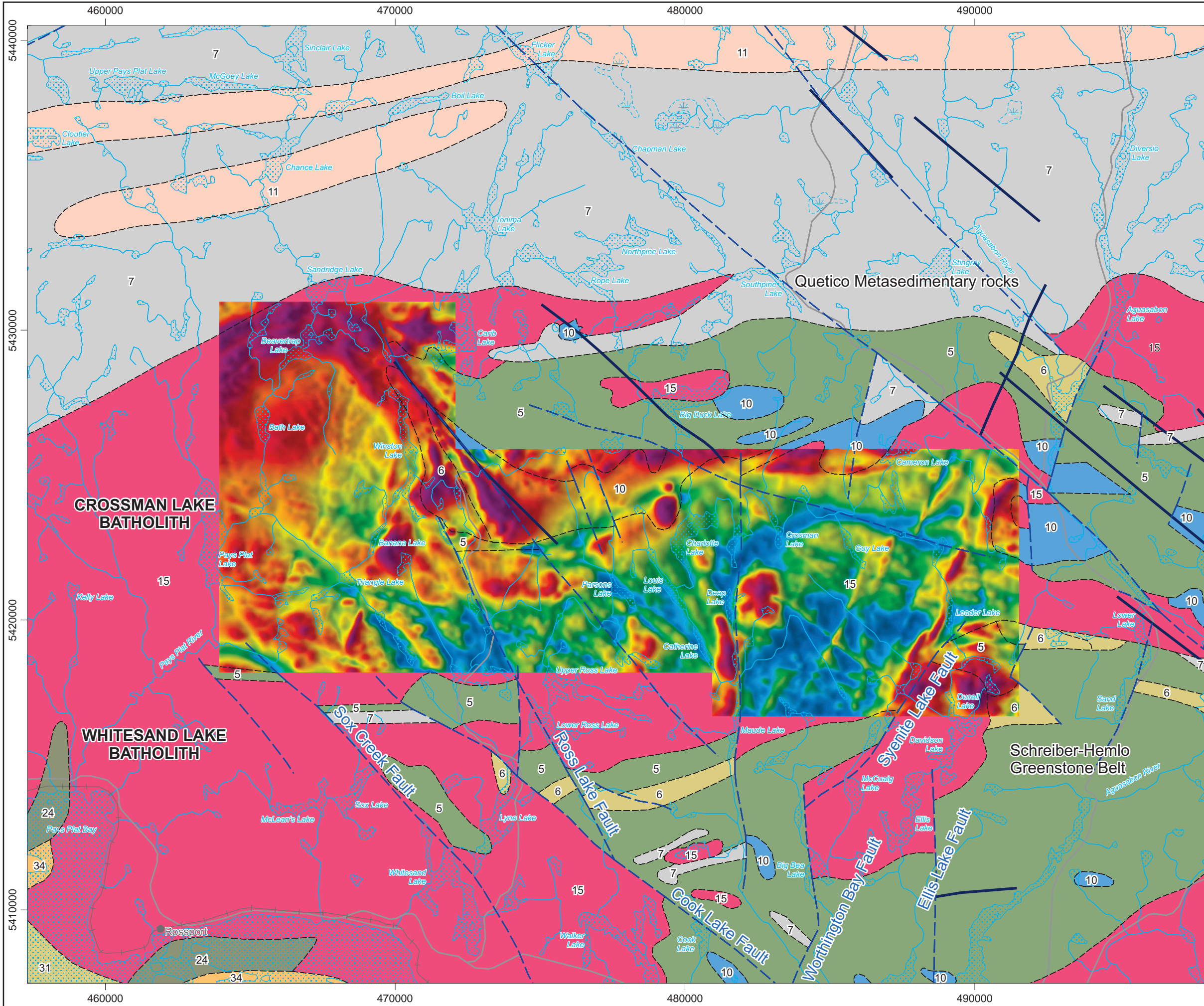


**Airborne Geophysics
 Acquisition and Interpretation**

Schreiber Area, Ontario 2014

Free Air Gravity (250 m cell)

	DESIGN	JK	29/01/2015	REV. 1.1
	GIS	YC, AP	04/02/2015	FIGURE: 4.4
	DATA	MM, DK	04/02/2015	
	QC	MB	04/02/2015	



Legend

Hydrography

Road

Railway

Geology

Fault

Dyke

- 5: Mafic to intermediate metavolcanic rocks
- 6: Felsic to intermediate metavolcanic rocks
- 7: Metasedimentary rocks
- 10: Mafic and ultramafic rocks
- 11: Gneissic tonalite suite
- 15: Massive granodiorite suite
- 24: Animikie Gp.
- 31: Sibley Gp.
- 32: Osler Gp., Mamainse Point Fm., Michipicoten Island Fm.
- 34: Mafic intrusive rocks (Keweenawan age)

Map Parameters

Illumination: inclination 50°, declination 270°

nT

2337.0
169.9
111.7
74.2
42.6
13.2
-11.5
-26.6
-38.5
-48.9
-57.8
-65.9
-73.5
-80.4
-87.1
-93.7
-99.9
-106.1
-112.1
-118.5
-124.7
-131.0
-137.3
-143.8
-150.4
-156.9
-163.6
-169.9
-175.9
-181.6
-187.2
-192.5
-197.7
-202.7
-207.6
-212.1
-216.6
-221.1
-225.5
-230.0
-234.7
-239.9
-245.5
-251.3
-257.5
-264.1
-271.0
-278.8
-288.4
-302.1
-368.7



BASE DATA: National Topographic Database - NRCAN
 GEOLOGY DATA: OGS Dataset MRD 126-Rev 1
 DATUM: NAD83
 PROJECTION: Universal Transverse Mercator (UTM Zone 16N)

Scale 1 : 130 000

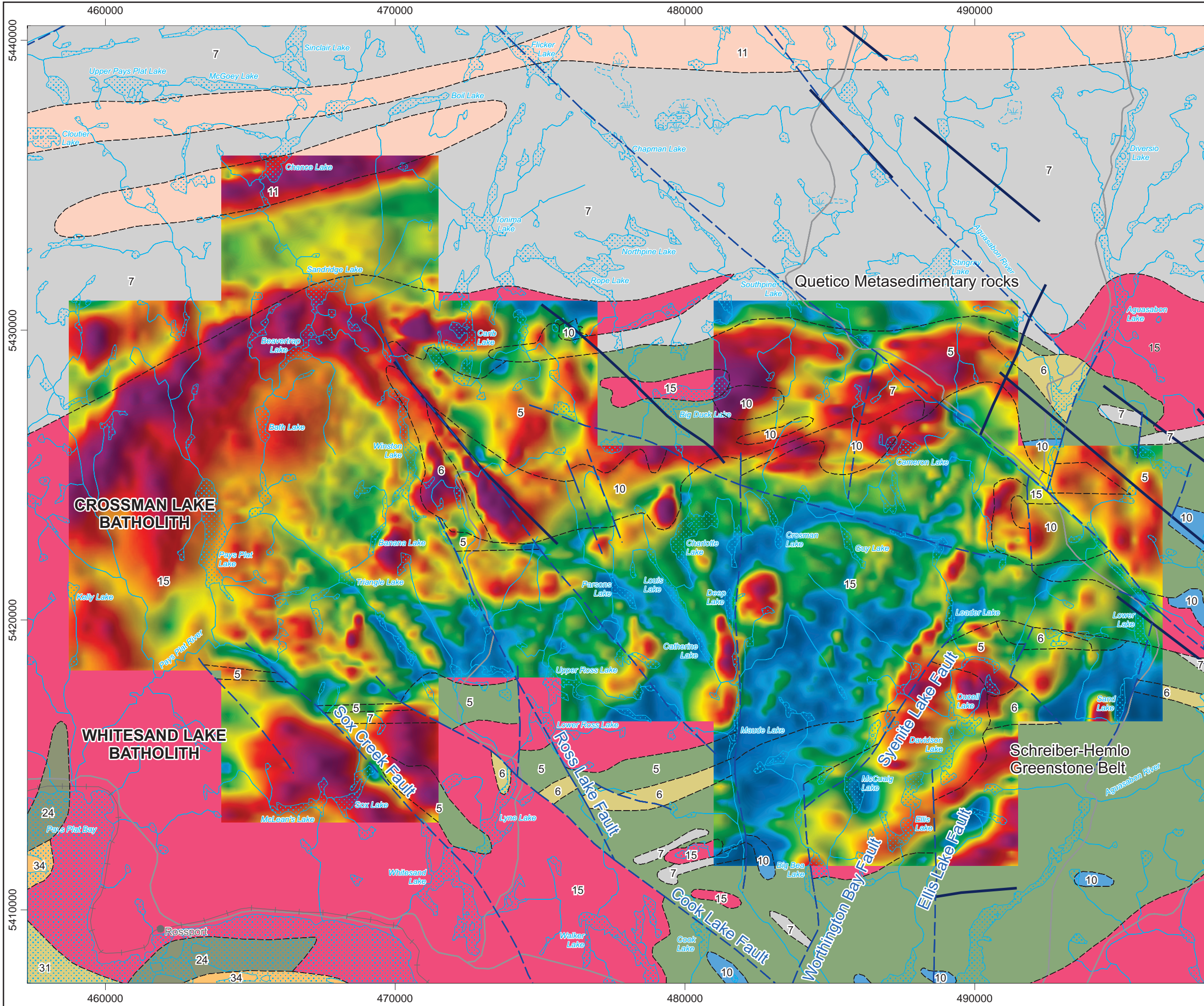
km 0 1 2 3 4 5 km

**Airborne Geophysics
 Acquisition and Interpretation**

Schreiber Area, Ontario 2014

Total Magnetic Intensity (25 m cell)

	DESIGN	JK	29/01/2015	REV. 1.1
	GIS	YC, AP	04/02/2015	FIGURE: 4.5
	DATA	MM, DK	04/02/2015	
	QC	MB	04/02/2015	



Legend

Hydrography

Road

Railway

Geology

Fault

Dyke

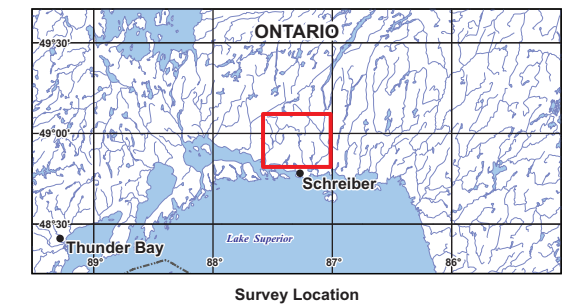
- 5: Mafic to intermediate metavolcanic rocks
- 6: Felsic to intermediate metavolcanic rocks
- 7: Metasedimentary rocks
- 10: Mafic and ultramafic rocks
- 11: Gneissic tonalite suite
- 15: Massive granodiorite suite
- 24: Animikie Gp.
- 31: Sibley Gp.
- 32: Osler Gp., Mamainse Point Fm., Michipicoten Island Fm.
- 34: Mafic intrusive rocks (Keweenawan age)

Map Parameters

Illumination: inclination 50°, declination 270°

nT

1319.2
218.4
151.5
113.9
85.3
62.0
40.6
22.9
6.6
-8.2
-21.2
-32.5
-42.9
-50.0
-60.8
-68.6
-76.0
-82.9
-89.6
-95.8
-102.2
-108.3
-114.7
-120.9
-127.1
-133.0
-138.8
-144.9
-151.2
-157.2
-163.1
-169.0
-174.7
-180.6
-186.4
-192.4
-198.7
-205.1
-211.3
-217.2
-222.8
-228.6
-234.9
-241.4
-248.5
-256.4
-265.8
-276.9
-289.7
-308.4
-514.2



BASE DATA: National Topographic Database - NRCAN
 GEOLOGY DATA: OGS Dataset MRD 126-Rev 1
 DATUM: NAD83
 PROJECTION: Universal Transverse Mercator (UTM Zone 16N)

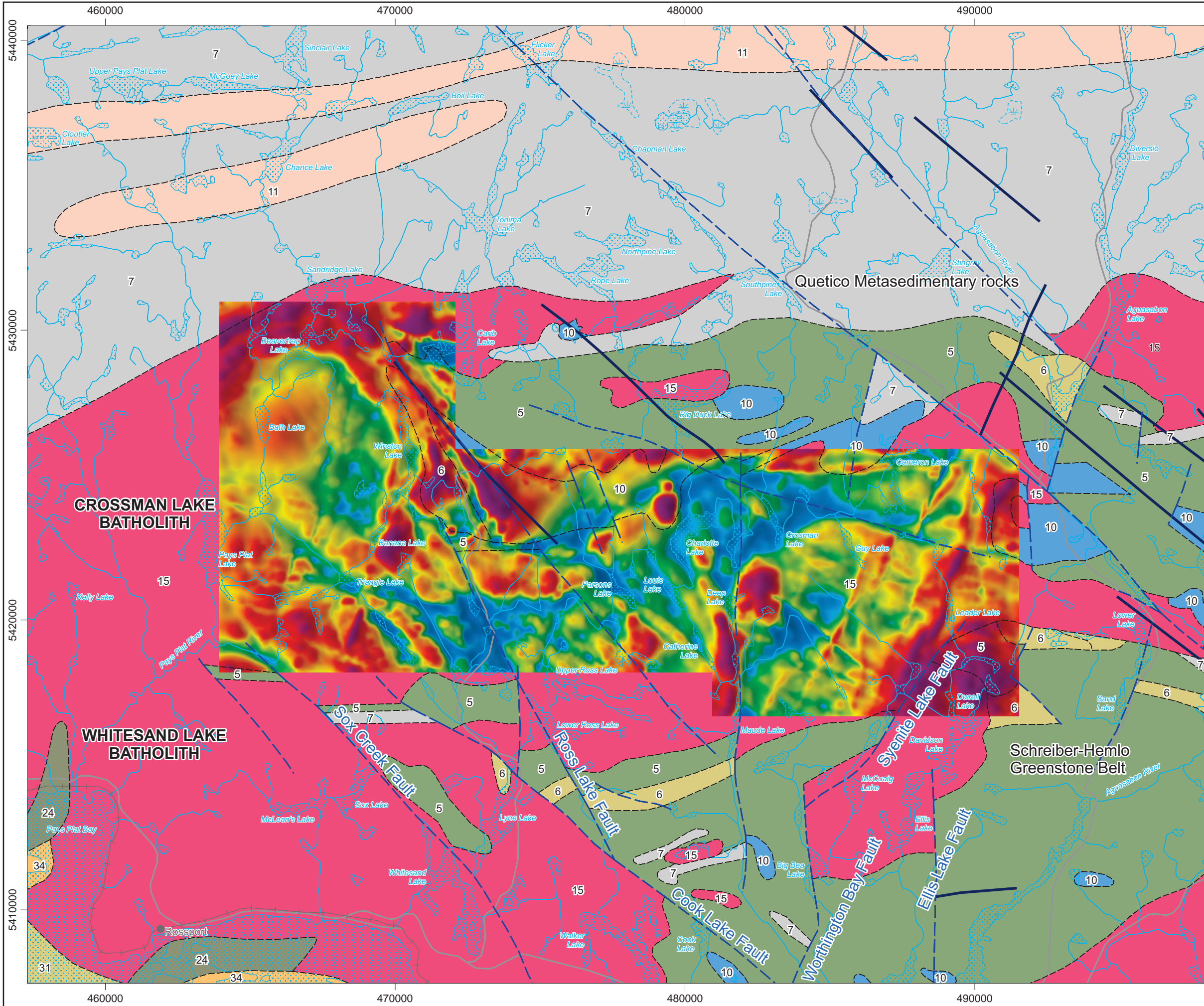


**Airborne Geophysics
 Acquisition and Interpretation**

Schreiber Area, Ontario 2014

Total Magnetic Intensity (250 m cell)

	DESIGN	JK	29/01/2015	REV. 1.1
	GIS	YC, AP	04/02/2015	FIGURE: 4.6
	DATA	MM, DK	04/02/2015	
	QC	MB	04/02/2015	



Legend

Hydrography

Road

Railway

Geology

Fault

Dyke

- 5: Mafic to intermediate metavolcanic rocks
- 6: Felsic to intermediate metavolcanic rocks
- 7: Metasedimentary rocks
- 10: Mafic and ultramafic rocks
- 11: Gneissic tonalite suite
- 15: Massive granodiorite suite
- 24: Animikie Gp.
- 31: Sibley Gp.
- 32: Osler Gp., Mamainse Point Fm., Michipicoten Island Fm.
- 34: Mafic intrusive rocks (Keweenawan age)

Map Parameters

Illumination: inclination 50°, declination 270°

nT

2468.5
326.9
243.4
196.8
163.5
137.4
115.4
96.4
80.4
67.5
56.4
46.8
38.5
31.2
24.6
18.4
12.6
6.9
1.4
-3.9
-9.3
-14.7
-19.6
-24.3
-29.0
-33.3
-37.3
-41.2
-45.4
-49.5
-53.7
-58.0
-62.1
-66.2
-69.9
-73.8
-77.9
-82.0
-86.3
-90.5
-94.6
-98.5
-102.7
-107.2
-111.9
-116.9
-122.4
-129.3
-138.4
-150.0
-281.8



BASE DATA: National Topographic Database - NRCAN
 GEOLOGY DATA: OGS Dataset MRD 126-Rev 1
 DATUM: NAD83
 PROJECTION: Universal Transverse Mercator (UTM Zone 16N)

Scale 1 : 130 000

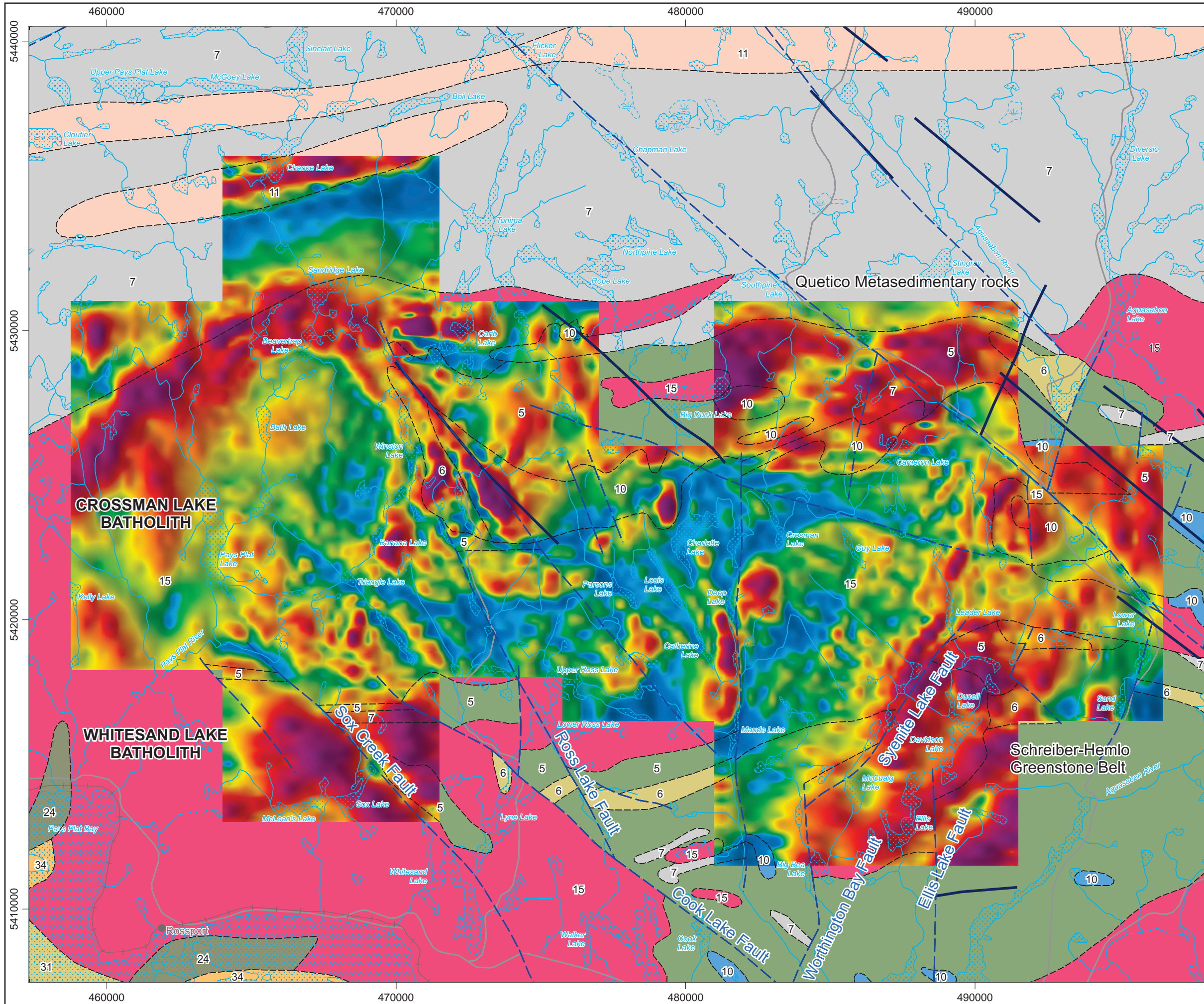
km 0 1 2 3 4 5 km

**Airborne Geophysics
 Acquisition and Interpretation**

Schreiber Area, Ontario 2014

**Reduction to the Pole
 of the Magnetic Field (25 m cell)**

	DESIGN	JK	29/01/2015	REV. 1.1
	GIS	YC, AP	04/02/2015	FIGURE: 4.7
	DATA	MM, DK	04/02/2015	
	QC	MB	04/02/2015	



Legend

Hydrography

Road

Railway

Geology

Fault

Dyke

5: Mafic to intermediate metavolcanic rocks

6: Felsic to intermediate metavolcanic rocks

7: Metasedimentary rocks

10: Mafic and ultramafic rocks

11: Gneissic tonalite suite

15: Massive granodiorite suite

24: Animikie Gp.

31: Sibley Gp.

32: Osler Gp., Mamainse Point Fm., Michipicoten Island Fm.

34: Mafic intrusive rocks (Keweenawan age)

Map Parameters

Illumination: inclination 50°, declination 270°

nT

1357.4

348.4

285.2

241.5

208.2

181.8

160.4

141.5

125.1

110.7

97.4

85.3

74.0

64.0

54.4

45.5

36.9

28.4

20.4

13.1

6.1

-0.7

-7.3

-13.5

-19.3

-24.8

-30.2

-35.8

-41.4

-46.9

-52.1

-57.1

-62.0

-66.8

-71.6

-76.4

-81.5

-86.9

-92.6

-98.7

-104.6

-110.6

-116.9

-123.6

-130.5

-137.5

-145.3

-154.0

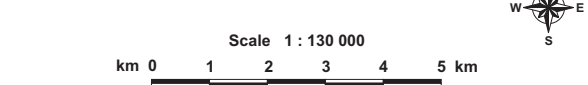
-165.7

-184.3

-339.9



BASE DATA: National Topographic Database - NRCAN
 GEOLOGY DATA: OGS Dataset MRD 126-Rev 1
 DATUM: NAD83
 PROJECTION: Universal Transverse Mercator (UTM Zone 16N)

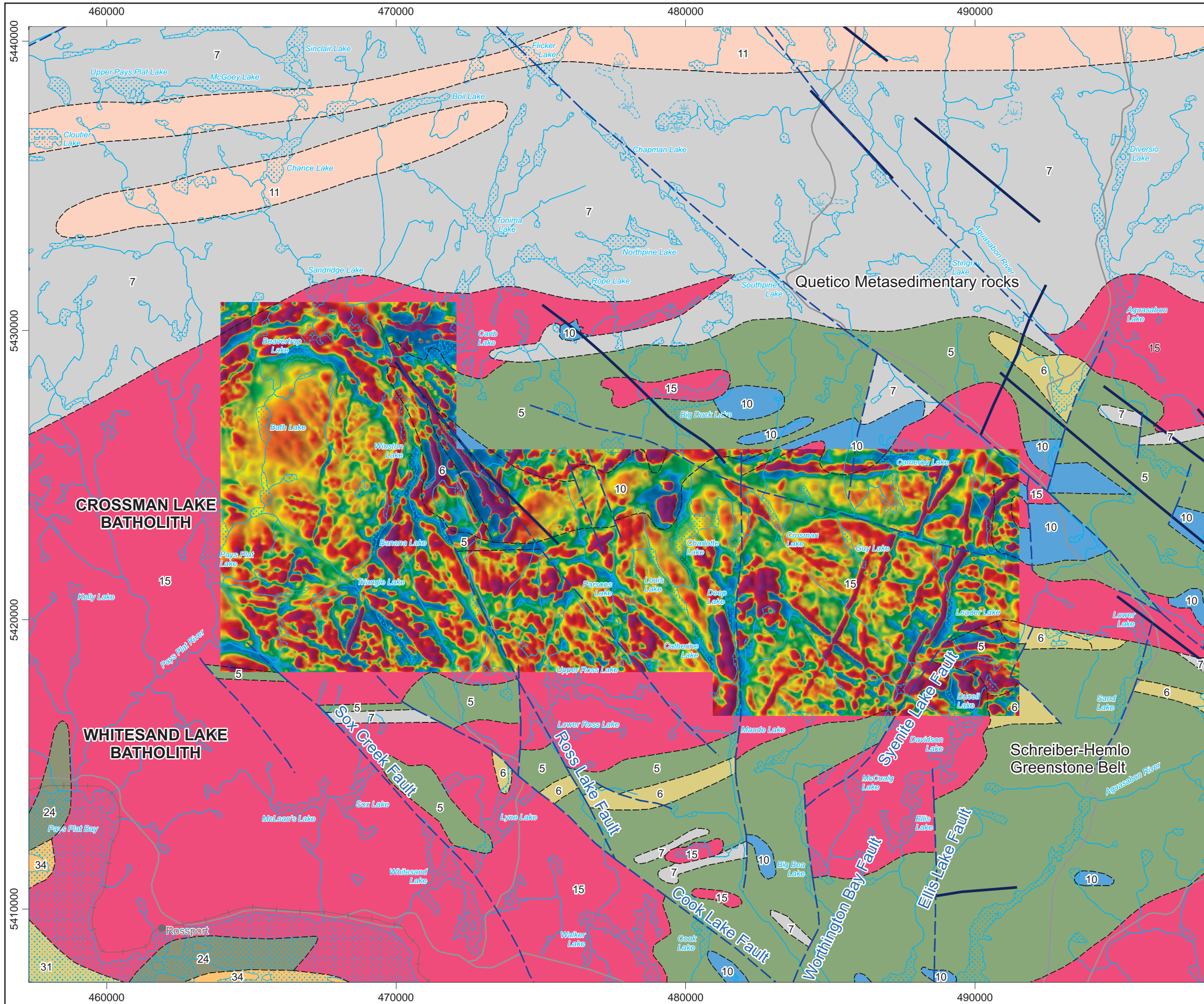


**Airborne Geophysics
 Acquisition and Interpretation**

Schreiber Area, Ontario 2014

**Reduction to the Pole
 of the Magnetic Field (250 m cell)**

	DESIGN	JK	29/01/2015	REV. 1.1
	GIS	YC, AP	04/02/2015	FIGURE: 4.8
	DATA	MM, DK	04/02/2015	
	QC	MB	04/02/2015	



Legend

Hydrography

Road

Railway

Geology

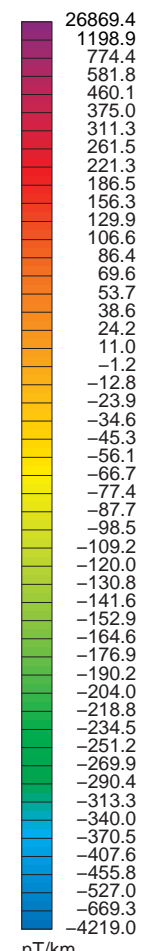
Fault

Dyke

- 5: Mafic to intermediate metavolcanic rocks
- 6: Felsic to intermediate metavolcanic rocks
- 7: Metasedimentary rocks
- 10: Mafic and ultramafic rocks
- 11: Gneissic tonalite suite
- 15: Massive granodiorite suite
- 24: Animikie Gp.
- 31: Sibley Gp.
- 32: Osler Gp., Mamainse Point Fm., Michipicoten Island Fm.
- 34: Mafic intrusive rocks (Keweenawan age)

Map Parameters

Illumination: inclination 50°, declination 270°



BASE DATA: National Topographic Database - NRCAN
 GEOLOGY DATA: OGS Dataset MRD 126-Rev 1
 DATUM: NAD83
 PROJECTION: Universal Transverse Mercator (UTM Zone 16N)

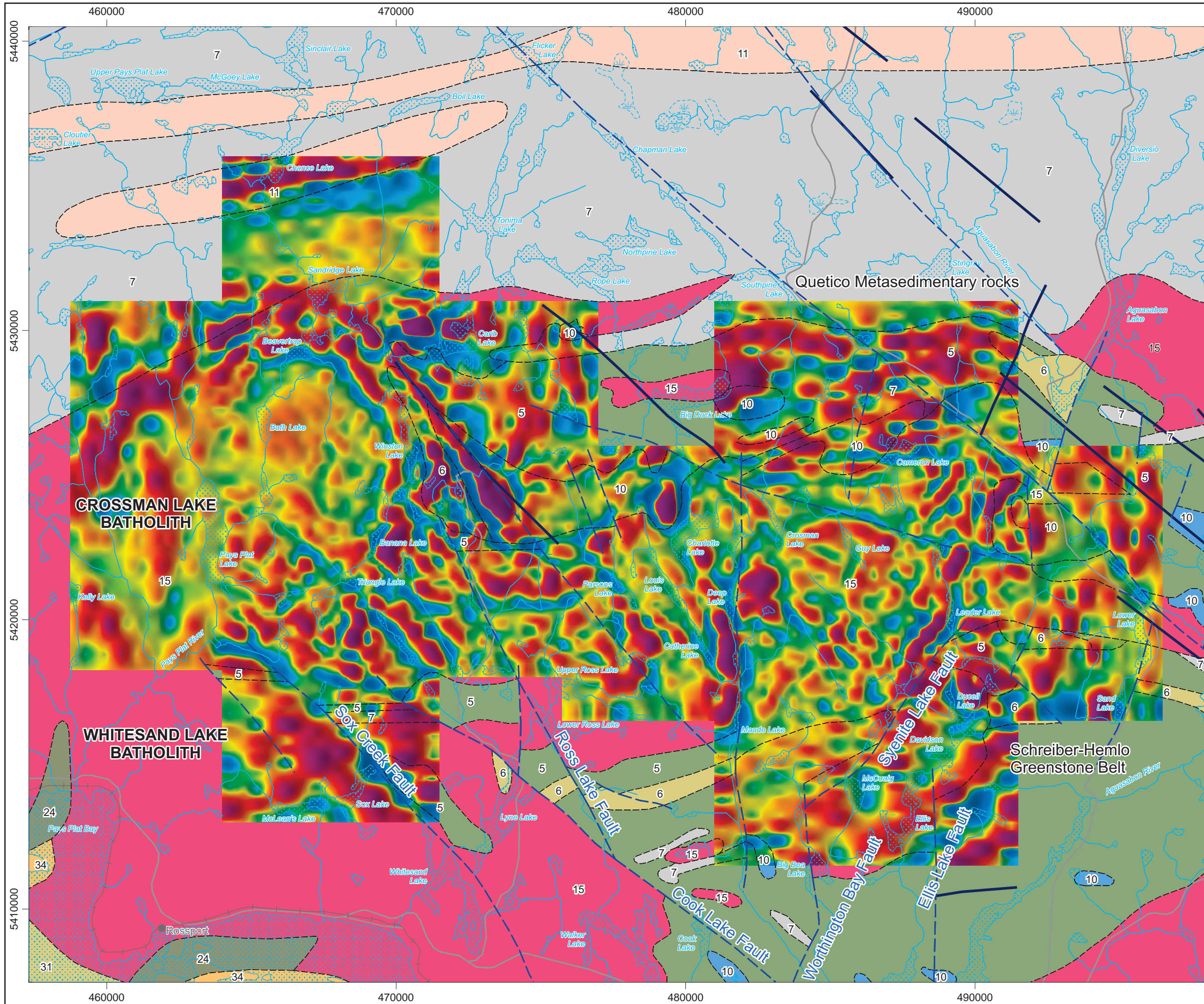


**Airborne Geophysics
 Acquisition and Interpretation**

Schreiber Area, Ontario 2014

First Vertical Derivative of the
 Reduction to the Pole of the Total Magnetic Intensity
 (25 m cell)

	DESIGN	JK	29/01/2015	REV. 1.1
	GIS	YC, AP	04/02/2015	FIGURE: 4.9
	DATA	MM, DK	04/02/2015	
	QC	MB	04/02/2015	



Legend

Hydrography

Road

Railway

Geology

Fault

Dyke

5: Mafic to intermediate metavolcanic rocks

6: Felsic to intermediate metavolcanic rocks

7: Metasedimentary rocks

10: Mafic and ultramafic rocks

11: Gneissic tonalite suite

15: Massive granodiorite suite

24: Animikie Gp.

31: Sibley Gp.

32: Osler Gp., Mamaise Point Fm., Michipicoten Island Fm.

34: Mafic intrusive rocks (Keweenawan age)

Map Parameters

Illumination: inclination 50°, declination 270°

nT/km

5320.9

741.3

531.4

425.5

355.2

304.2

261.7

226.4

196.1

170.2

147.2

126.8

107.8

90.6

75.2

61.5

48.5

37.0

26.3

16.0

6.2

-3.3

-12.6

-21.7

-30.5

-39.1

-47.7

-55.9

-64.1

-72.1

-80.1

-88.2

-96.5

-104.8

-113.8

-123.5

-133.7

-144.3

-155.2

-166.9

-179.4

-193.0

-208.1

-225.0

-244.1

-266.5

-292.9

-327.3

-377.2

-465.6

-2097.7



BASE DATA: National Topographic Database - NRCAN

GEOLOGY DATA: OGS Dataset MRD 126-Rev 1

DATUM: NAD83

PROJECTION: Universal Transverse Mercator (UTM Zone 16N)

Scale 1 : 130 000

km 0 1 2 3 4 5 km

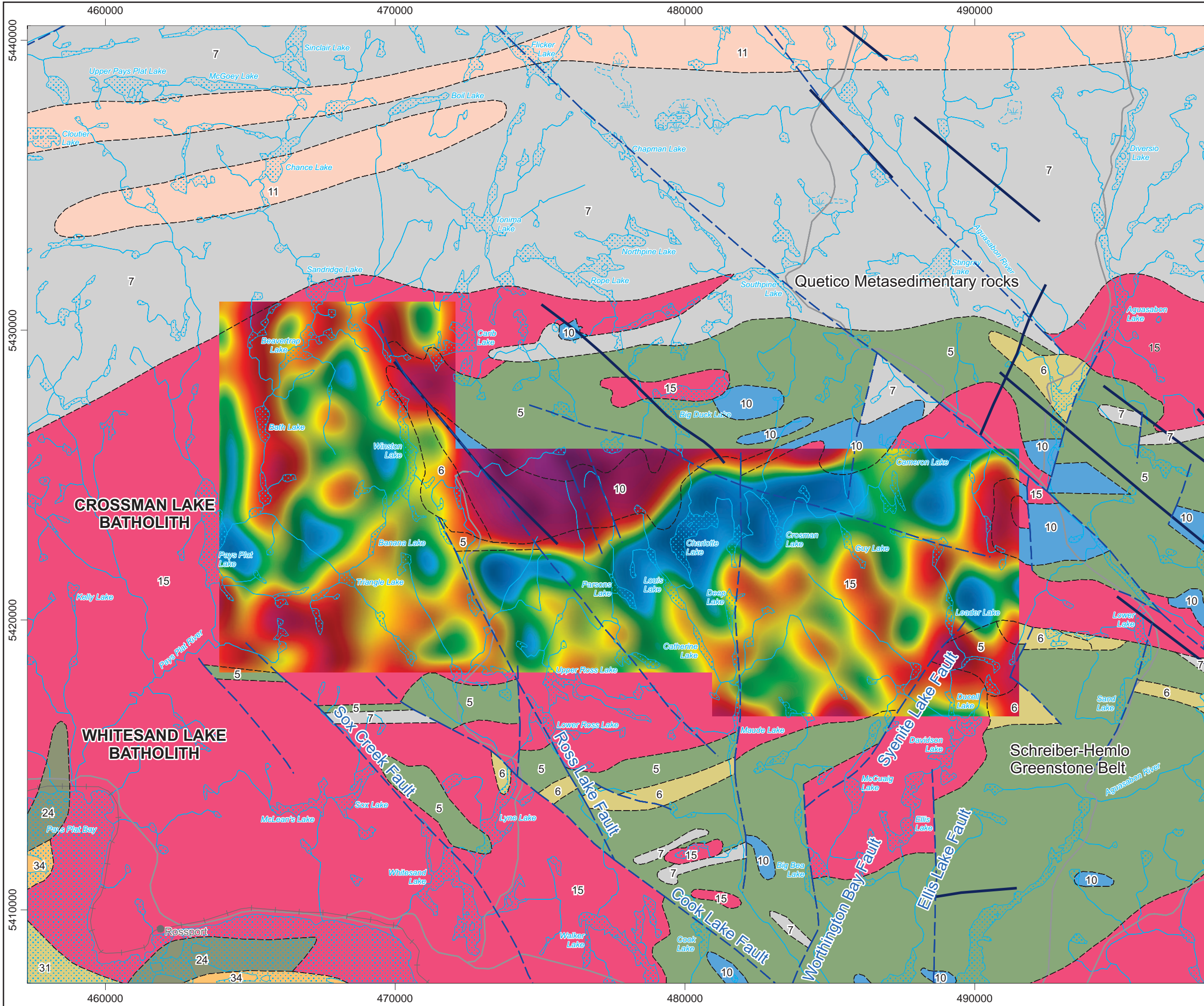
Airborne Geophysics

Acquisition and Interpretation

Schreiber Area, Ontario 2014

First Vertical Derivative of the Reduction to the Pole of the Total Magnetic Intensity (250 m cell)

	DESIGN	JK	29/01/2015	REV. 1.1
	GIS	YC, AP	04/02/2015	FIGURE: 4.10
	DATA	MM, DK	04/02/2015	
	QC	MB	04/02/2015	



Legend

Hydrography

Road

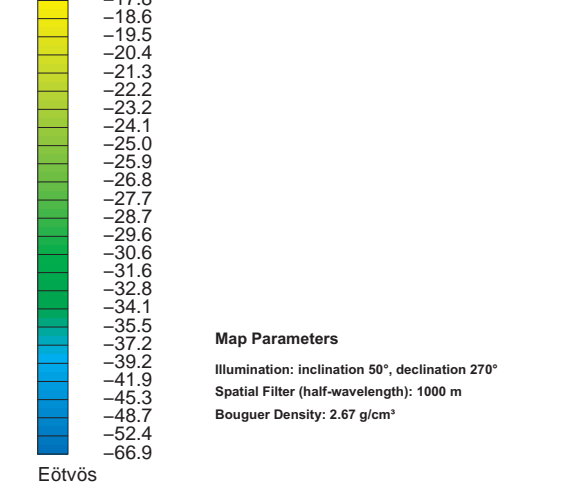
Railway

Geology

Fault

Dyke

- 5: Mafic to intermediate metavolcanic rocks
- 6: Felsic to intermediate metavolcanic rocks
- 7: Metasedimentary rocks
- 10: Mafic and ultramafic rocks
- 11: Gneissic tonalite suite
- 15: Massive granodiorite suite
- 24: Animikie Gp.
- 31: Sibley Gp.
- 32: Osler Gp., Mamainse Point Fm., Michipicoten Island Fm.
- 34: Mafic intrusive rocks (Keweenawan age)



BASE DATA: National Topographic Database - NRCAN
 GEOLOGY DATA: OGS Dataset MRD 126-Rev 1
 DATUM: NAD83
 PROJECTION: Universal Transverse Mercator (UTM Zone 16N)

Scale 1 : 130 000

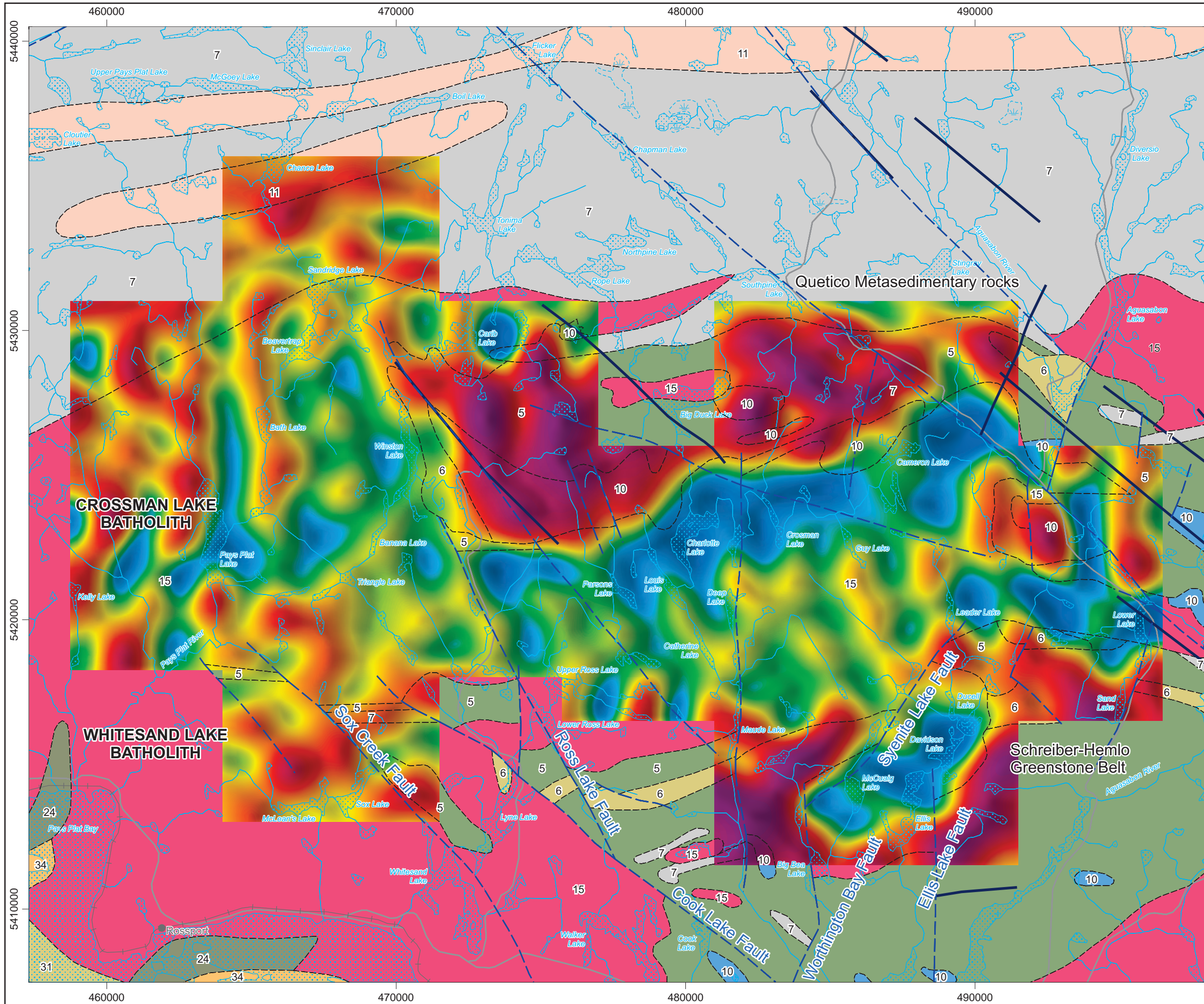
km 0 1 2 3 4 5 km

**Airborne Geophysics
 Acquisition and Interpretation**

Schreiber Area, Ontario 2014

**First Vertical Derivative of the Bouguer Gravity
 (Density: 2.67 g/cm³) (25 m cell)**

	DESIGN	JK	29/01/2015	REV. 1.1
	GIS	YC, AP	04/02/2015	FIGURE: 4.11
	DATA	MM, DK	04/02/2015	
	QC	MB	04/02/2015	



Legend

Hydrography

Road

Railway

Geology

Fault

Dyke

5: Mafic to intermediate metavolcanic rocks

6: Felsic to intermediate metavolcanic rocks

7: Metasedimentary rocks

10: Mafic and ultramafic rocks

11: Gneissic tonalite suite

15: Massive granodiorite suite

24: Animikie Gp.

31: Sibley Gp.

32: Osler Gp., Mamainse Point Fm., Michipicoten Island Fm.

34: Mafic intrusive rocks (Keweenawan age)

Map Parameters

Illumination: inclination 50°, declination 270°

Spatial Filter (half-wavelength): 1000 m

Bouguer Density: 2.67 g/cm³

Eötvös

90.0
66.2
56.1
49.8
44.1
38.3
32.9
28.6
25.0
21.9
19.4
17.0
15.0
13.1
11.3
9.4
7.6
5.8
4.2
2.6
0.9
-0.7
-2.3
-4.0
-5.7
-7.4
-8.8
-10.2
-11.5
-12.9
-14.2
-15.5
-16.8
-18.0
-19.4
-20.8
-22.2
-23.6
-25.1
-26.6
-28.0
-29.5
-31.1
-32.8
-34.9
-37.3
-40.1
-43.7
-48.2
-53.4
-78.3



BASE DATA: National Topographic Database - NRCAN
 GEOLOGY DATA: OGS Dataset MRD 126-Rev 1
 DATUM: NAD83
 PROJECTION: Universal Transverse Mercator (UTM Zone 16N)

Scale 1 : 130 000

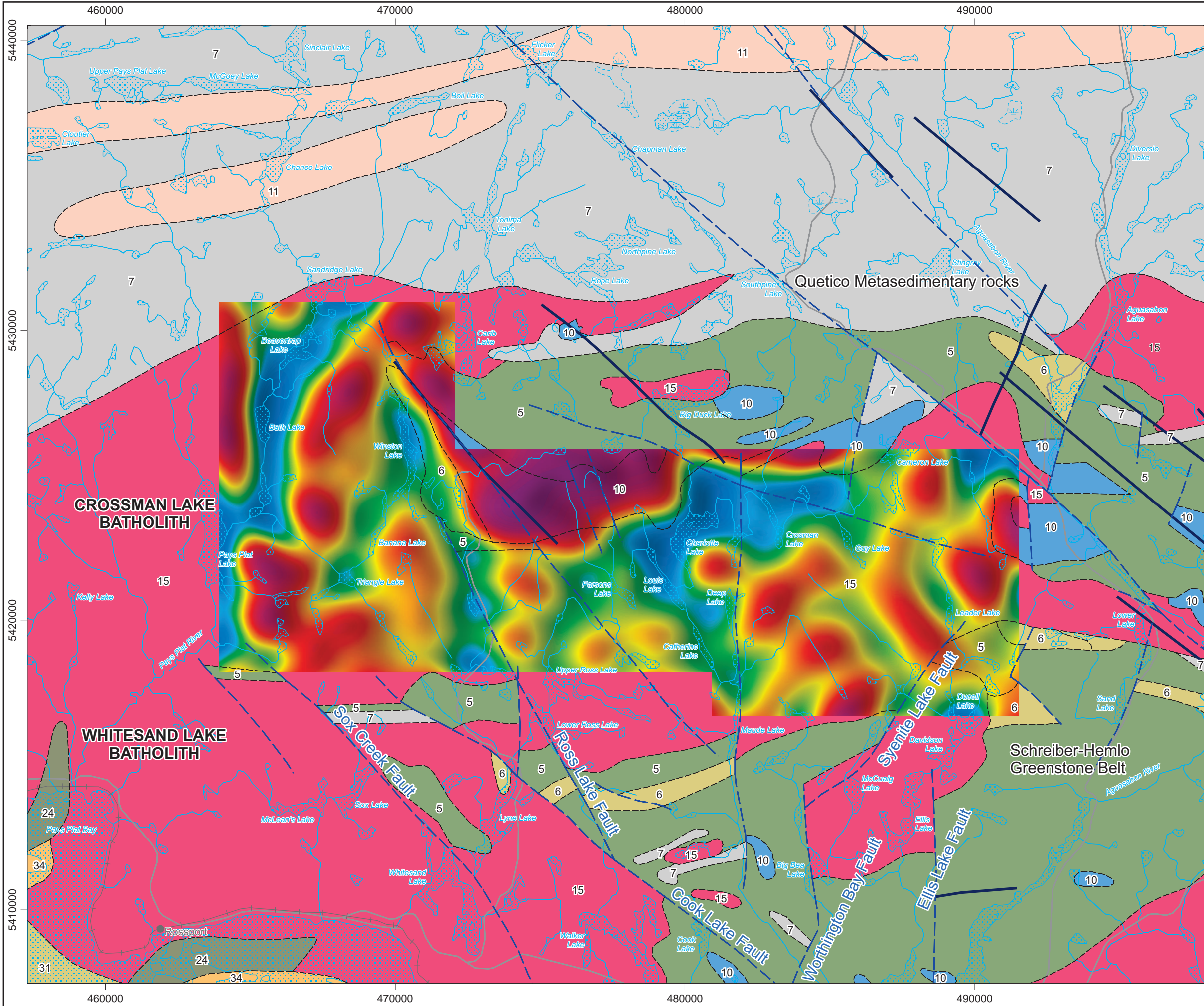
km 0 1 2 3 4 5 km

**Airborne Geophysics
 Acquisition and Interpretation**

Schreiber Area, Ontario 2014

**First Vertical Derivative of the Bouguer Gravity
 (Density: 2.67 g/cm³) (250 m cell)**

	DESIGN	JK	29/01/2015	REV. 1.1
	GIS	YC, AP	04/02/2015	FIGURE: 4.12
	DATA	MM, DK	04/02/2015	
	QC	MB	04/02/2015	



Legend

Hydrography

Road

Railway

Geology

Fault

Dyke

5: Mafic to intermediate metavolcanic rocks

6: Felsic to intermediate metavolcanic rocks

7: Metasedimentary rocks

10: Mafic and ultramafic rocks

11: Gneissic tonalite suite

15: Massive granodiorite suite

24: Animikie Gp.

31: Sibley Gp.

32: Osler Gp., Mamainse Point Fm., Michipicoten Island Fm.

34: Mafic intrusive rocks (Keweenawan age)

Map Parameters

Illumination: inclination 50°, declination 270°

Spatial Filter (half-wavelength): 1000 m

Eötvös

141.1

107.4

81.3

65.6

57.2

48.5

39.7

32.8

28.5

24.3

20.2

16.4

13.1

10.1

7.3

4.6

2.1

-0.2

-2.3

-4.2

-5.9

-7.6

-9.4

-11.3

-13.1

-14.9

-16.8

-18.8

-20.9

-23.0

-25.2

-27.4

-29.6

-31.8

-34.0

-36.3

-38.6

-41.1

-43.6

-46.3

-49.2

-52.5

-55.7

-59.7

-64.3

-69.6

-74.3

-80.3

-88.0

-100.7

-142.5



BASE DATA: National Topographic Database - NRCAN

GEOLOGY DATA: OGS Dataset MRD 126-Rev 1

DATUM: NAD83

PROJECTION: Universal Transverse Mercator (UTM Zone 16N)

Scale 1 : 130 000

km 0 1 2 3 4 5 km

Airborne Geophysics

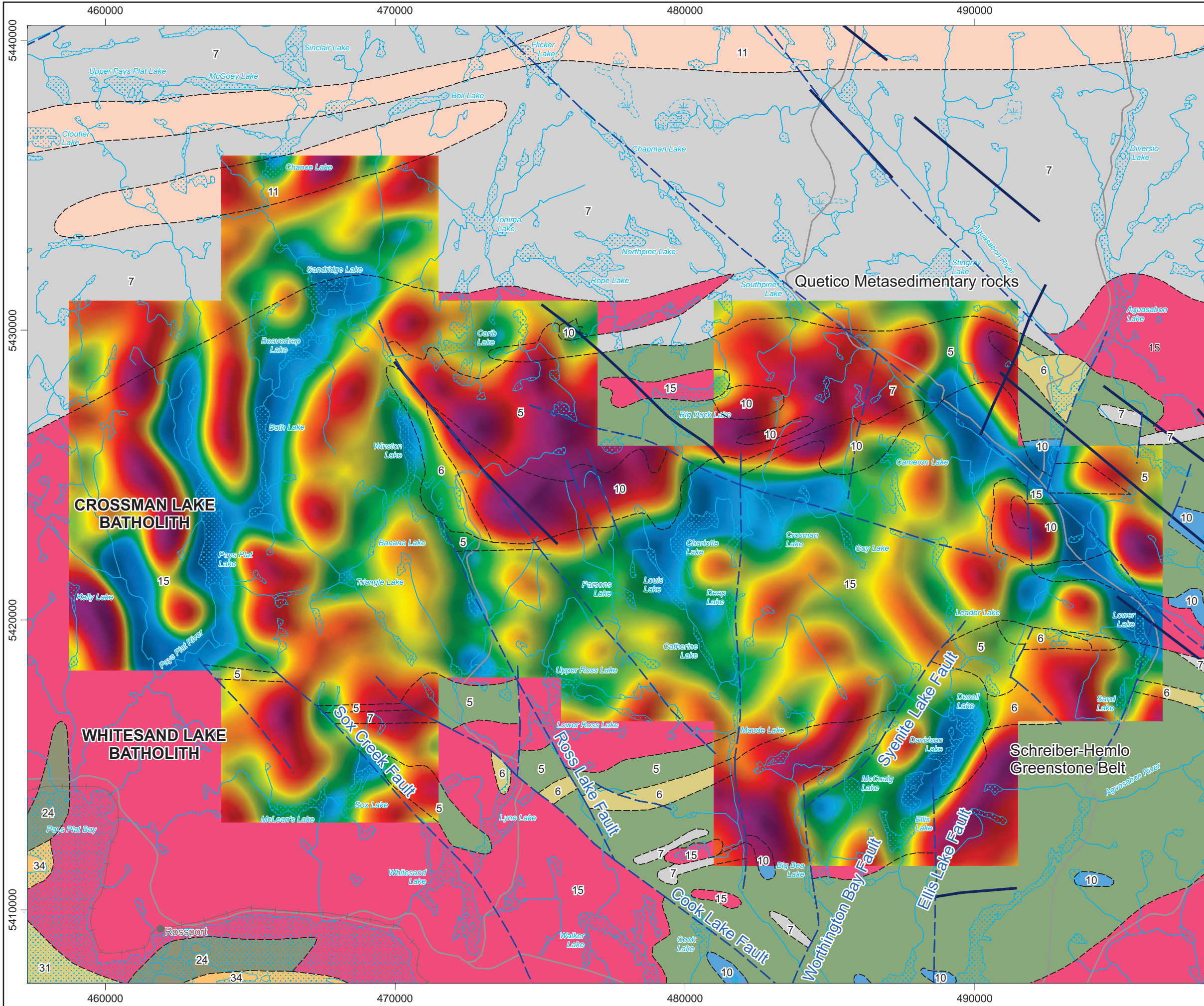
Acquisition and Interpretation

Schreiber Area, Ontario 2014

First Vertical Derivative

of the Free Air Gravity (25 m cell)

	DESIGN	JK	29/01/2015	REV. 1.1
	GIS	YC, AP	04/02/2015	FIGURE: 4.13
	DATA	MM, DK	04/02/2015	
	QC	MB	04/02/2015	



Legend

Hydrography

Road

Railway

Geology

Fault

Dyke

- 5: Mafic to intermediate metavolcanic rocks
- 6: Felsic to intermediate metavolcanic rocks
- 7: Metasedimentary rocks
- 10: Mafic and ultramafic rocks
- 11: Gneissic tonalite suite
- 15: Massive granodiorite suite
- 24: Animikie Gp.
- 31: Sibley Gp.
- 32: Osler Gp., Mamaise Point Fm., Michipicoten Island Fm.
- 34: Mafic intrusive rocks (Keweenawan age)

Map Parameters

Illumination: inclination 50°, declination 270°

Spatial Filter (half-wavelength): 1000 m

Eötvös

157.7
109.6
94.4
84.4
76.0
68.9
62.8
57.8
52.9
47.9
43.0
38.3
33.9
30.1
26.4
22.8
19.4
16.2
13.3
10.3
7.4
4.4
1.7
-0.9
-3.3
-5.5
-7.6
-9.7
-12.0
-14.2
-16.6
-19.1
-21.7
-24.5
-27.3
-30.3
-33.3
-36.5
-39.7
-42.9
-46.4
-50.4
-54.5
-59.5
-65.5
-72.2
-79.7
-89.4
-102.8
-120.7
-181.1



BASE DATA: National Topographic Database - NRCAN
 GEOLOGY DATA: OGS Dataset MRD 126-Rev 1
 DATUM: NAD83
 PROJECTION: Universal Transverse Mercator (UTM Zone 16N)

Scale 1 : 130 000

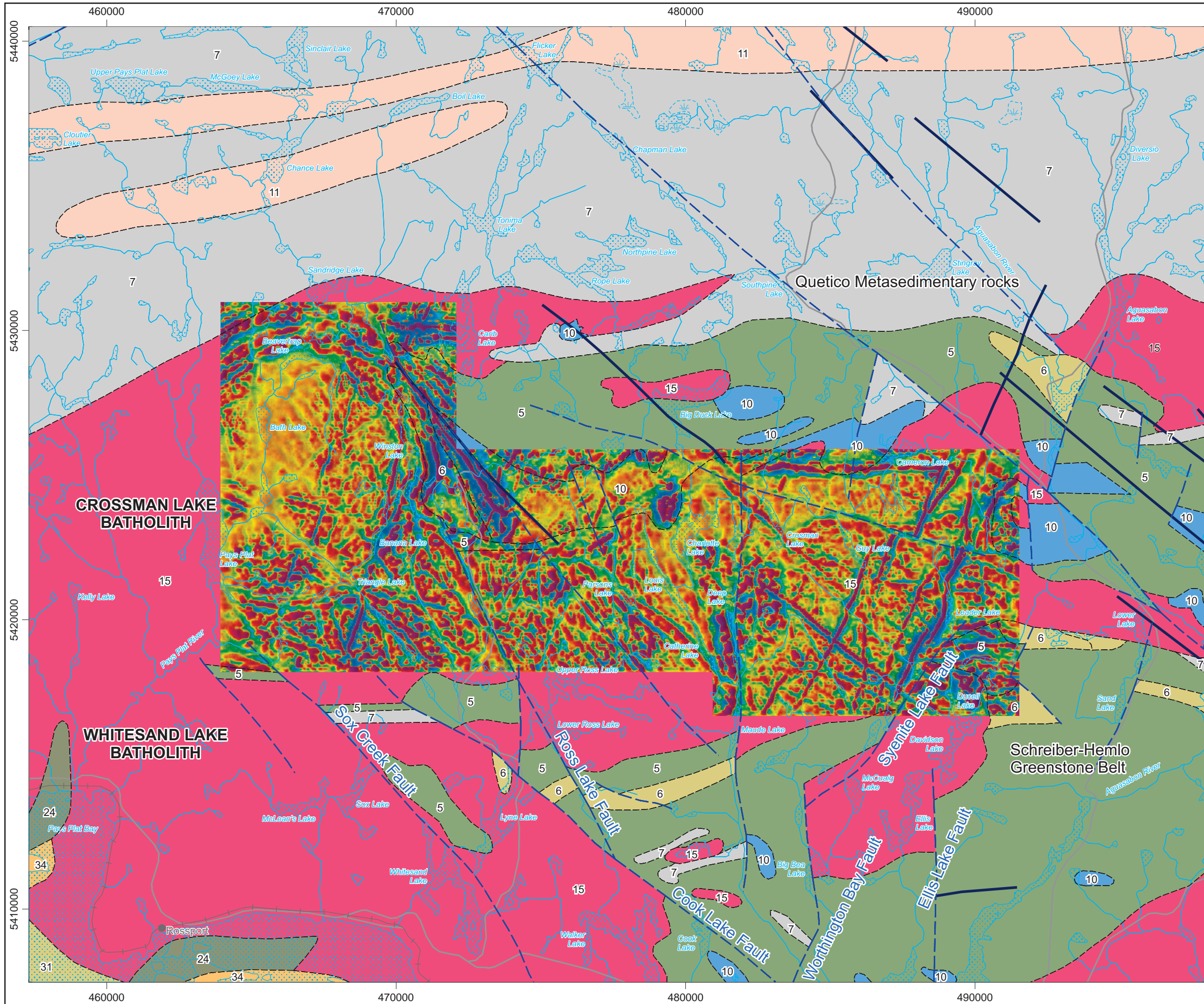
km 0 1 2 3 4 5 km

**Airborne Geophysics
 Acquisition and Interpretation**

Schreiber Area, Ontario 2014

**First Vertical Derivative
 of the Free Air Gravity (250 m cell)**

	DESIGN	JK	29/01/2015	REV. 1.1
	GIS	YC, AP	04/02/2015	FIGURE: 4.14
	DATA	MM, DK	04/02/2015	
	QC	MB	04/02/2015	



Legend

Hydrography

Road

Railway

Geology

Fault

Dyke

5: Mafic to intermediate metavolcanic rocks

6: Felsic to intermediate metavolcanic rocks

7: Metasedimentary rocks

10: Mafic and ultramafic rocks

11: Gneissic tonalite suite

15: Massive granodiorite suite

24: Animikie Gp.

31: Sibley Gp.

32: Osler Gp., Mamainse Point Fm., Michipicoten Island Fm.

34: Mafic intrusive rocks (Keweenawan age)

Map Parameters

Illumination: inclination 50°, declination 270°

nT/km2

499330.6

13192.1

8321.0

6133.3

4791.1

3880.2

3224.5

2696.4

2287.8

1939.5

1644.8

1390.1

1167.6

977.2

806.3

654.8

520.2

399.8

294.8

200.0

110.7

23.6

-59.8

-142.6

-224.6

-309.3

-396.2

-488.2

-583.8

-683.7

-790.6

-902.4

-1020.5

-1147.1

-1278.8

-1418.6

-1576.3

-1747.6

-1934.7

-2136.5

-2361.5

-2612.4

-2902.7

-3231.2

-3636.7

-4108.6

-4727.6

-5601.7

-7004.9

-10142.1

-187107.4



BASE DATA: National Topographic Database - NRCAN
 GEOLOGY DATA: OGS Dataset MRD 126-Rev 1
 DATUM: NAD83
 PROJECTION: Universal Transverse Mercator (UTM Zone 16N)

Scale 1 : 130 000

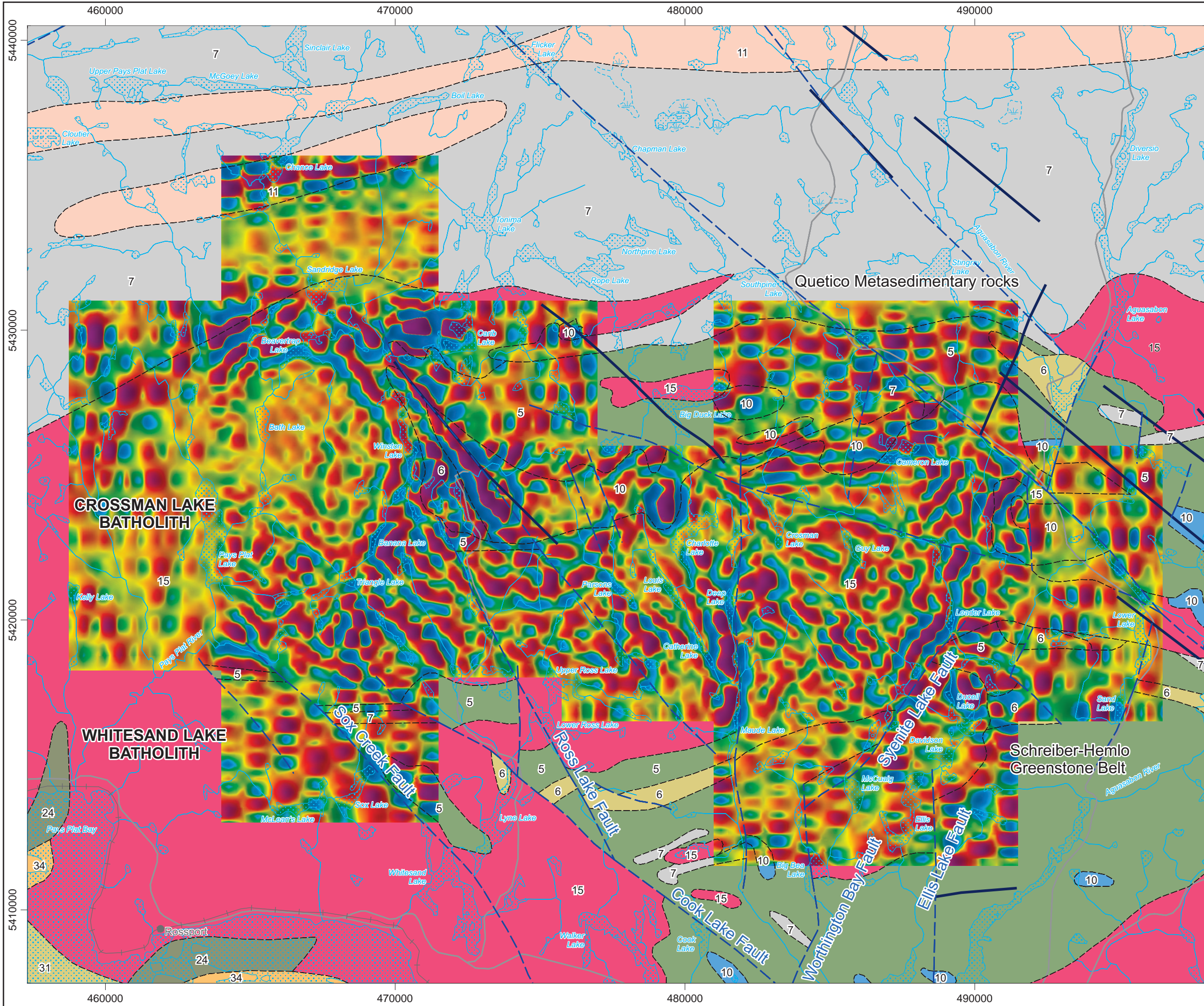
km 0 1 2 3 4 5 km

**Airborne Geophysics
 Acquisition and Interpretation**

Schreiber Area, Ontario 2014

**Second Vertical Derivative of the
 Reduction to the Pole of the Total Magnetic Intensity
 (25 m cell)**

	DESIGN	JK	29/01/2015	REV. 1.1
	GIS	YC, AP	04/02/2015	FIGURE: 4.15
	DATA	MM, DK	04/02/2015	
	QC	MB	04/02/2015	



Legend

Hydrography

Road

Railway

Geology

Fault

Dyke

5: Mafic to intermediate metavolcanic rocks

6: Felsic to intermediate metavolcanic rocks

7: Metasedimentary rocks

10: Mafic and ultramafic rocks

11: Gneissic tonalite suite

15: Massive granodiorite suite

24: Animikie Gp.

31: Sibley Gp.

32: Osler Gp., Mamainse Point Fm., Michipicoten Island Fm.

34: Mafic intrusive rocks (Keweenawan age)

Map Parameters

Illumination: inclination 50°, declination 270°

nT/km²

29788.6

3535.3

2434.2

1891.1

1535.6

1281.1

1087.8

930.3

804.6

699.1

607.9

529.4

459.8

395.8

339.0

287.5

240.4

197.7

158.4

121.3

86.6

53.7

22.2

-8.2

-38.8

-68.5

-98.0

-127.2

-157.0

-188.4

-221.3

-255.9

-292.4

-332.5

-375.7

-423.4

-476.0

-532.5

-594.0

-661.4

-734.9

-817.4

-912.0

-1020.8

-1146.9

-1299.7

-1488.5

-1737.2

-2103.1

-2835.3

-15047.3



BASE DATA: National Topographic Database - NRCAN
 GEOLOGY DATA: OGS Dataset MRD 126-Rev 1
 DATUM: NAD83
 PROJECTION: Universal Transverse Mercator (UTM Zone 16N)

Scale 1 : 130 000

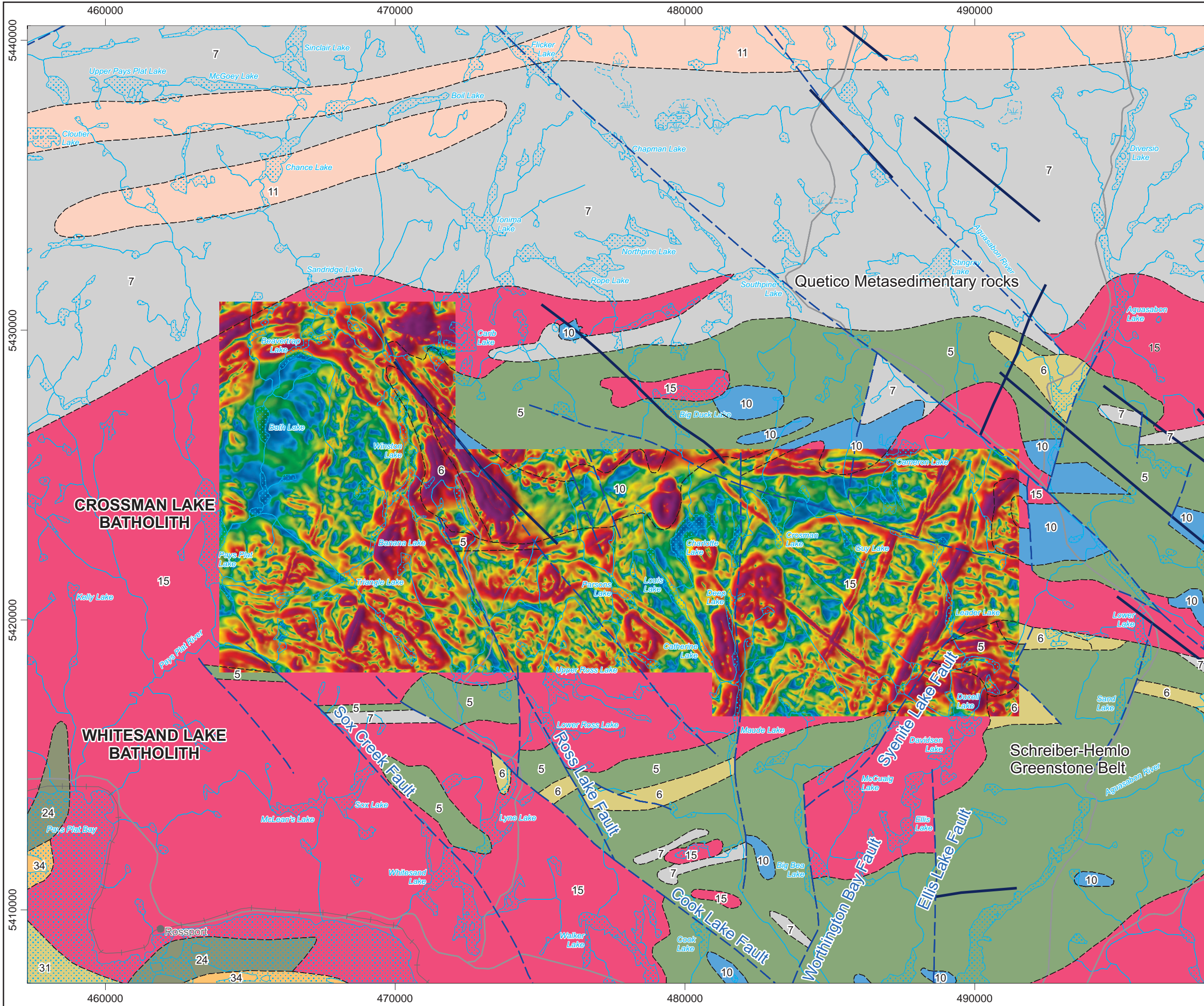
km 0 1 2 3 4 5 km

**Airborne Geophysics
 Acquisition and Interpretation**

Schreiber Area, Ontario 2014

**Second Vertical Derivative of the
 Reduction to the Pole of the Total Magnetic Intensity
 (250 m cell)**

	DESIGN	JK	29/01/2015	REV. 1.1
	GIS	YC, AP	04/02/2015	FIGURE: 4.16
	DATA	MM, DK	04/02/2015	
	QC	MB	04/02/2015	



Legend

Hydrography

Road

Railway

Geology

Fault

Dyke

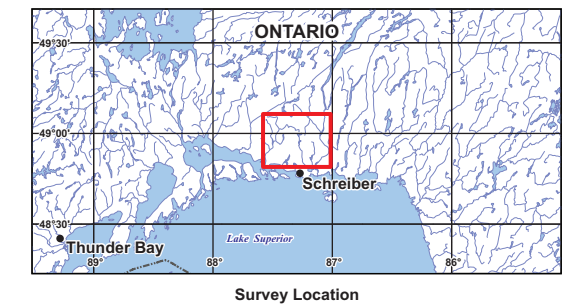
- 5: Mafic to intermediate metavolcanic rocks
- 6: Felsic to intermediate metavolcanic rocks
- 7: Metasedimentary rocks
- 10: Mafic and ultramafic rocks
- 11: Gneissic tonalite suite
- 15: Massive granodiorite suite
- 24: Animikie Gp.
- 31: Sibley Gp.
- 32: Osler Gp., Mamainse Point Fm., Michipicoten Island Fm.
- 34: Mafic intrusive rocks (Keweenawan age)

Map Parameters

Illumination: inclination 50°, declination 270°

nT/km

14941.2
1393.8
975.7
796.6
689.5
614.8
557.0
509.5
468.6
434.0
404.3
378.2
355.5
334.8
316.0
299.1
283.7
269.4
256.1
243.6
231.6
220.4
209.8
199.9
190.4
181.4
172.7
164.4
156.5
149.0
141.8
134.8
128.1
121.5
115.1
108.9
103.0
97.2
91.5
86.1
80.6
75.4
70.0
64.4
58.7
52.6
46.2
39.4
31.8
21.9
0.5



BASE DATA: National Topographic Database - NRCAN
 GEOLOGY DATA: OGS Dataset MRD 126-Rev 1
 DATUM: NAD83
 PROJECTION: Universal Transverse Mercator (UTM Zone 16N)

Scale 1 : 130 000

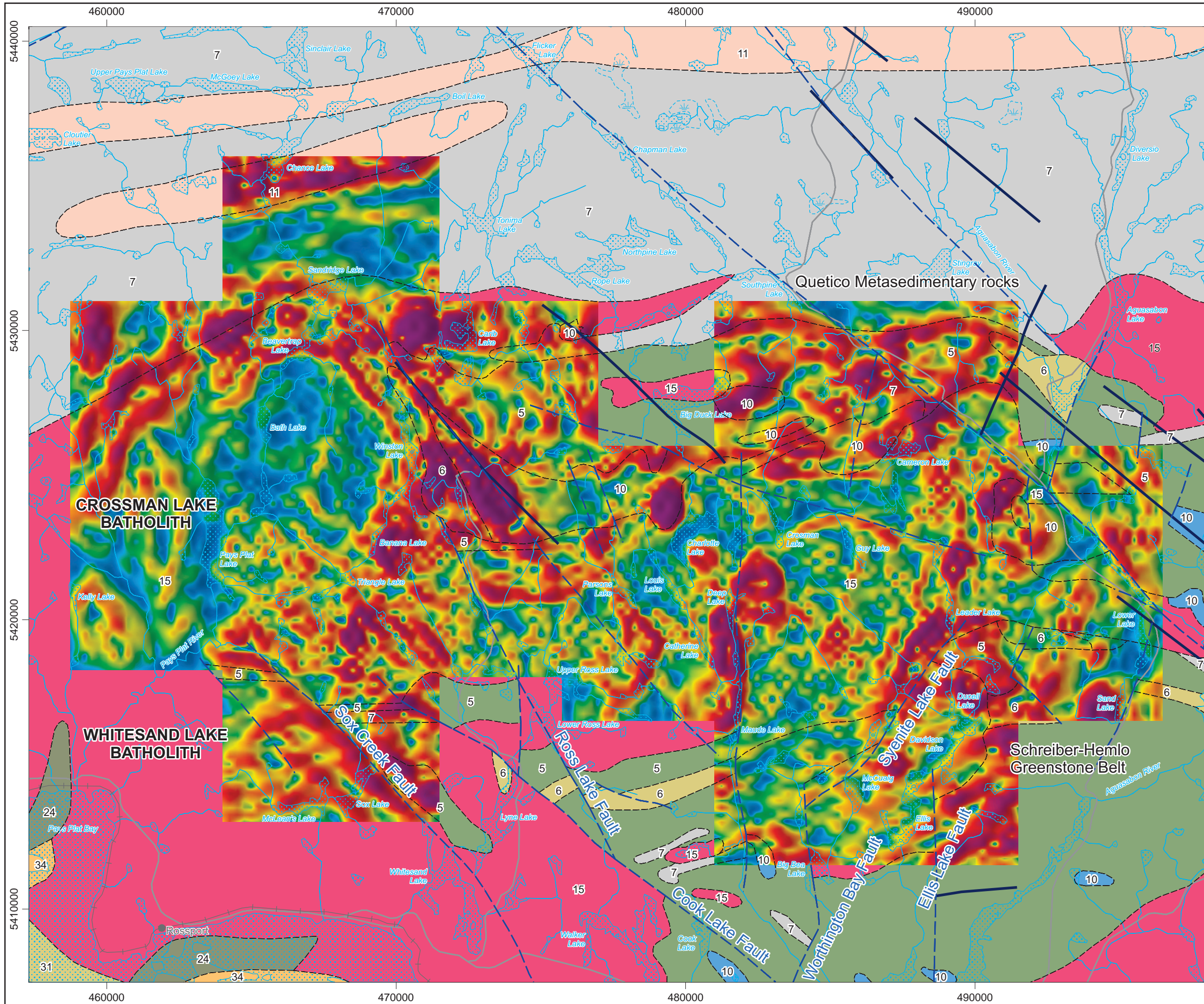
km 0 1 2 3 4 5 km

**Airborne Geophysics
 Acquisition and Interpretation**

Schreiber Area, Ontario 2014

Total Horizontal Derivative of the
 Reduction to the Pole of the Total Magnetic Intensity
 (25 m cell)

	DESIGN	JK	29/01/2015	REV. 1.1
	GIS	YC, AP	04/02/2015	FIGURE: 4.17
	DATA	MM, DK	04/02/2015	
	QC	MB	04/02/2015	



Legend

Hydrography

Road

Railway

Geology

Fault

Dyke

- 5: Mafic to intermediate metavolcanic rocks
- 6: Felsic to intermediate metavolcanic rocks
- 7: Metasedimentary rocks
- 10: Mafic and ultramafic rocks
- 11: Gneiss tonalite suite
- 15: Massive granodiorite suite
- 24: Animikie Gp.
- 31: Sibley Gp.
- 32: Osler Gp., Mamainse Point Fm., Michipicoten Island Fm.
- 34: Mafic intrusive rocks (Keweenawan age)

Map Parameters

Illumination: inclination 50°, declination 270°

nT/km

3248.8
780.6
607.5
516.1
460.9
420.4
388.0
360.6
337.1
316.5
298.8
283.5
269.8
257.0
245.1
234.0
223.9
214.3
205.4
197.0
189.1
181.6
174.4
167.6
161.1
155.0
149.1
143.5
138.0
132.6
127.3
122.2
117.2
112.2
107.4
102.4
97.5
92.6
87.9
83.4
78.8
74.3
69.8
65.2
60.2
55.1
49.7
43.8
37.1
28.1
-18.9



BASE DATA: National Topographic Database - NRCAN
 GEOLOGY DATA: OGS Dataset MRD 126-Rev 1
 DATUM: NAD83
 PROJECTION: Universal Transverse Mercator (UTM Zone 16N)

Scale 1 : 130 000

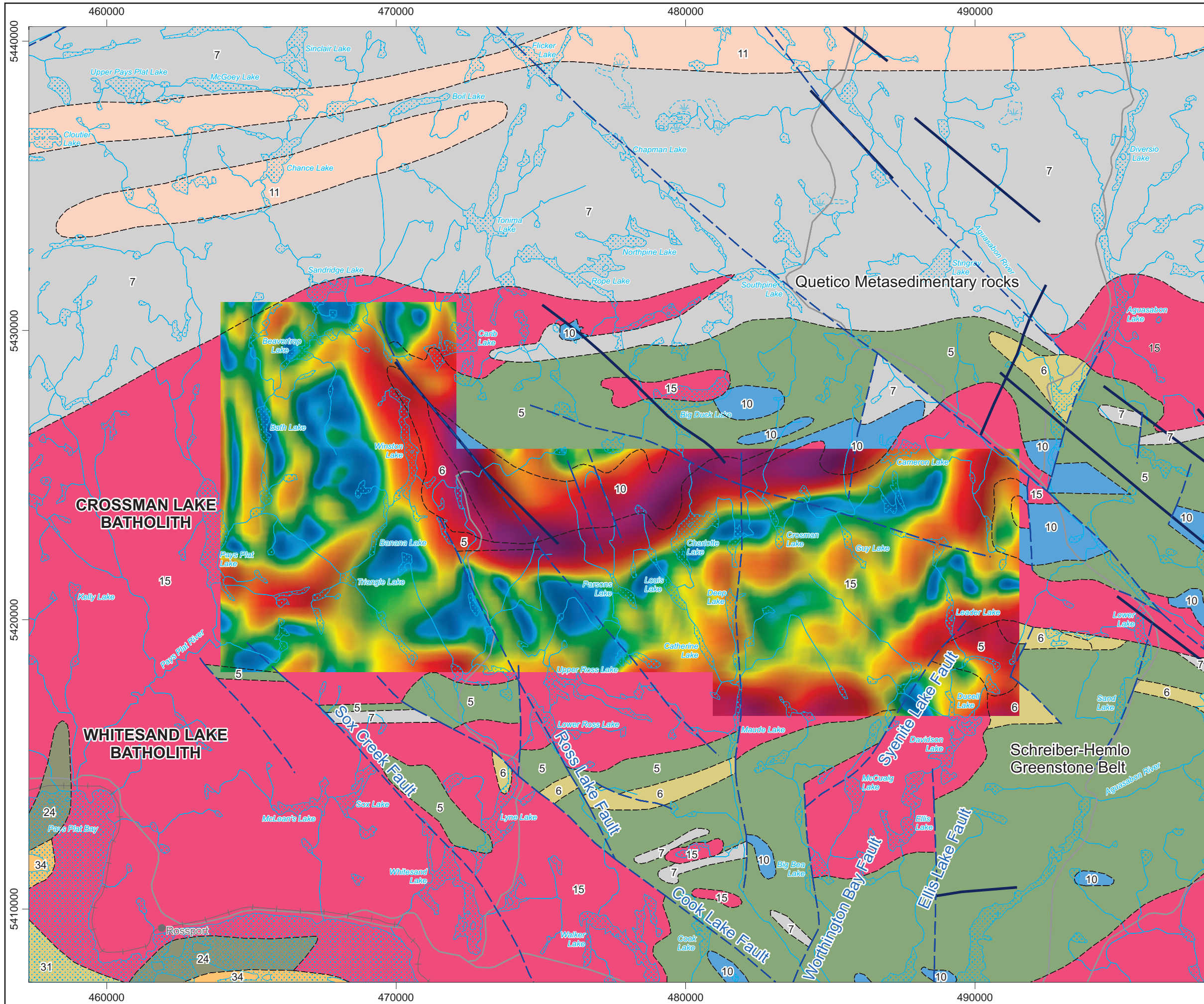
km 0 1 2 3 4 5 km

**Airborne Geophysics
 Acquisition and Interpretation**

Schreiber Area, Ontario 2014

**Total Horizontal Derivative of the
 Reduction to the Pole of the Total Magnetic Intensity
 (250 m cell)**

	DESIGN	JK	29/01/2015	REV. 1.1
	GIS	YC, AP	04/02/2015	FIGURE: 4.18
	DATA	MM, DK	04/02/2015	
	QC	MB	04/02/2015	



Legend

- Hydrography
- Road
- Railway

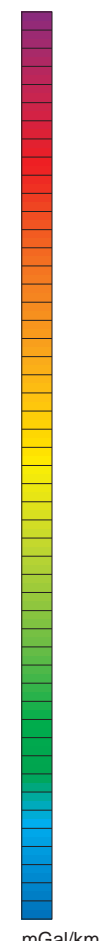
Geology

- Fault
- Dyke

- 5: Mafic to intermediate metavolcanic rocks
- 6: Felsic to intermediate metavolcanic rocks
- 7: Metasedimentary rocks
- 10: Mafic and ultramafic rocks
- 11: Gneissic tonalite suite
- 15: Massive granodiorite suite
- 24: Animikie Gp.
- 31: Sibley Gp.
- 32: Osler Gp., Mamainse Point Fm., Michipicoten Island Fm.
- 34: Mafic intrusive rocks (Keweenawan age)

Map Parameters

Illumination: inclination 50°, declination 270°
 Spatial Filter (half-wavelength): 1000 m
 Bouguer Density: 2.67 g/cm³



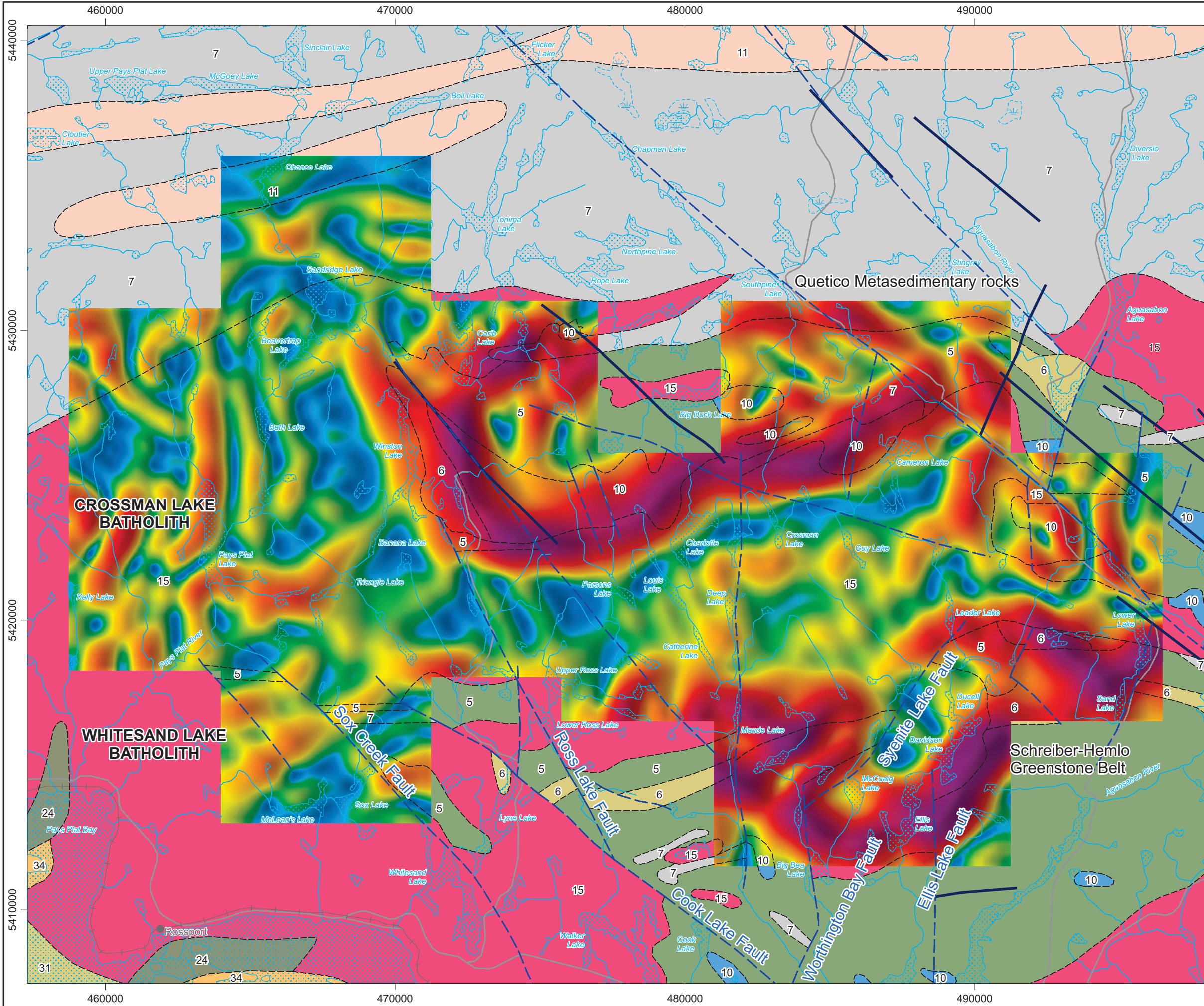
BASE DATA: National Topographic Database - NRCAN
 GEOLOGY DATA: OGS Dataset MRD 126-Rev 1
 DATUM: NAD83
 PROJECTION: Universal Transverse Mercator (UTM Zone 16N)



**Airborne Geophysics
 Acquisition and Interpretation**
 Schreiber Area, Ontario 2014

**Total Horizontal Derivative of the Bouguer Gravity
 (Density: 2.67 g/cm³) (25 m cell)**

	DESIGN	JK	29/01/2015	REV. 1.1
	GIS	YC, AP	04/02/2015	FIGURE: 4.19
	DATA	MM, DK	04/02/2015	
	QC	MB	04/02/2015	



Legend

Hydrography

Road

Railway

Geology

Fault

Dyke

5: Mafic to intermediate metavolcanic rocks

6: Felsic to intermediate metavolcanic rocks

7: Metasedimentary rocks

10: Mafic and ultramafic rocks

11: Gneissic tonalite suite

15: Massive granodiorite suite

24: Animikie Gp.

31: Sibley Gp.

32: Osler Gp., Mamainse Point Fm., Michipicoten Island Fm.

34: Mafic intrusive rocks (Keweenawan age)

Map Parameters

Illumination: inclination 50°, declination 270°

Spatial Filter (half-wavelength): 1000 m

Bouguer Density: 2.67 g/cm³

mGal/km



BASE DATA: National Topographic Database - NRCAN
 GEOLOGY DATA: OGS Dataset MRD 126-Rev 1
 DATUM: NAD83
 PROJECTION: Universal Transverse Mercator (UTM Zone 16N)

Scale 1 : 130 000

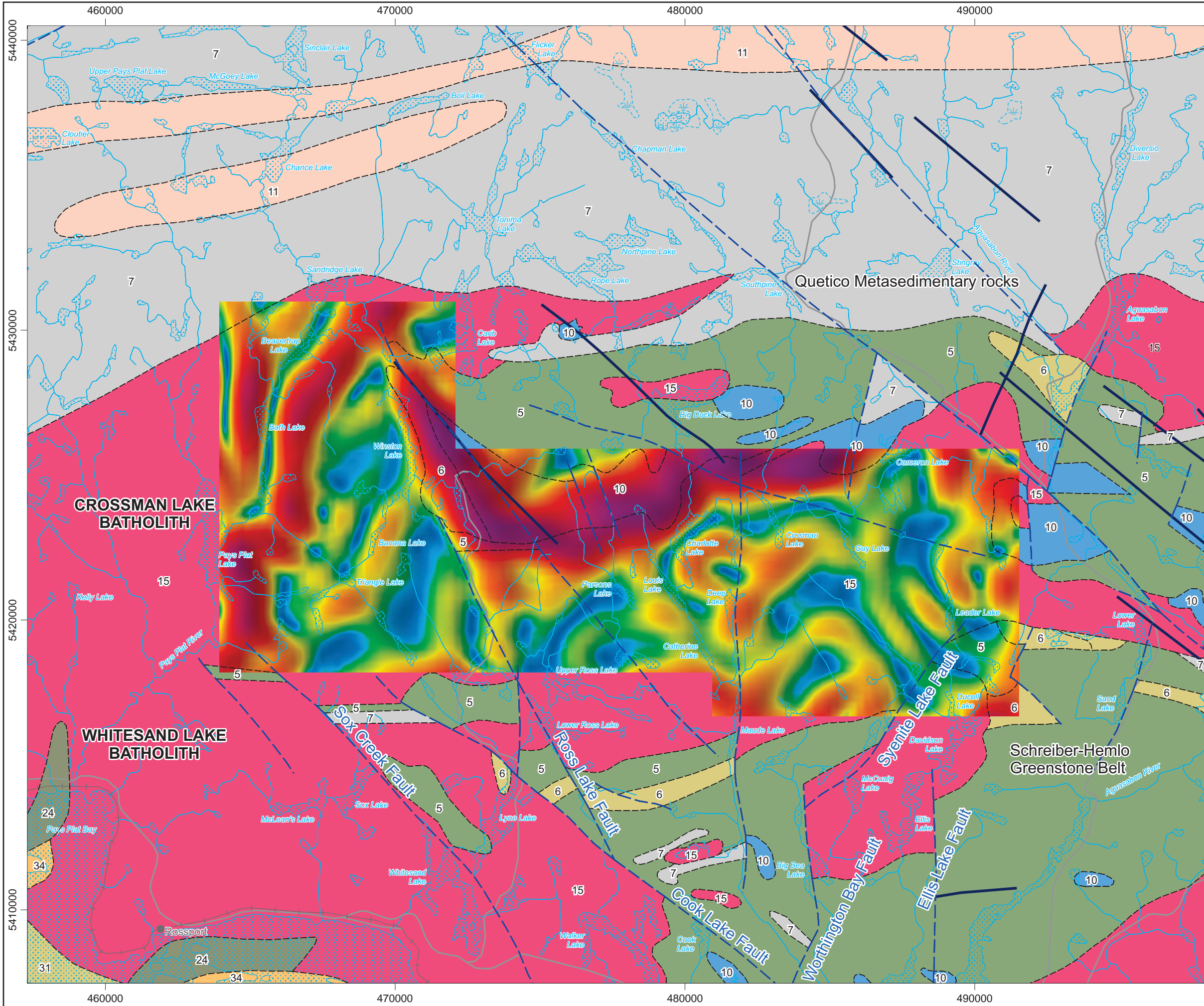
km 0 1 2 3 4 5 km

**Airborne Geophysics
 Acquisition and Interpretation**

Schreiber Area, Ontario 2014

**Total Horizontal Derivative of the Bouguer Gravity
 (Density: 2.67 g/cm³) (250 m cell)**

	DESIGN	JK	29/01/2015	REV. 1.1
	GIS	YC, AP	04/02/2015	FIGURE: 4.20
	DATA	MM, DK	04/02/2015	
	QC	MB	04/02/2015	



Legend

Hydrography

Road

Railway

Geology

Fault

Dyke

- 5: Mafic to intermediate metavolcanic rocks
- 6: Felsic to intermediate metavolcanic rocks
- 7: Metasedimentary rocks
- 10: Mafic and ultramafic rocks
- 11: Gneissic tonalite suite
- 15: Massive granodiorite suite
- 24: Animikie Gp.
- 31: Sibley Gp.
- 32: Osler Gp., Mamainse Point Fm., Michipicoten Island Fm.
- 34: Mafic intrusive rocks (Keweenawan age)

Map Parameters

Illumination: inclination 50°, declination 270°

Spatial Filter (half-wavelength): 1000 m

mGal/km



BASE DATA: National Topographic Database - NRCAN
 GEOLOGY DATA: OGS Dataset MRD 126-Rev 1
 DATUM: NAD83
 PROJECTION: Universal Transverse Mercator (UTM Zone 16N)

Scale 1 : 130 000

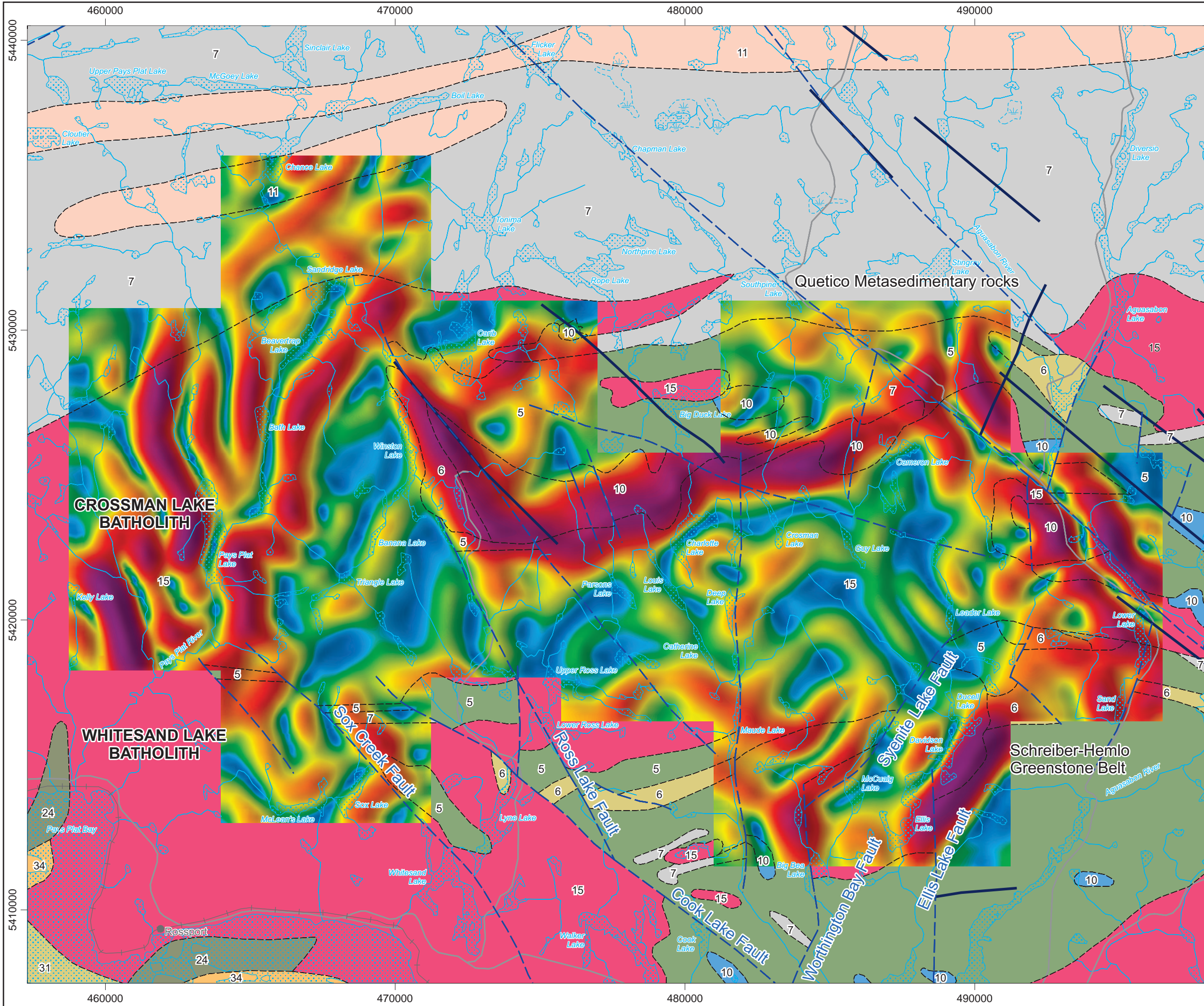
km 0 1 2 3 4 5 km

**Airborne Geophysics
 Acquisition and Interpretation**

Schreiber Area, Ontario 2014

**Total Horizontal Derivative
 of the Free Air Gravity (25 m cell)**

	DESIGN	JK	29/01/2015	REV. 1.1
	GIS	YC, AP	04/02/2015	FIGURE: 4.21
	DATA	MM, DK	04/02/2015	
	QC	MB	04/02/2015	



Legend

Hydrography

Road

Railway

Geology

Fault

Dyke

5: Mafic to intermediate metavolcanic rocks

6: Felsic to intermediate metavolcanic rocks

7: Metasedimentary rocks

10: Mafic and ultramafic rocks

11: Gneissic tonalite suite

15: Massive granodiorite suite

24: Animikie Gp.

31: Sibley Gp.

32: Osler Gp., Mamaise Point Fm., Michipicoten Island Fm.

34: Mafic intrusive rocks (Keweenawan age)

Map Parameters

Illumination: inclination 50°, declination 270°

Spatial Filter (half-wavelength): 1000 m

mGal/km

17.20
12.02
10.87
10.06
9.34
8.77
8.23
7.77
7.39
7.04
6.73
6.46
6.22
6.01
5.80
5.60
5.41
5.22
5.05
4.89
4.74
4.60
4.46
4.32
4.17
4.03
3.89
3.76
3.63
3.50
3.37
3.25
3.13
3.00
2.87
2.75
2.63
2.50
2.38
2.25
2.12
1.98
1.83
1.69
1.54
1.39
1.23
1.06
0.86
0.61
-0.06



BASE DATA: National Topographic Database - NRCAN
 GEOLOGY DATA: OGS Dataset MRD 126-Rev 1
 DATUM: NAD83
 PROJECTION: Universal Transverse Mercator (UTM Zone 16N)

Scale 1 : 130 000

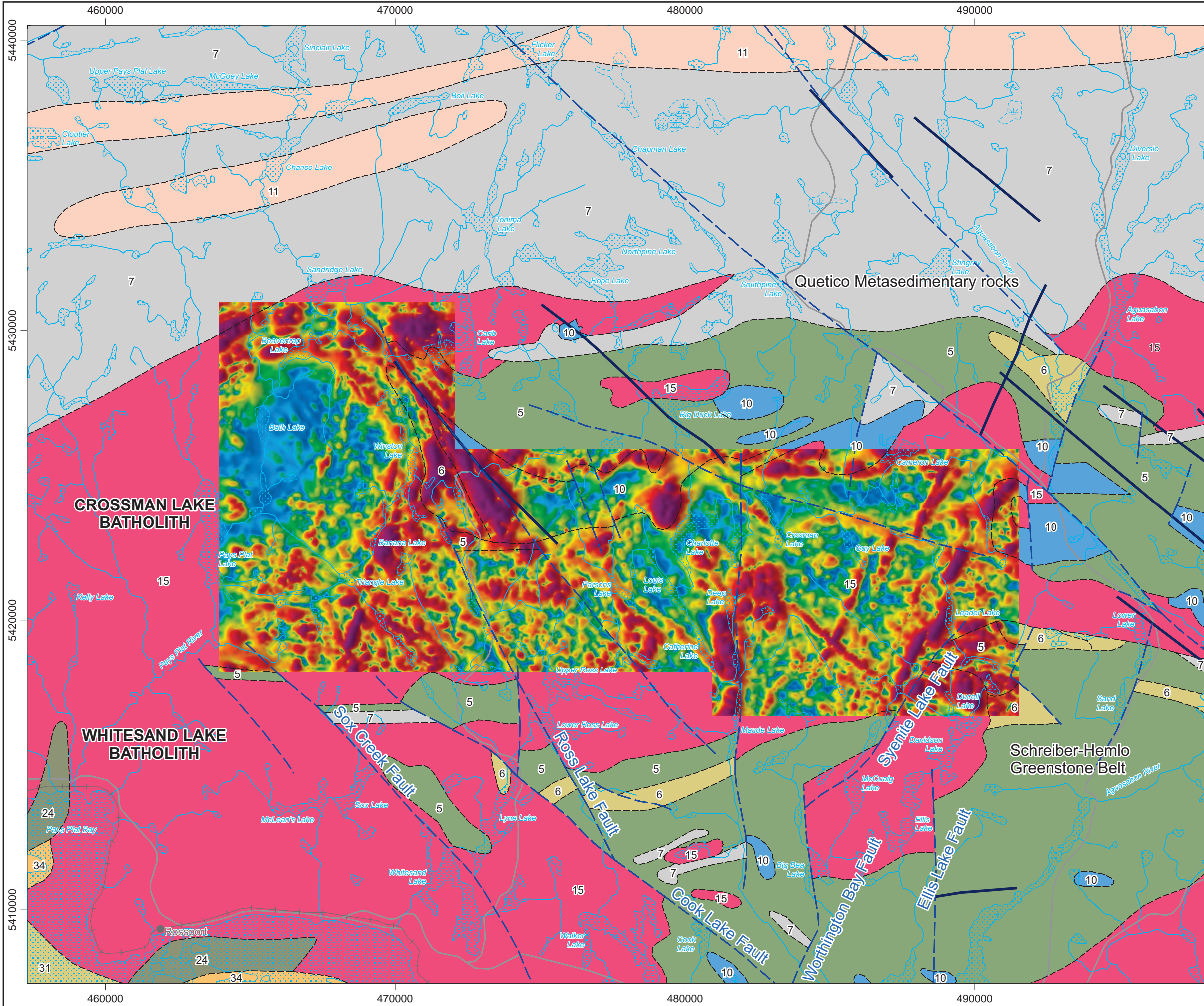
km 0 1 2 3 4 5 km

**Airborne Geophysics
 Acquisition and Interpretation**

Schreiber Area, Ontario 2014

**Total Horizontal Derivative
 of the Free Air Gravity (250 m cell)**

	DESIGN	JK	29/01/2015	REV. 1.1
	GIS	YC, AP	04/02/2015	FIGURE: 4.22
	DATA	MM, DK	04/02/2015	
	QC	MB	04/02/2015	



Legend

Hydrography

Road

Railway

Geology

Fault

Dyke

- 5: Mafic to intermediate metavolcanic rocks
- 6: Felsic to intermediate metavolcanic rocks
- 7: Metasedimentary rocks
- 10: Mafic and ultramafic rocks
- 11: Gneissic tonalite suite
- 15: Massive granodiorite suite
- 24: Animikie Gp.
- 31: Sibley Gp.
- 32: Osler Gp., Mamainse Point Fm., Michipicoten Island Fm.
- 34: Mafic intrusive rocks (Keweenawan age)

Map Parameters

Illumination: inclination 50°, declination 270°

nT/km



BASE DATA: National Topographic Database - NRCAN
 GEOLOGY DATA: OGS Dataset MRD 126-Rev 1
 DATUM: NAD83
 PROJECTION: Universal Transverse Mercator (UTM Zone 16N)

Scale 1 : 130 000

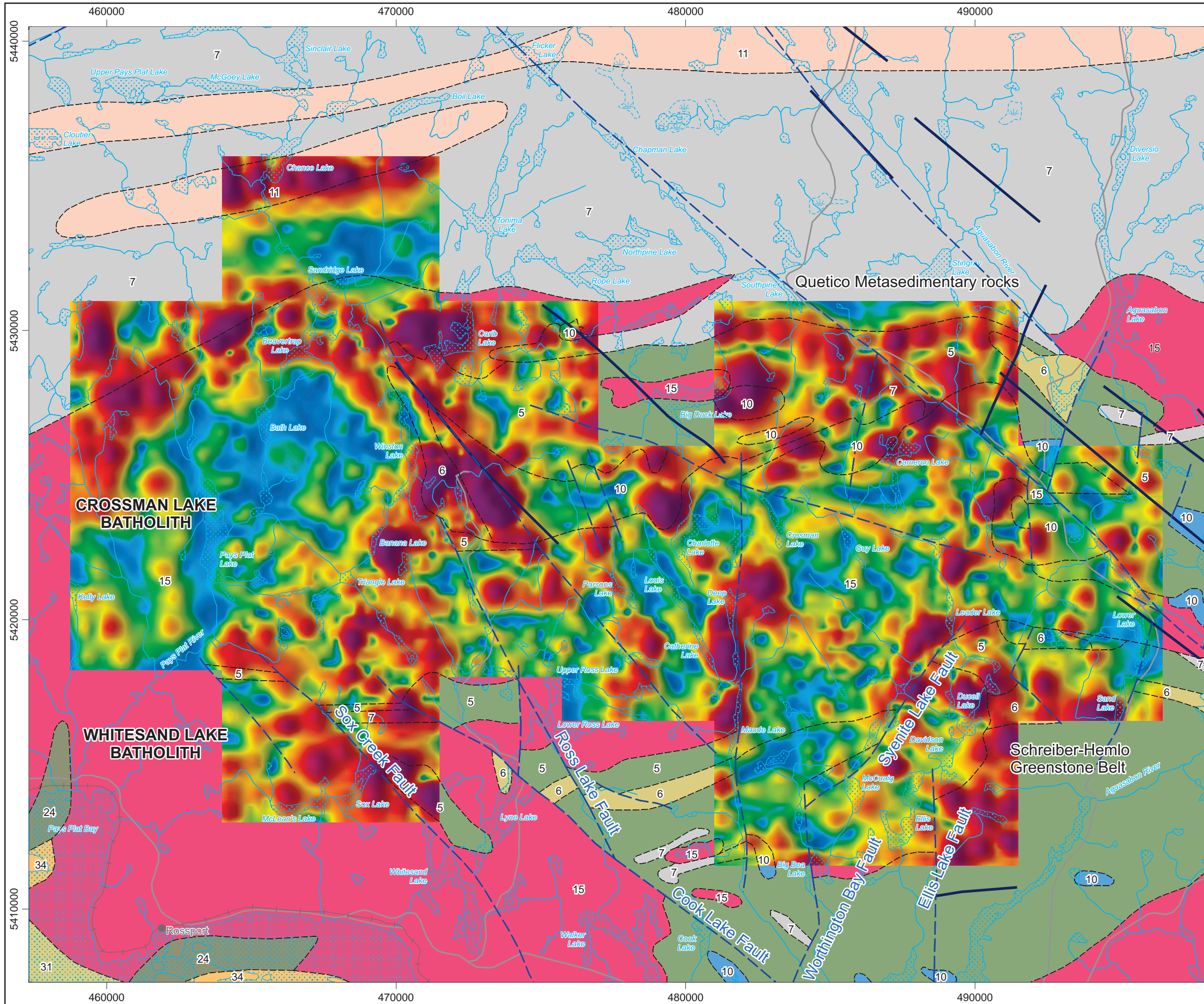
km 0 1 2 3 4 5 km

**Airborne Geophysics
 Acquisition and Interpretation**

Schreiber Area, Ontario 2014

**Analytic Signal
 of the Total Magnetic Intensity (25 m cell)**

	DESIGN	JK	29/01/2015	REV. 1.1
	GIS	YC, AP	04/02/2015	FIGURE: 4.23
	DATA	MM, DK	04/02/2015	
	QC	MB	04/02/2015	



Legend

Hydrography

Road

Railway

Geology

Fault

Dyke

- 5: Mafic to intermediate metavolcanic rocks
- 6: Felsic to intermediate metavolcanic rocks
- 7: Metasedimentary rocks
- 10: Mafic and ultramafic rocks
- 11: Gneissic tonalite suite
- 15: Massive granodiorite suite
- 24: Animikie Gp.
- 31: Sibley Gp.
- 32: Osler Gp., Mamainse Point Fm., Michipicoten Island Fm.
- 34: Mafic intrusive rocks (Keweenawan age)

Map Parameters

Illumination: inclination 50°, declination 270°

nT/km



BASE DATA: National Topographic Database - NRCAN
 GEOLOGY DATA: OGS Dataset MRD 126-Rev 1
 DATUM: NAD83
 PROJECTION: Universal Transverse Mercator (UTM Zone 16N)

Scale 1 : 130 000

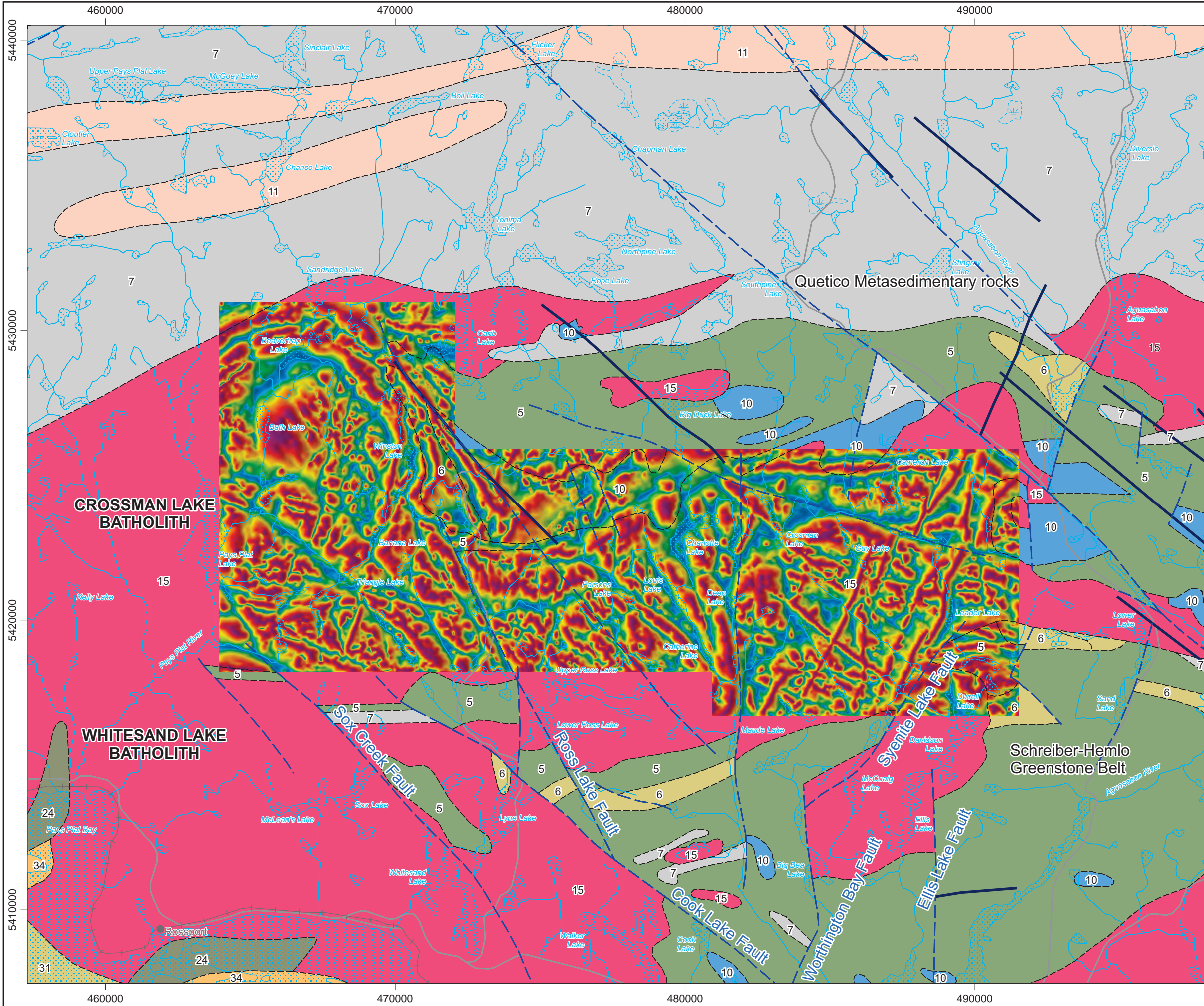
km 0 1 2 3 4 5 km

**Airborne Geophysics
 Acquisition and Interpretation**

Schreiber Area, Ontario 2014

**Analytic Signal
 of the Total Magnetic Intensity (250 m cell)**

	DESIGN	JK	29/01/2015	REV. 1.1
	GIS	YC, AP	04/02/2015	FIGURE: 4.24
	DATA	MM, DK	04/02/2015	
	QC	MB	04/02/2015	



Legend

Hydrography

Road

Railway

Geology

Fault

Dyke

5: Mafic to intermediate metavolcanic rocks

6: Felsic to intermediate metavolcanic rocks

7: Metasedimentary rocks

10: Mafic and ultramafic rocks

11: Gneissic tonalite suite

15: Massive granodiorite suite

24: Animikie Gp.

31: Sibley Gp.

32: Osler Gp., Mamainse Point Fm., Michipicoten Island Fm.

34: Mafic intrusive rocks (Keweenawan age)

Map Parameters

Illumination: inclination 50°, declination 270°

degrees



BASE DATA: National Topographic Database - NRCAN
 GEOLOGY DATA: OGS Dataset MRD 126-Rev 1
 DATUM: NAD83
 PROJECTION: Universal Transverse Mercator (UTM Zone 16N)

Scale 1 : 130 000

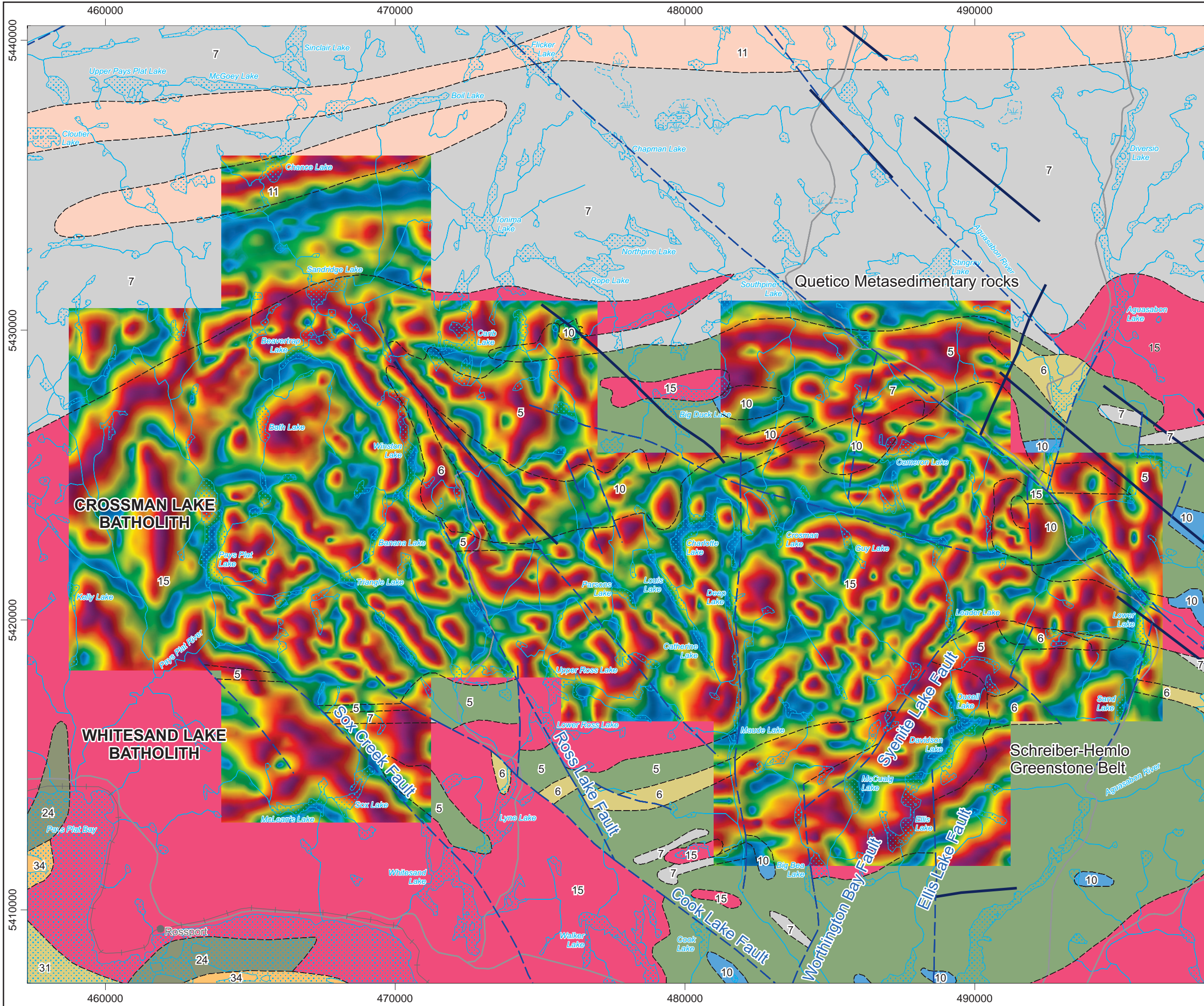
km 0 1 2 3 4 5 km

**Airborne Geophysics
 Acquisition and Interpretation**

Schreiber Area, Ontario 2014

Tilt Angle of the Reduction to the Pole
 of the Total Magnetic Intensity (25 m cell)

	DESIGN	JK	29/01/2015	REV. 1.1
	GIS	YC, AP	04/02/2015	FIGURE: 4.25
	DATA	MM, DK	04/02/2015	
	QC	MB	04/02/2015	



Legend

Hydrography

Road

Railway

Geology

Fault

Dyke

5: Mafic to intermediate metavolcanic rocks

6: Felsic to intermediate metavolcanic rocks

7: Metasedimentary rocks

10: Mafic and ultramafic rocks

11: Gneissic tonalite suite

15: Massive granodiorite suite

24: Animikie Gp.

31: Sibley Gp.

32: Osler Gp., Mamainse Point Fm., Michipicoten Island Fm.

34: Mafic intrusive rocks (Keweenawan age)

Map Parameters

Illumination: inclination 50°, declination 270°

degrees



BASE DATA: National Topographic Database - NRCAN
 GEOLOGY DATA: OGS Dataset MRD 126-Rev 1
 DATUM: NAD83
 PROJECTION: Universal Transverse Mercator (UTM Zone 16N)

Scale 1 : 130 000

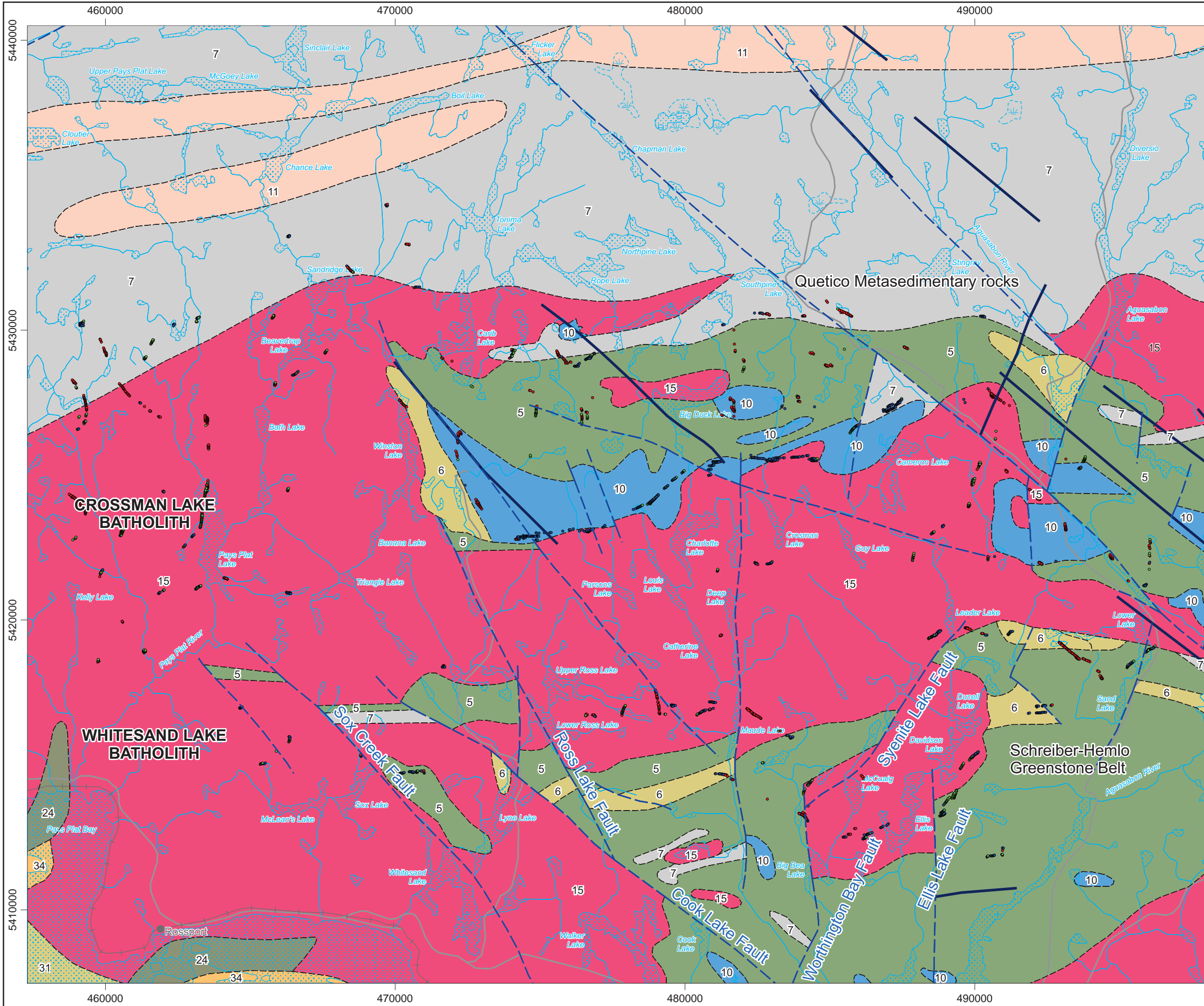
km 0 1 2 3 4 5 km

**Airborne Geophysics
 Acquisition and Interpretation**

Schreiber Area, Ontario 2014

Tilt Angle of the Reduction to the Pole
 of the Total Magnetic Intensity (250 m cell)

	DESIGN	JK	29/01/2015	REV. 1.1
	GIS	YC, AP	04/02/2015	FIGURE: 4.26
	DATA	MM, DK	04/02/2015	
	QC	MB	04/02/2015	

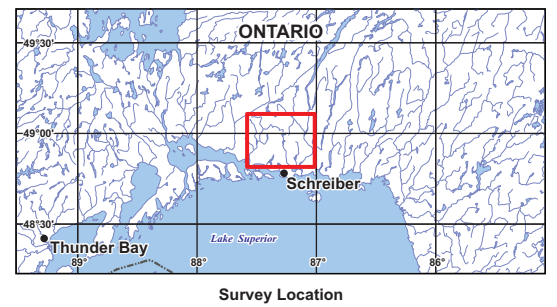


- Legend**
- Hydrography
 - Road
 - Railway
- Geology**
- Fault
 - Dyke
- 5: Mafic to intermediate metavolcanic rocks
 - 6: Felsic to intermediate metavolcanic rocks
 - 7: Metasedimentary rocks
 - 10: Mafic and ultramafic rocks
 - 11: Gneissic tonalite suite
 - 15: Massive granodiorite suite
 - 24: Animikie Gp.
 - 31: Sibley Gp.
 - 32: Osler Gp., Mamainse Point Fm., Michipicoten Island Fm.
 - 34: Mafic intrusive rocks (Keweenawan age)

- Interpreted and Mapped Features**
- OGS Dataset MRD 126-Rev 1 Surface Geology Mapping
- Trend analysis solutions**
- 0 - 50 m
 - 51 - 100 m
 - > 100 m

Map Parameters

Spatial Filter (half-wavelength): 1000 m
 Bouguer Density: 2.67 g/cm³



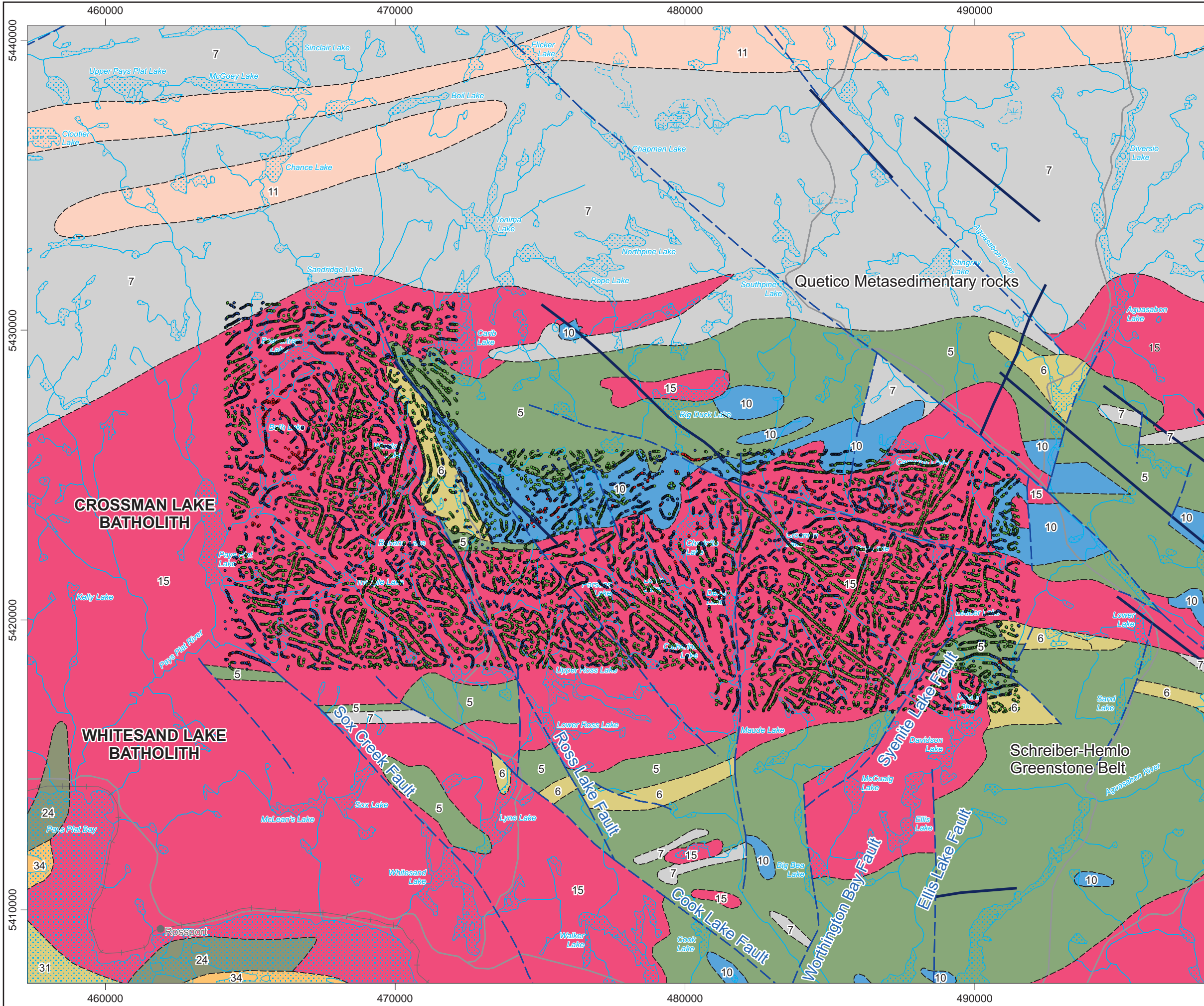
BASE DATA: National Topographic Database - NRCAN
 GEOLOGY DATA: OGS Dataset MRD 126-Rev 1
 DATUM: NAD83
 PROJECTION: Universal Transverse Mercator (UTM Zone 16N)



**Airborne Geophysics
 Acquisition and Interpretation**
 Schreiber Area, Ontario 2014

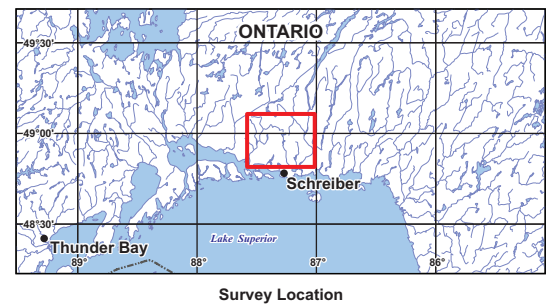
**Trend Analysis Solutions of Bouguer Gravity
 (terrain correction density = 2.67 g/cc)**

	DESIGN	JK	29/01/2015	REV. 1.1
	GIS	YC, AP	04/02/2015	FIGURE: 4.27
	DATA	MM, DK	04/02/2015	
	QC	MB	04/02/2015	



- Legend**
- Hydrography
 - Road
 - Railway
- Geology**
- Fault
 - Dyke
- 5: Mafic to intermediate metavolcanic rocks
 - 6: Felsic to intermediate metavolcanic rocks
 - 7: Metasedimentary rocks
 - 10: Mafic and ultramafic rocks
 - 11: Gneissic tonalite suite
 - 15: Massive granodiorite suite
 - 24: Animikie Gp.
 - 31: Sibley Gp.
 - 32: Osler Gp., Mamainse Point Fm., Michipicoten Island Fm.
 - 34: Mafic intrusive rocks (Keweenawan age)

- Interpreted and Mapped Features**
- OGS Dataset MRD 126-Rev 1 Surface Geology Mapping
- Trend analysis solutions**
- 0 - 100 m
 - 101 - 200 m
 - > 200 m



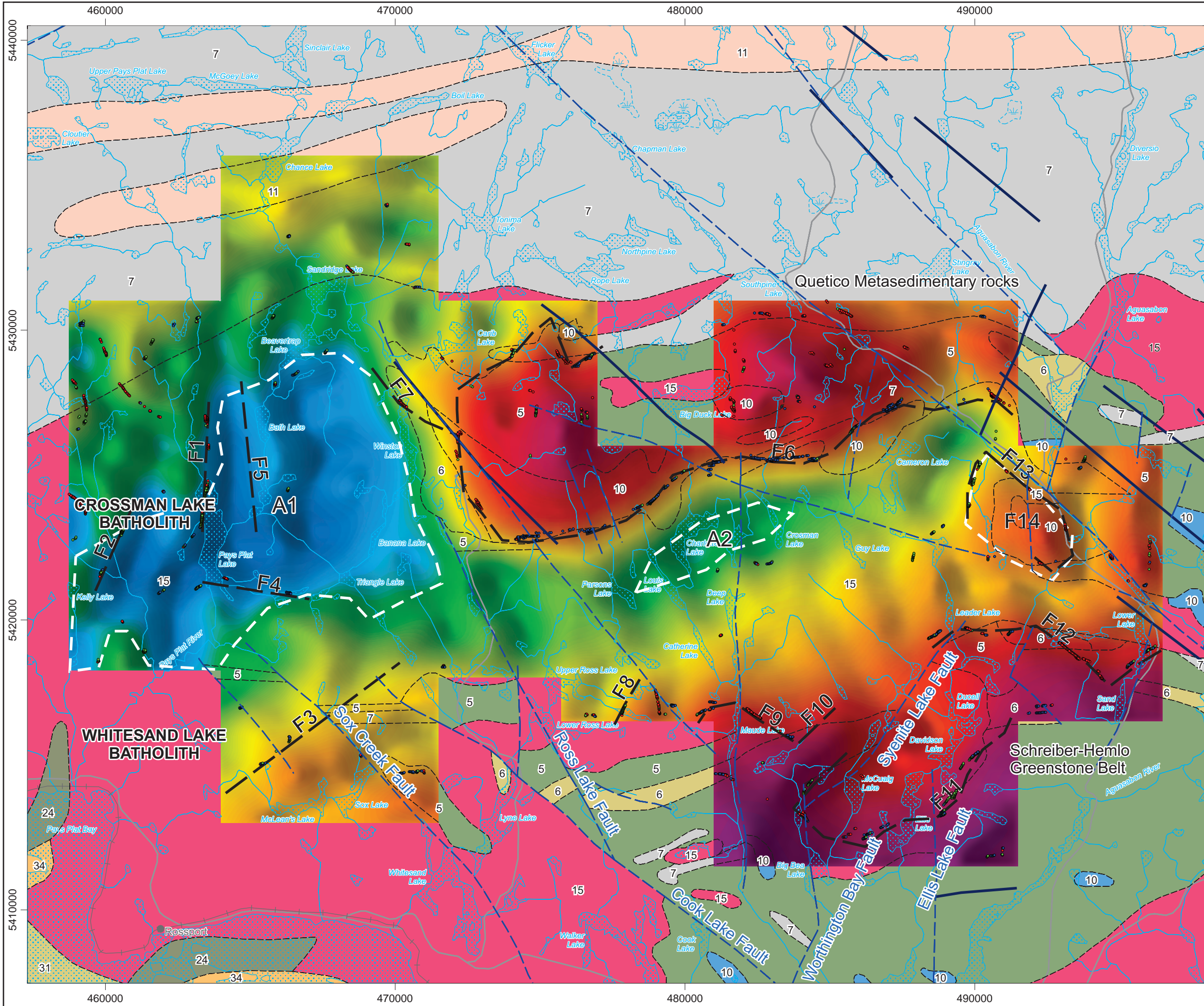
BASE DATA: National Topographic Database - NRCAN
 GEOLOGY DATA: OGS Dataset MRD 126-Rev 1
 DATUM: NAD83
 PROJECTION: Universal Transverse Mercator (UTM Zone 16N)



**Airborne Geophysics
 Acquisition and Interpretation**
 Schreiber Area, Ontario 2014

**Trend Analysis Solutions of Reduction to the Pole
 of the Total Magnetic Intensity**

	DESIGN	JK	29/01/2015	REV. 1.1
	GIS	YC, AP	04/02/2015	FIGURE: 4.28
	DATA	MM, DK	04/02/2015	
	QC	MB	04/02/2015	



Legend

Hydrography

Road

Railway

Geology

Fault

Dyke

5: Mafic to intermediate metavolcanic rocks

6: Felsic to intermediate metavolcanic rocks

7: Metasedimentary rocks

10: Mafic and ultramafic rocks

11: Gneissic tonalite suite

15: Massive granodiorite suite

24: Animikie Gp.

31: Sibley Gp.

32: Osler Gp., Mamaine Point Fm., Michipicoten Island Fm.

34: Mafic intrusive rocks (Keweenaw age)

Interpreted and Mapped Features

- - - Feature interpreted from horizontal derivative of Bouguer gravity

□ Area defined from horizontal derivative of Bouguer gravity

- - - OGS Dataset MRD 126-Rev 1 Surface Geology Mapping

Trend analysis solutions

• 0 - 100 m

• 101 - 200 m

• > 200 m

Map Parameters

Illumination: inclination 50°, declination 270°

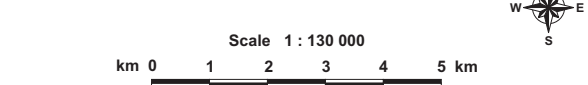
Spatial Filter (half-wavelength): 1000 m

Bouguer Density: 2.67 g/cm³

mGal



BASE DATA: National Topographic Database - NRCAN
 GEOLOGY DATA: OGS Dataset MRD 126-Rev 1
 DATUM: NAD83
 PROJECTION: Universal Transverse Mercator (UTM Zone 16N)

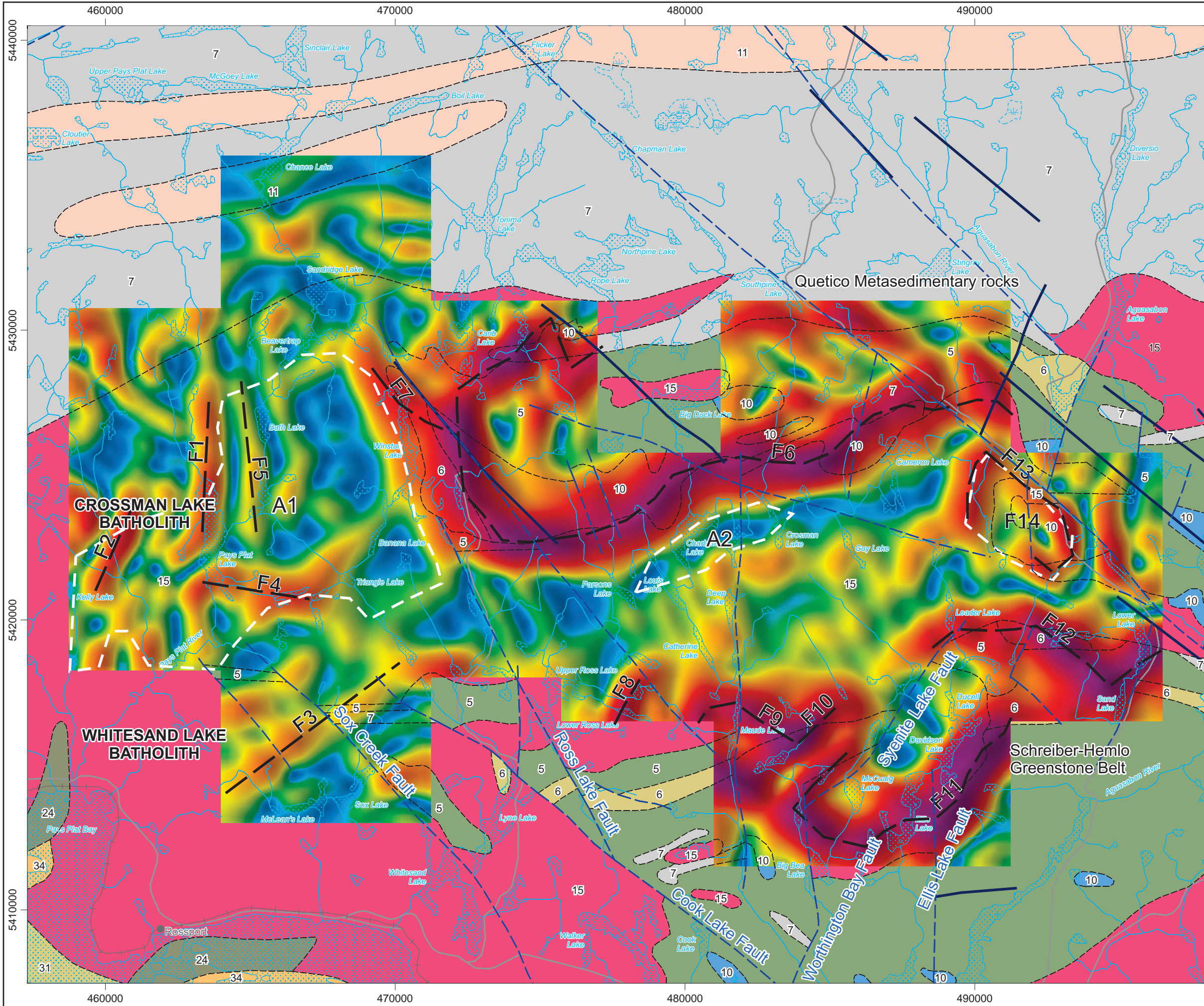


**Airborne Geophysics
 Acquisition and Interpretation**

Schreiber Area, Ontario 2014

**Bouguer Gravity
 (terrain correction density = 2.67 g/cc) (250 m cell)
 with Selected Interpreted Features
 and Trend Analysis solutions**

	DESIGN	JK	29/01/2015	REV. 1.1
	GIS	YC, AP	04/02/2015	FIGURE: 5.1
	DATA	MM, DK	04/02/2015	
	QC	MB	04/02/2015	



Legend

Hydrography

Road

Railway

Geology

Fault

Dyke

5: Mafic to intermediate metavolcanic rocks

6: Felsic to intermediate metavolcanic rocks

7: Metasedimentary rocks

10: Mafic and ultramafic rocks

11: Gneissic tonalite suite

15: Massive granodiorite suite

24: Animikie Gp.

31: Sibley Gp.

32: Osler Gp., Mamaine Point Fm., Michipicoten Island Fm.

34: Mafic intrusive rocks (Keweenawan age)

Interpreted and Mapped Features

- - - Feature interpreted from horizontal derivative of Bouguer gravity

□ Area defined from horizontal derivative of Bouguer gravity

- - - OGS Dataset MRD 126-Rev 1 Surface Geology Mapping

Map Parameters

Illumination: inclination 50°, declination 270°

Spatial Filter (half-wavelength): 1000 m

Bouguer Density: 2.67 g/cm³

mGal/km



BASE DATA: National Topographic Database - NRCAN
 GEOLOGY DATA: OGS Dataset MRD 126-Rev 1
 DATUM: NAD83
 PROJECTION: Universal Transverse Mercator (UTM Zone 16N)

Scale 1 : 130 000

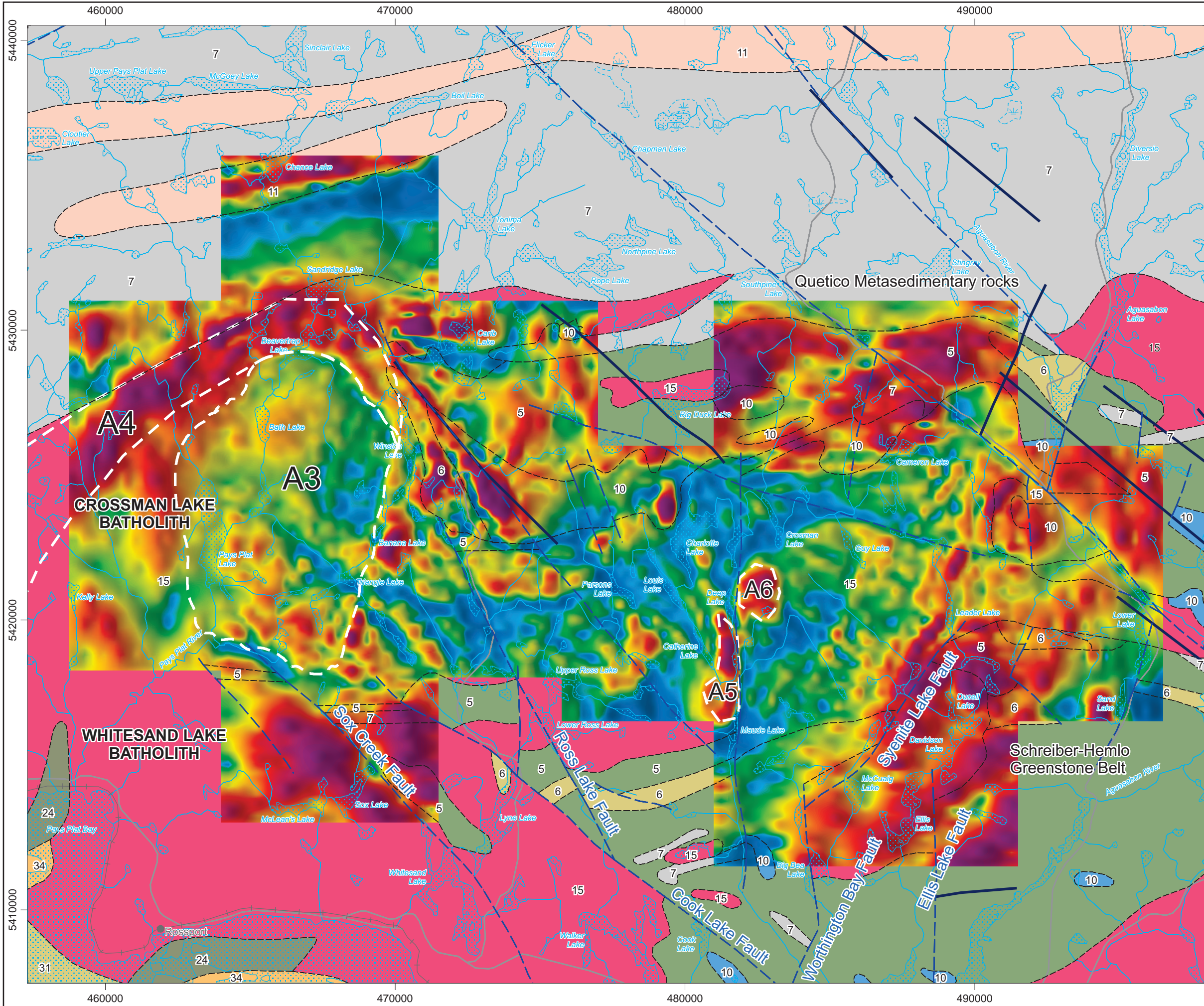
km 0 1 2 3 4 5 km

**Airborne Geophysics
 Acquisition and Interpretation**

Schreiber Area, Ontario 2014

**Horizontal Derivative of Bouguer Gravity
 (terrain correction density = 2.67 g/cc) (250 m cell)
 with Selected Interpreted Features**

	DESIGN	JK	29/01/2015	REV. 1.1
	GIS	YC, AP	04/02/2015	FIGURE: 5.2
	DATA	MM, DK	04/02/2015	
	QC	MB	04/02/2015	



Legend

Hydrography

Road

Railway

Geology

Fault

Dyke

5: Mafic to intermediate metavolcanic rocks

6: Felsic to intermediate metavolcanic rocks

7: Metasedimentary rocks

10: Mafic and ultramafic rocks

11: Gneissic tonalite suite

15: Massive granodiorite suite

24: Animikie Gp.

31: Sibley Gp.

32: Osler Gp., Mamaine Point Fm., Michipicoten Island Fm.

34: Mafic intrusive rocks (Keweenawan age)

Interpreted and Mapped Features

Area defined from Reduction to the Pole of the Total Magnetic Intensity

Area defined from First Vertical Derivative of the Reduction to the Pole of the Total Magnetic Intensity

OGS Dataset MRD 126-Rev 1 Surface Geology Mapping

Map Parameters

Illumination: inclination 50°, declination 270°

nT

1357.4

348.4

285.2

241.5

208.2

181.8

160.4

141.5

125.1

110.7

97.4

85.3

74.0

64.0

54.4

45.5

36.9

28.4

20.4

13.1

6.1

-0.7

-7.3

-13.5

-19.3

-24.8

-30.2

-35.8

-41.4

-46.9

-52.1

-57.1

-62.0

-66.8

-71.6

-76.4

-81.5

-86.9

-92.6

-98.7

-104.6

-110.6

-116.9

-123.6

-130.5

-137.5

-145.3

-154.0

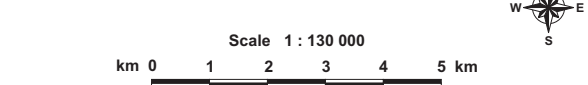
-165.7

-184.3

-339.9



BASE DATA: National Topographic Database - NRCAN
 GEOLOGY DATA: OGS Dataset MRD 126-Rev 1
 DATUM: NAD83
 PROJECTION: Universal Transverse Mercator (UTM Zone 16N)

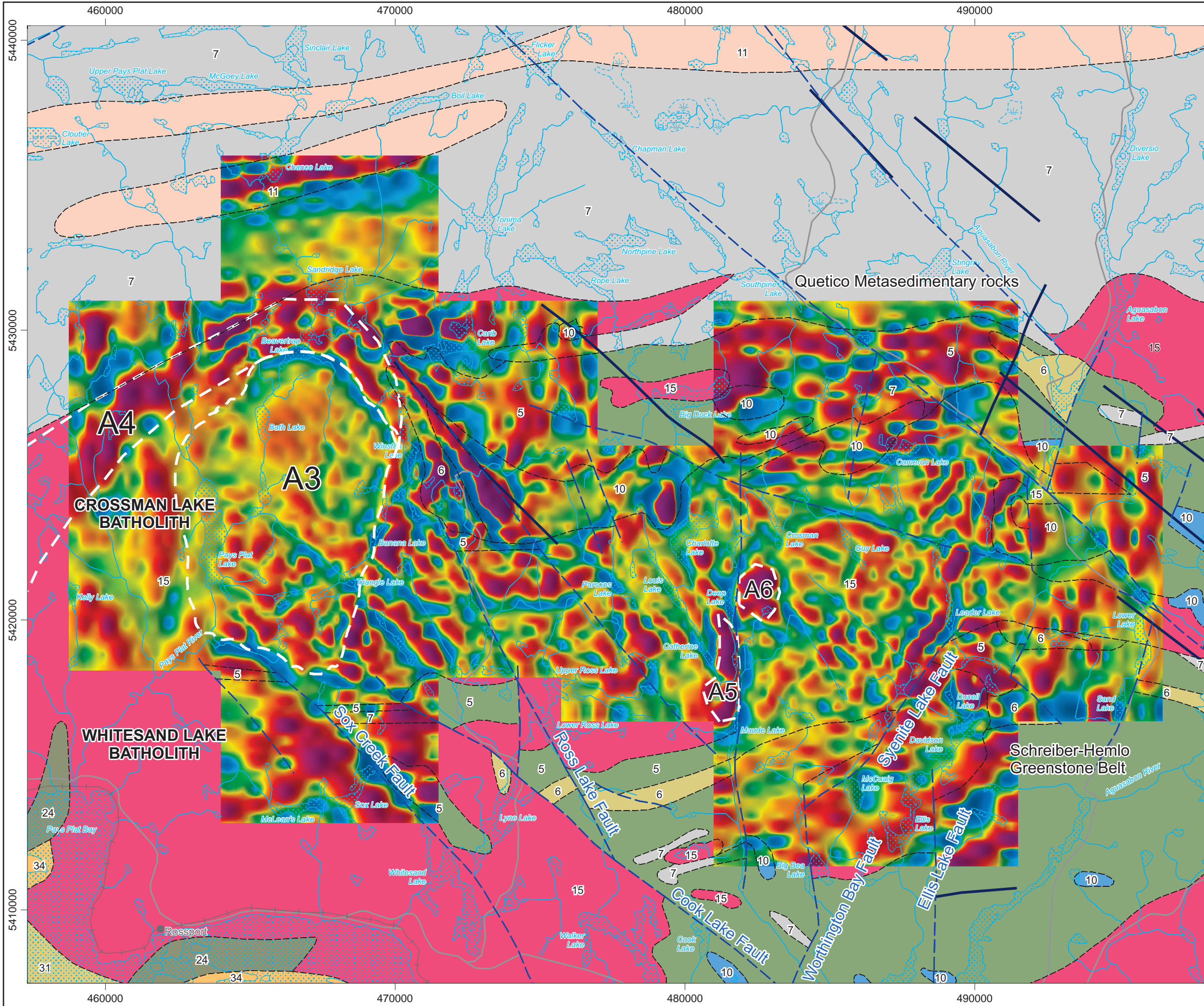


**Airborne Geophysics
 Acquisition and Interpretation**

Schreiber Area, Ontario 2014

**Reduction to the Pole
 of the Total Magnetic Intensity (250 m cell)
 with Selected Interpreted Features**

	DESIGN	JK	29/01/2015	REV. 1.1
	GIS	YC, AP	04/02/2015	FIGURE: 5.3
	DATA	MM, DK	04/02/2015	
	QC	MB	04/02/2015	



Legend

Hydrography

Road

Railway

Geology

Fault

Dyke

5: Mafic to intermediate metavolcanic rocks

6: Felsic to intermediate metavolcanic rocks

7: Metasedimentary rocks

10: Mafic and ultramafic rocks

11: Gneissic tonalite suite

15: Massive granodiorite suite

24: Animikie Gp.

31: Sibley Gp.

32: Osler Gp., Mamaine Point Fm., Michipicoten Island Fm.

34: Mafic intrusive rocks (Keweenaw age)

Interpreted and Mapped Features

- - - Feature interpreted from horizontal derivative of Bouguer gravity

Area defined from Reduction to the Pole of the Total Magnetic Intensity

Area defined from First Vertical Derivative of the Reduction to the Pole of the Total Magnetic Intensity

- - - OGS Dataset MRD 126-Rev 1 Surface Geology Mapping

Map Parameters

Illumination: inclination 50°, declination 270°

nT/km



BASE DATA: National Topographic Database - NRCAN
 GEOLOGY DATA: OGS Dataset MRD 126-Rev 1
 DATUM: NAD83
 PROJECTION: Universal Transverse Mercator (UTM Zone 16N)

Scale 1 : 130 000

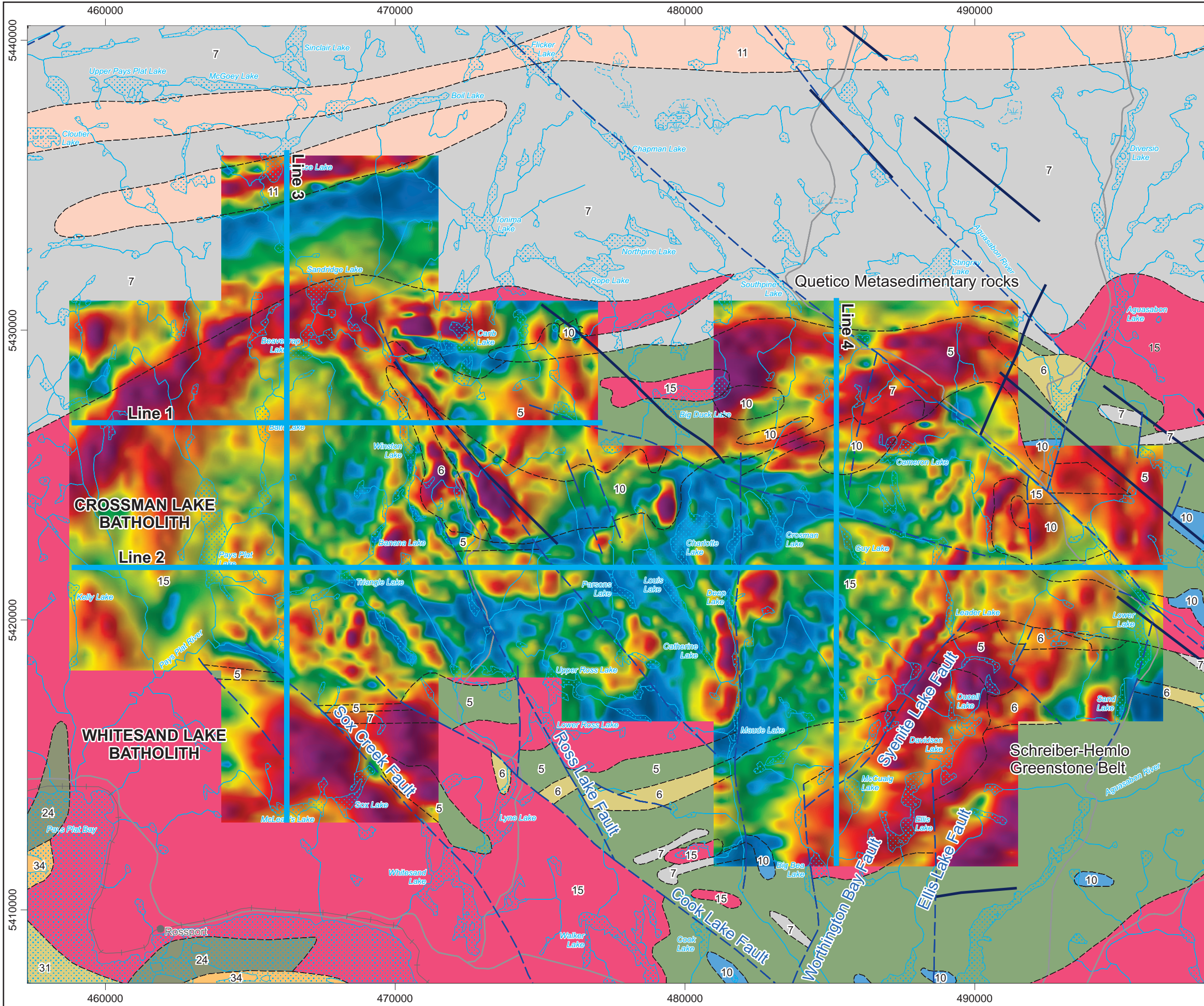
km 0 1 2 3 4 5 km

**Airborne Geophysics
 Acquisition and Interpretation**

Schreiber Area, Ontario 2014

First Vertical Derivative of the Reduction to the Pole
 of the Total Magnetic Intensity (250 m cell)
 with Selected Interpreted Features

	DESIGN	JK	29/01/2015	REV. 1.1
	GIS	YC, AP	04/02/2015	FIGURE: 5.4
	DATA	MM, DK	04/02/2015	
	QC	MB	04/02/2015	



Legend

Hydrography

Road

Railway

Geology

Fault

Dyke

5: Mafic to intermediate metavolcanic rocks

6: Felsic to intermediate metavolcanic rocks

7: Metasedimentary rocks

10: Mafic and ultramafic rocks

11: Gneissic tonalite suite

15: Massive granodiorite suite

24: Animikie Gp.

31: Sibley Gp.

32: Osler Gp., Mamainse Point Fm., Michipicoten Island Fm.

34: Mafic intrusive rocks (Keweenawan age)

Interpreted and Mapped Features

--- OGS Dataset MRD 126-Rev 1 Surface Geology Mapping

— 2.5D model line

Map Parameters

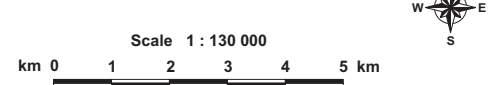
Illumination: inclination 50°, declination 270°

nT

1357.4
348.4
285.2
241.5
208.2
181.8
160.4
141.5
125.1
110.7
97.4
85.3
74.0
64.0
54.4
45.5
36.9
28.4
20.4
13.1
6.1
-0.7
-7.3
-13.5
-19.3
-24.8
-30.2
-35.8
-41.4
-46.9
-52.1
-57.1
-62.0
-66.8
-71.6
-76.4
-81.5
-86.9
-92.6
-98.7
-104.6
-110.6
-116.9
-123.6
-130.5
-137.5
-145.3
-154.0
-165.7
-184.3
-339.9



BASE DATA: National Topographic Database - NRCAN
 GEOLOGY DATA: OGS Dataset MRD 126-Rev 1
 DATUM: NAD83
 PROJECTION: Universal Transverse Mercator (UTM Zone 16N)

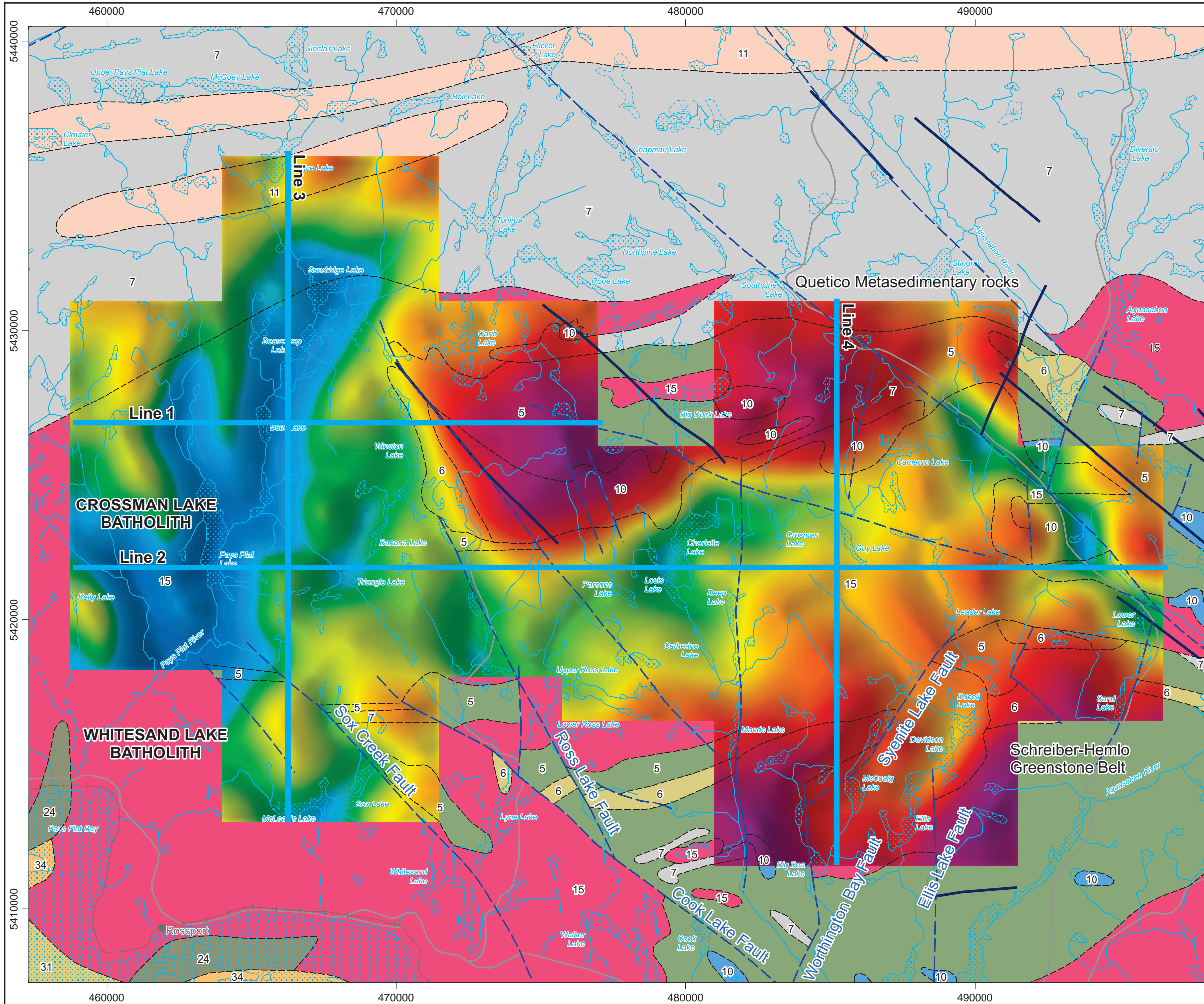


**Airborne Geophysics
 Acquisition and Interpretation**

Schreiber Area, Ontario 2014

Location of 2.5D Model Lines shown with
 Reduction to the Pole
 of the Total Magnetic Intensity (250 m cell)

	DESIGN	JK	29/01/2015	REV. 1.1
	GIS	YC, AP	04/02/2015	FIGURE: 5.5
	DATA	MM, DK	04/02/2015	
	QC	MB	04/02/2015	



Legend

Hydrography

Road

Railway

Geology

Fault

Dyke

5: Mafic to intermediate metavolcanic rocks

6: Felsic to intermediate metavolcanic rocks

7: Metasedimentary rocks

10: Mafic and ultramafic rocks

11: Gneissic tonalite suite

15: Massive granodiorite suite

24: Animikie Gp.

31: Sibley Gp.

32: Osler Gp., Mamaine Point Fm., Michipicoten Island Fm.

34: Mafic intrusive rocks (Keweenawan age)

Interpreted and Mapped Features

--- OGS Dataset MRD 126-Rev 1 Surface Geology Mapping

— 2.5D model line

Map Parameters

Illumination: inclination 50°, declination 270°

Spatial Filter (half-wavelength): 1000 m

mGal



BASE DATA: National Topographic Database - NRCAN
 GEOLOGY DATA: OGS Dataset MRD 126-Rev 1
 DATUM: NAD83
 PROJECTION: Universal Transverse Mercator (UTM Zone 16N)

Scale 1 : 130 000

km 0 1 2 3 4 5 km

**Airborne Geophysics
 Acquisition and Interpretation**

Schreiber Area, Ontario 2014

Location of 2.5D Model Lines shown with
 Free Air Gravity (250 m cell)

	DESIGN	JK	29/01/2015	REV. 1.1
	GIS	YC, AP	04/02/2015	FIGURE: 5.6
	DATA	MM, DK	04/02/2015	
	QC	MB	04/02/2015	

Figure 5.7 - Forward Modeling Results: Line 1, Model 1.5, Schreiber, Ontario

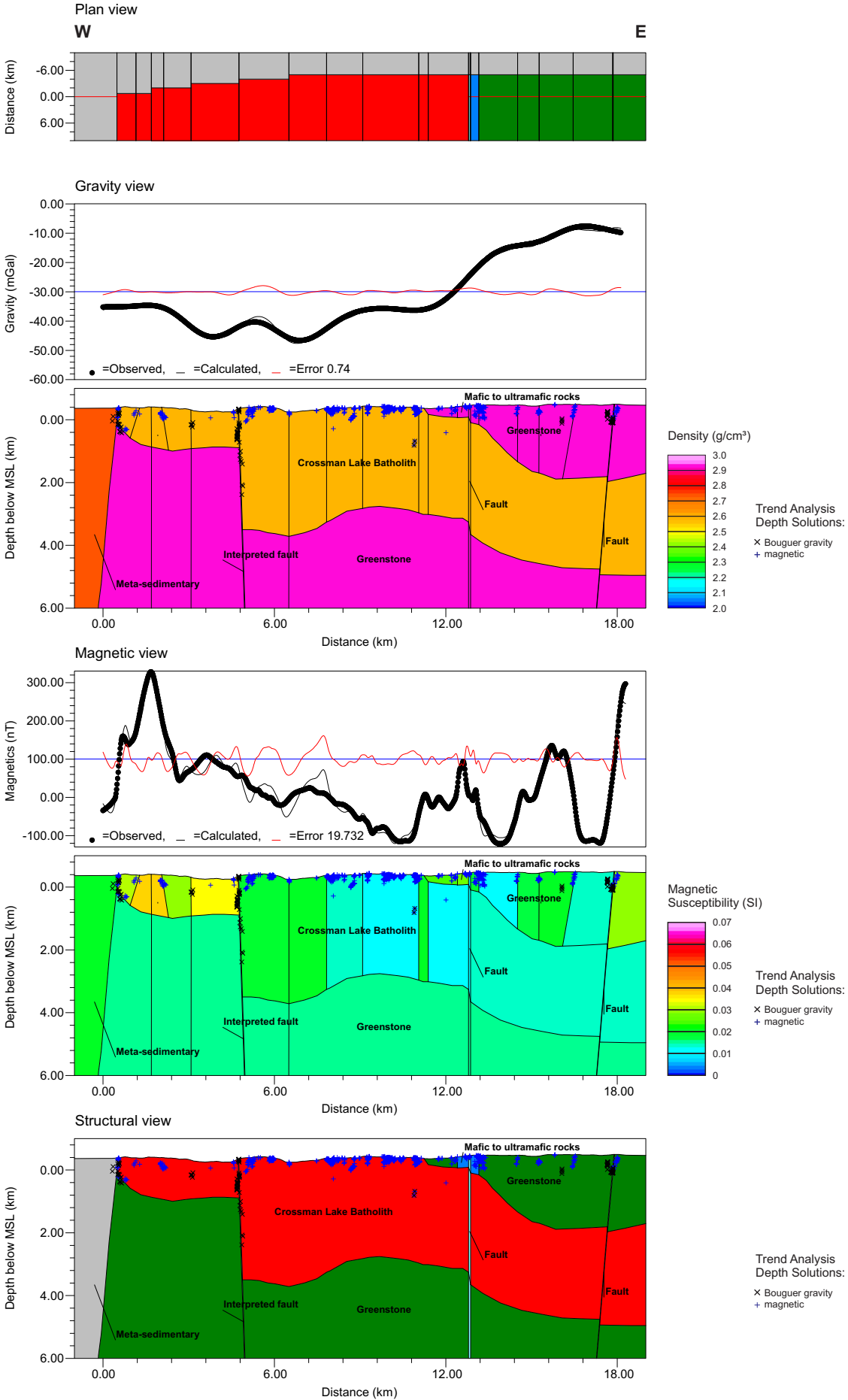


Figure 5.8 - Forward Modeling Results: Line 1, Model 1.6, Schreiber, Ontario

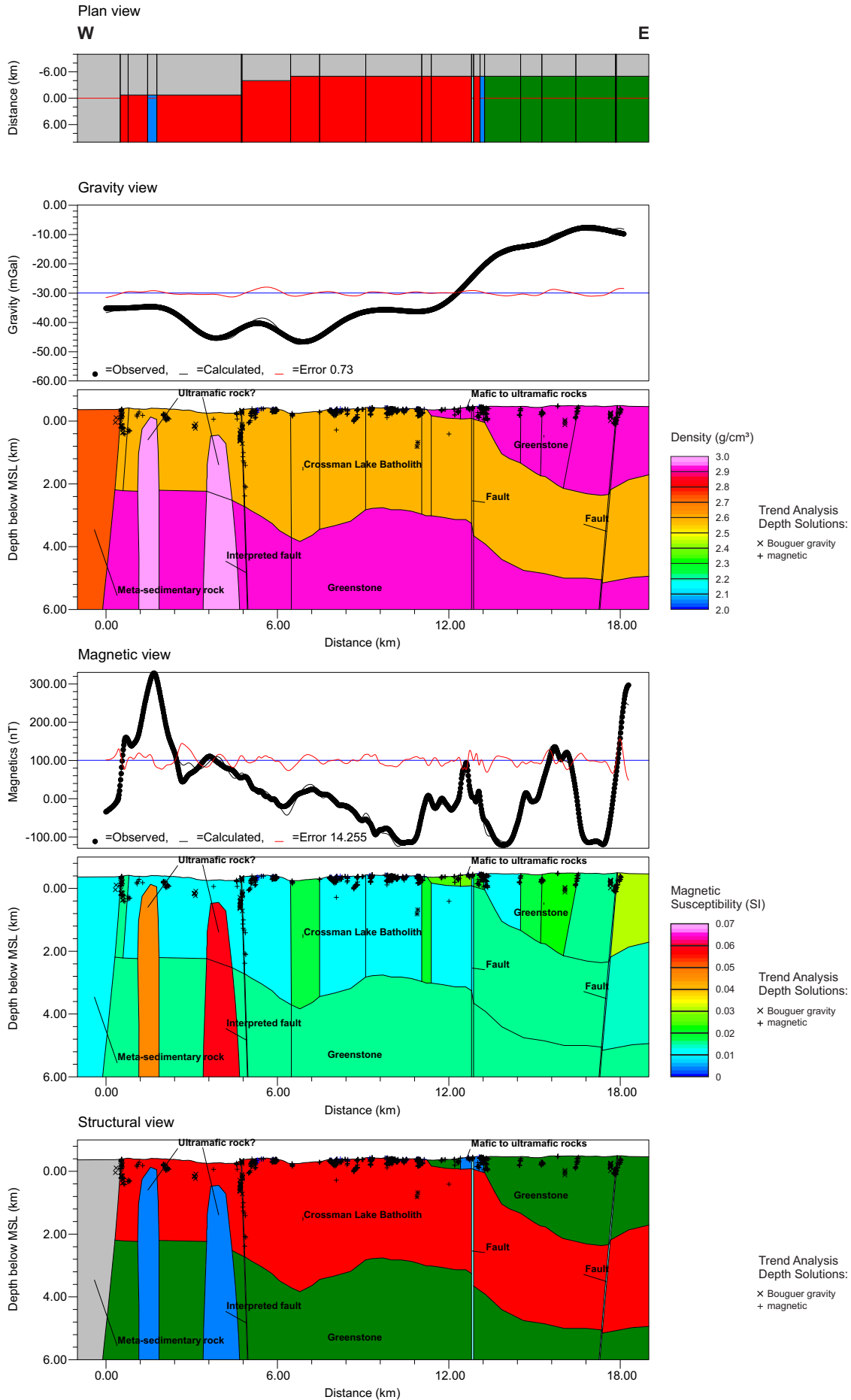


Figure 5.9 - Forward Modeling Results: Line 1, Alternative Model 1.5, Gneiss Basement, Schreiber, Ontario

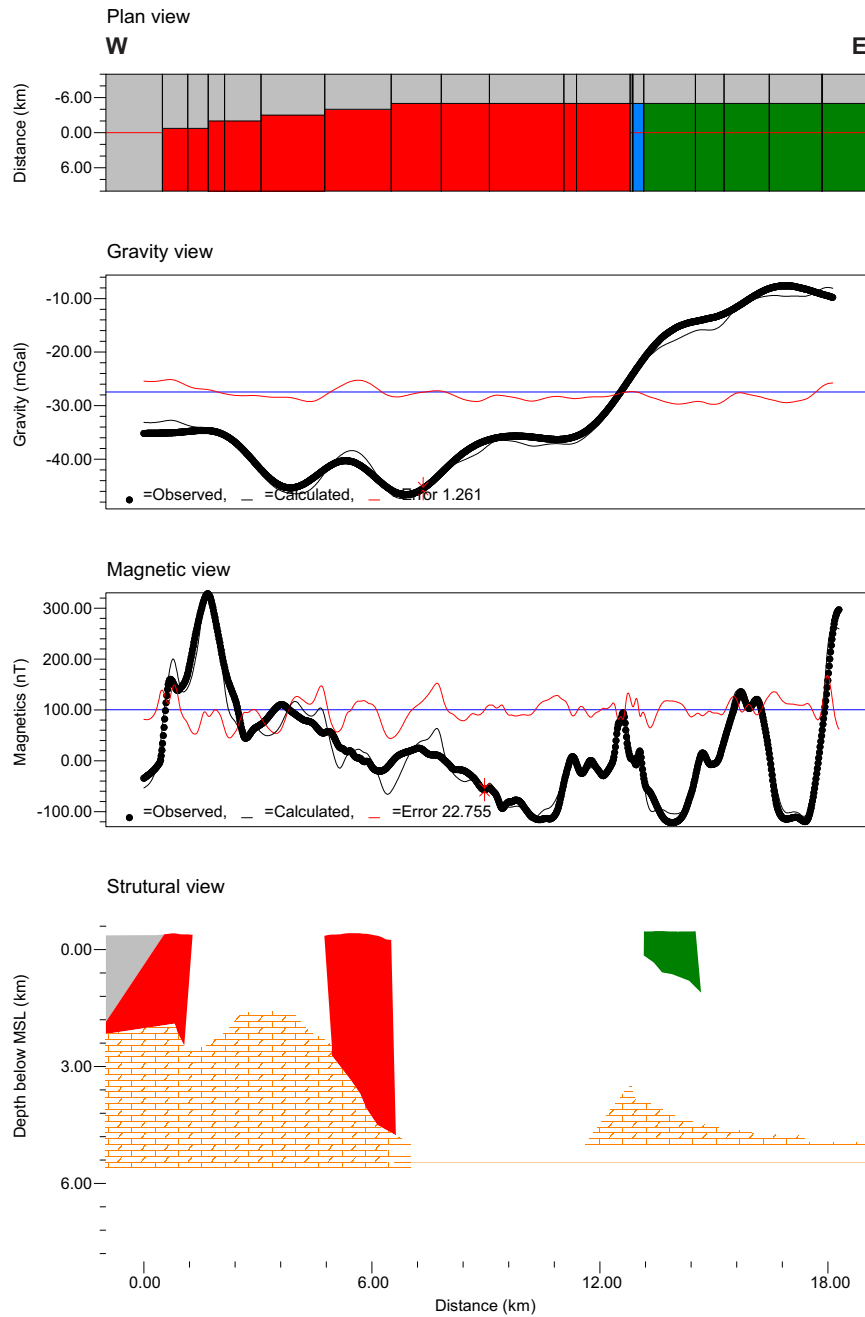


Figure 5.10 - Forward Modeling Results: Line 2, Model 2.2, Schreiber, Ontario

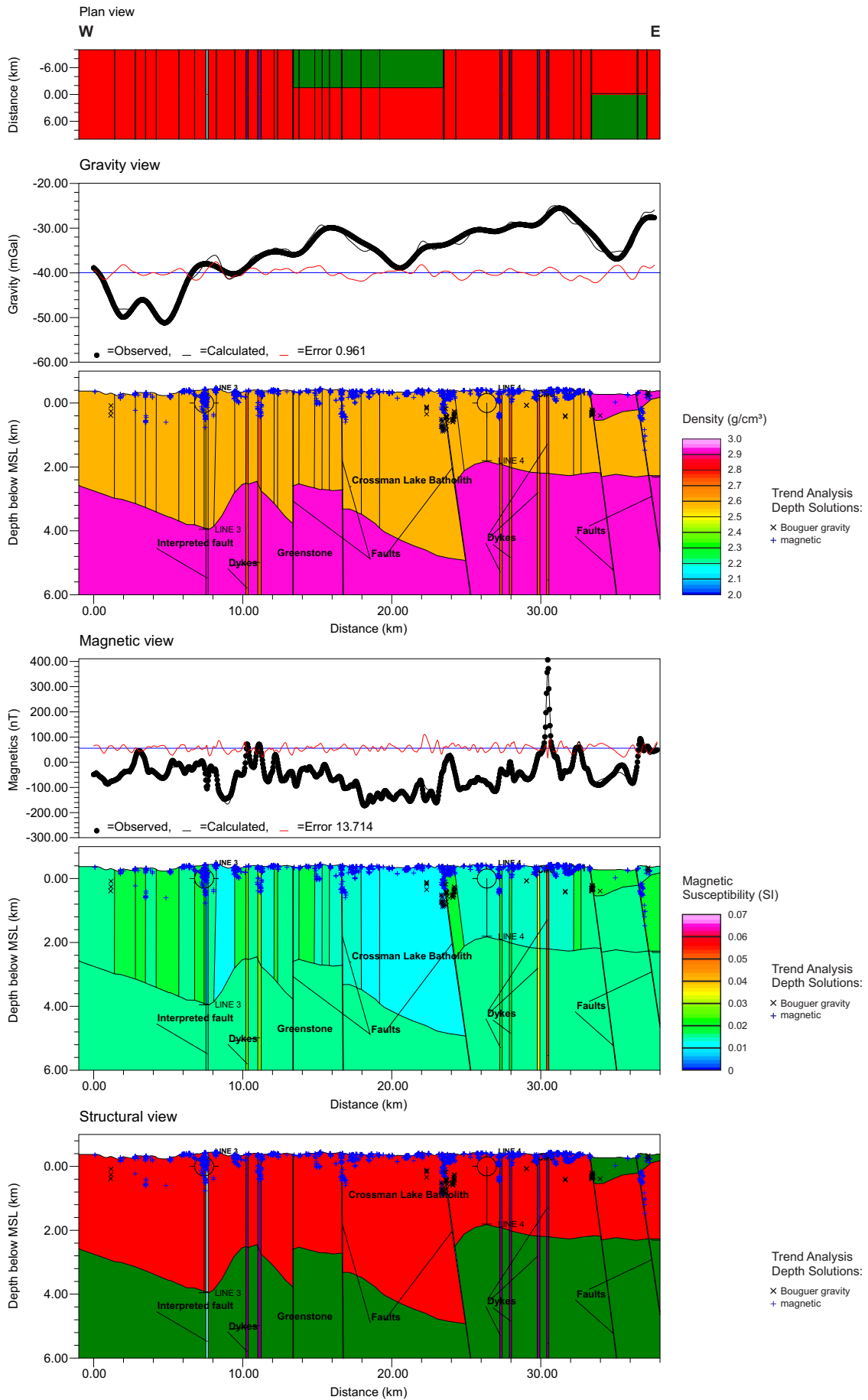


Figure 5.11 - Forward Modeling Results: Line 2, Model 2.1.2, Schreiber, Ontario

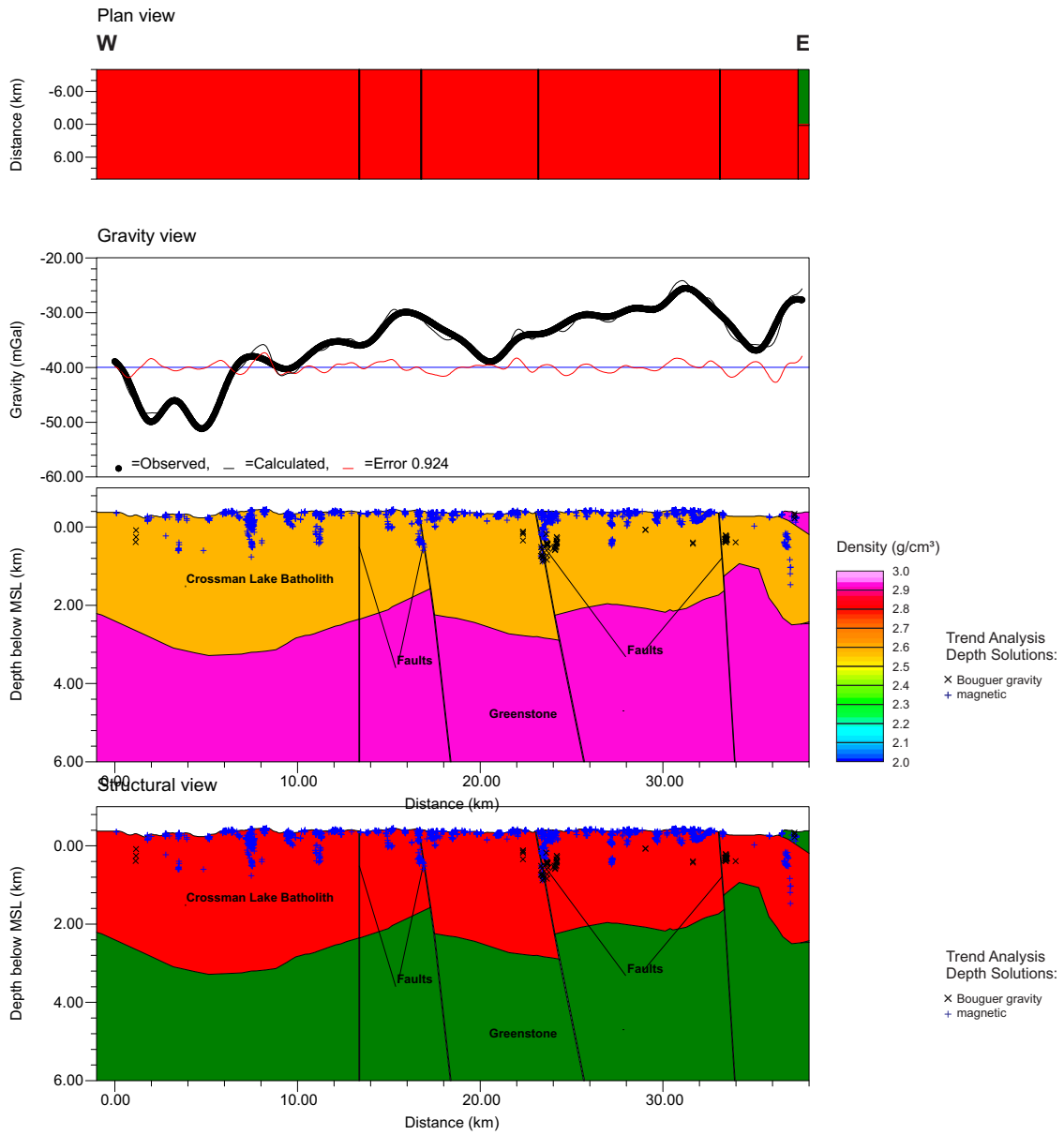


Figure 5.12 - Forward Modeling Results: Line 2, Alternative Model 2.1.2, Gneiss Basement, Schreiber, Ontario

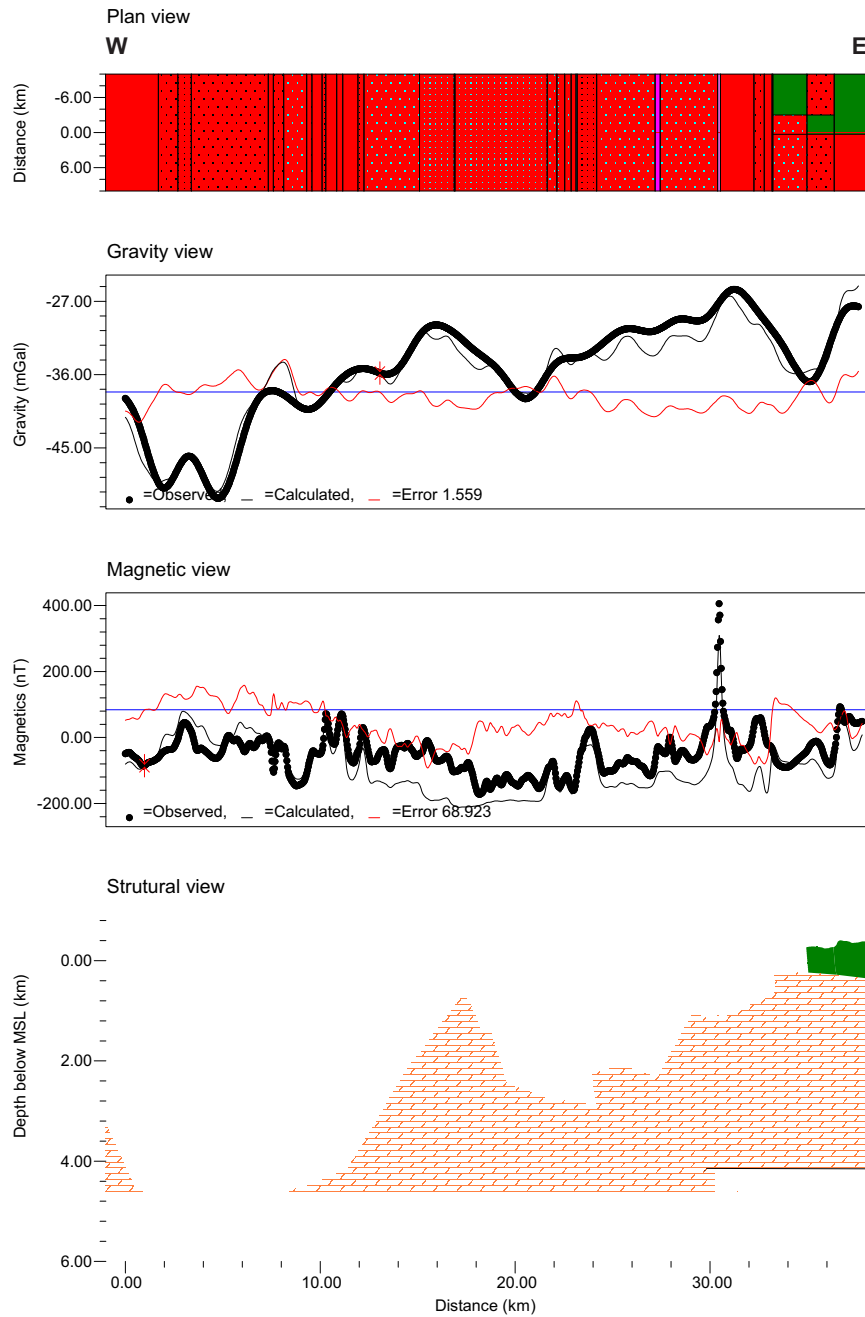


Figure 5.13 - Forward Modeling Results: Line 3, Model 3.4, Schreiber, Ontario

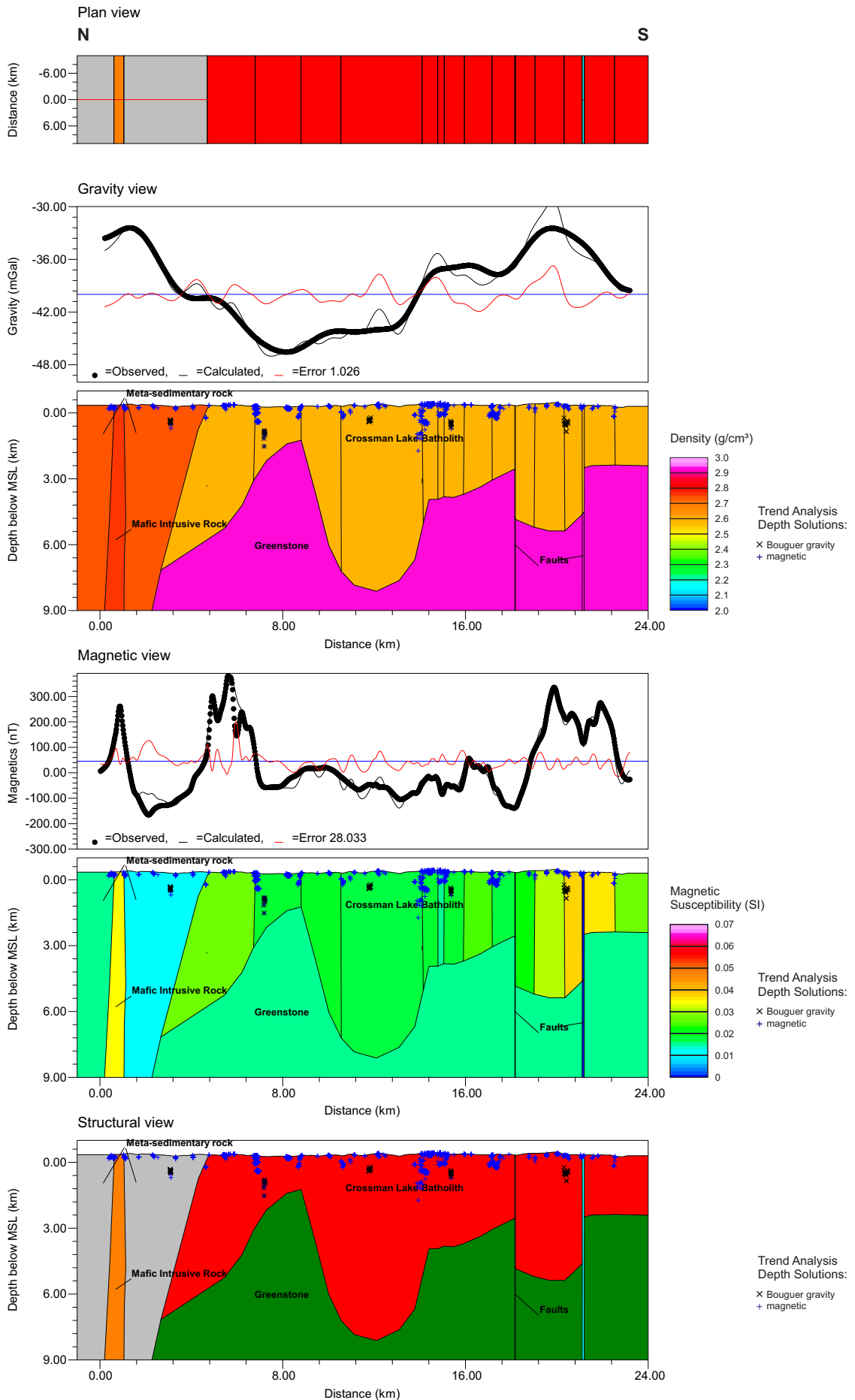


Figure 5.14 - Forward Modeling Results: Line 3, Alternative Model 3.4, Gneiss Basement, Schreiber, Ontario

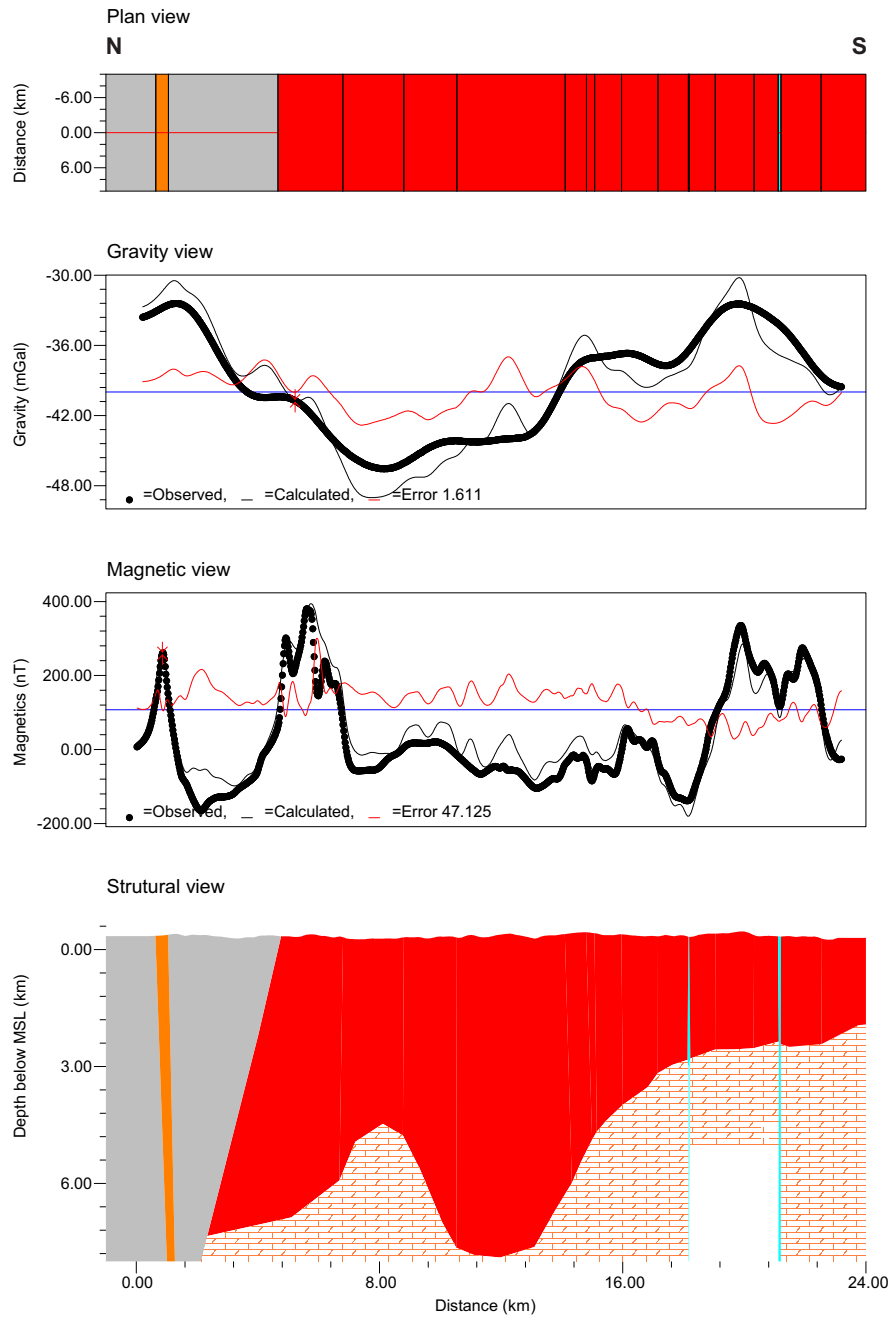


Figure 5.15 - Forward Modeling Results: Line 4, Model 4.4.3.2, Schreiber, Ontario

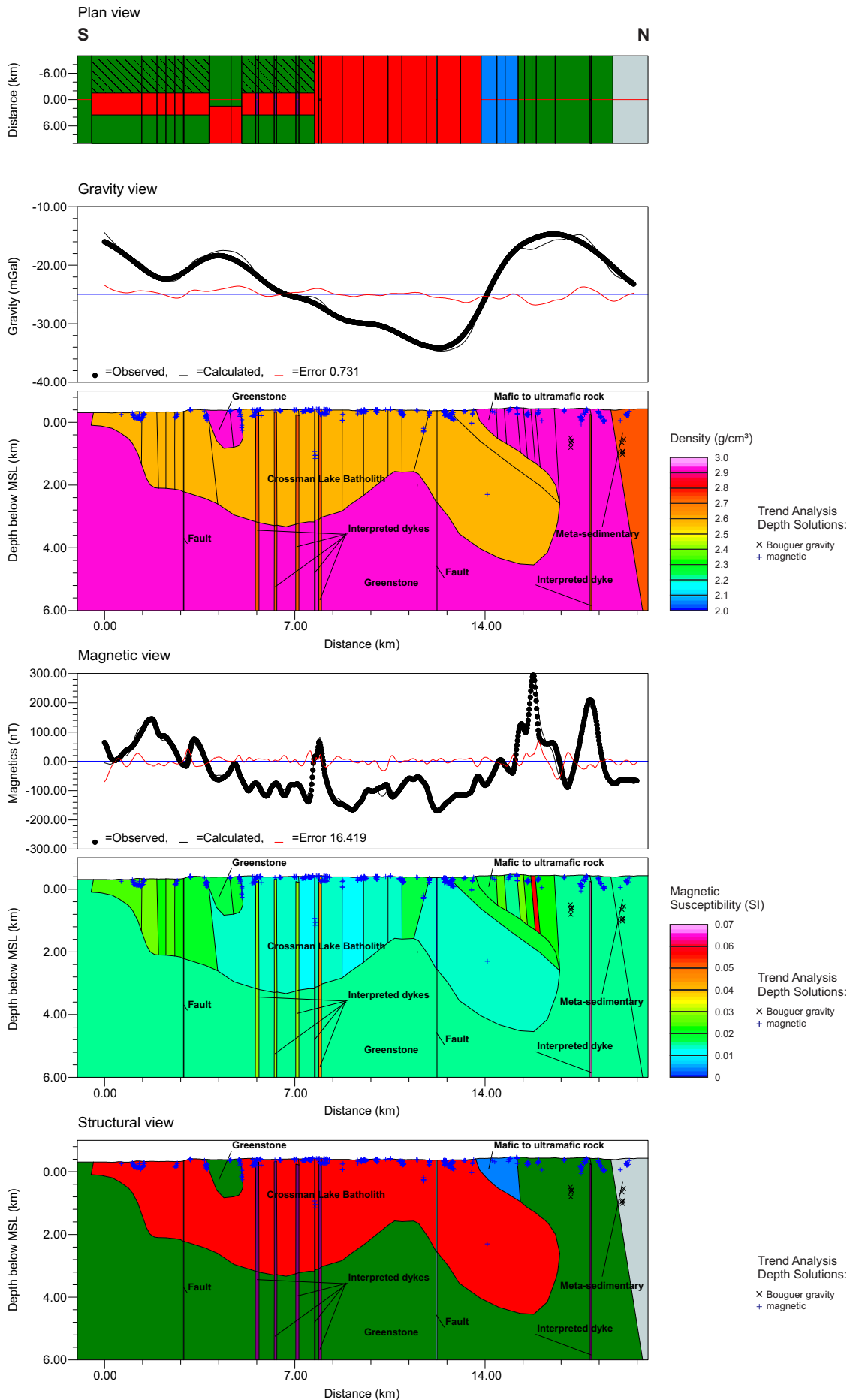


Figure 5.16 - Forward Modeling Results: Line 4, Alternative Model 4.4.3.2, Gneiss Basement, Schreiber, Ontario

